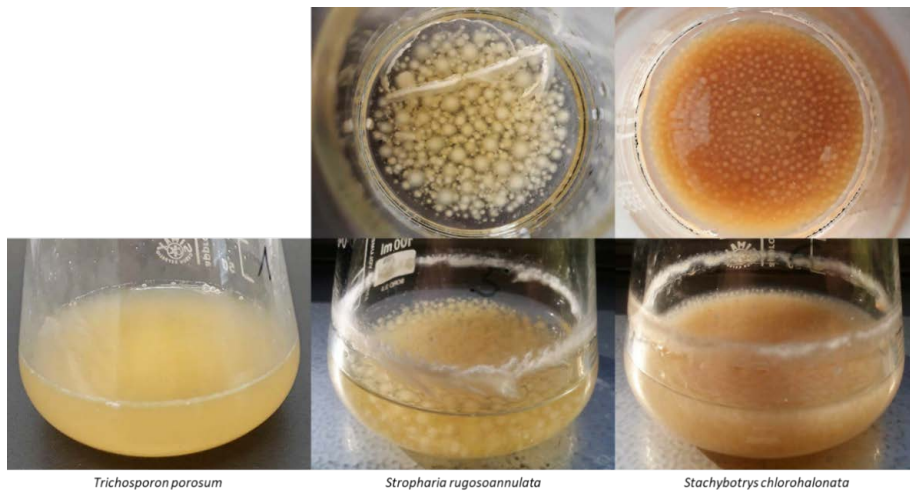


Biodegradation of Organic Micropollutants Dibutyl Phthalate and Bisphenol A by Fungi

Lena Carstens



Trichosporon porosum

Stropharia rugosoannulata

Stachybotrys chlorohalonata

Master's thesis • 30 credits
Environmental Science
Molecular Sciences, 2018:15
Uppsala 2018

Biodegradation of Organic Micropollutants Dibutyl Phthalate and Bisphenol A by Fungi

Lena Carstens

Supervisor:	Dr. Harald Cederlund, SLU, Department of Molecular Science
Assistant supervisor:	Dr. Dietmar Schlosser, Helmholtz Centre for Environmental Research - UFZ, Department of Environmental Microbiology
Examiner:	Prof. Dr. John Stenström, SLU, Department of Molecular Science
Credits:	30 credits
Level:	Second cycle, A2E, Master's level
Course title:	Independent project in environmental science – master's thesis
Course code:	EX0431
Programme/education:	Environmental Science
Title of series	Molecular Sciences
Part number:	2018:15
Place of publication:	Uppsala
Year of publication:	2018
Cover picture:	Lena Carstens
Online publication:	https://stud.epsilon.slu.se
Keywords:	micropollutant, dibutyl phthalate, bisphenol A, fungi, biodegradation, biosorption, endocrine disrupting chemical

Swedish University of Agricultural Sciences

Faculty of Natural Resources and Agricultural Sciences

Department of Molecular Sciences

Can Fungi Help to Solve Problems Related to Plastic Pollution?

Popular scientific summary

Plastics are everywhere around us in many products that we use. To produce the plastic, different chemicals are used. Phthalates are utilized to make rigid plastic flexible and increase its applicability, while bisphenol A is a raw material for plastic. When plastics are used or after their deposition, these compounds can escape into the environment. They can affect health in wildlife and humans by disrupting hormones, or acting as one themselves. Some microorganisms, such as fungi living in soil and water actually learned to grow on these pollutants and can degrade them enzymatically. In this study some selected fungi from different habitats were tested to see if and how they actually remove or degrade the pollutants.

The fungi were cultivated in flasks containing the pollutant (dibutyl phthalate or bisphenol A) in a liquid growth medium. The time course of degradation was followed and degradation products of phthalate were investigated. In both experiments, additional chemicals facilitated determination of removal by sorption to the biomass, and elucidation of the contribution to removal of a versatile oxidative enzyme found inside of cells named cytochrome P450. The activities of lignin-modifying enzymes were concomitantly monitored.

The removal of both micropollutants was very effective in all investigated fungi except one, and no pollutant could be detected after 3.5 h to 9 days of incubation. The fungi were capable to degrade the micropollutants to varying extent. Most effective degradation of both pollutants was observed in a wood-decaying and an aquatic fungus. This implies that phthalate degraders are present all around in the environment. The same fungi plus a fungus isolated from a constructed wetland were utilizing cytochrome P450 to degrade the micropollutants. The lignin-modifying enzyme laccase was possibly involved in transformation of bisphenol A in the wood-decaying fungus. Oxidative and hydrolytic degradation products were formed by the investigated wood-decaying fungi and the wetland isolate, and only hydrolytic degradation products by a soil inhabiting yeast. With the information about degradation

products, further conclusions could be drawn about how phthalate is degraded and which enzymes are involved. However, in most fungi removal was dominated by biosorption.

In conclusion, fungi represent a promising and relatively untapped resource with regard to the bioremediation of micropollutants. The results in this study indicate that fungi of diverse habitats remove phthalate and bisphenol A by different processes. To follow up these results, investigation of degradation of pollutant mixtures, removal by a fungal consortium, and ultimately removal of micropollutants in the environment should be conducted.

Abstract

Fungi represent a promising and relatively untapped resource in regard to the bioremediation of micropollutants. Degradation efficiencies of the ubiquitous endocrine disrupting chemicals dibutyl phthalate (DBP) and bisphenol A (BPA) by selected fungal strains with different ecophysiologicals were determined via ultra performance liquid chromatography (UPLC). The micropollutants were almost completely (about 100% of the initial concentration) removed by all fungi except the wetland isolate *Stachybotrys chlorohalonata*. Biotransformation of micropollutants tested was observed, but the degree of transformation varied between individual strains. Strongest biocatalytic DBP degradation was observed for the white-rot fungus *Stropharia rugosoannulata* followed by the aquatic *Clavariopsis aquatica*, implying wide-spread presence of DBP degraders in the environment. Contribution of P450 monooxygenase(s) to DBP degradation in *Stropharia rugosoannulata* and *Clavariopsis aquatica*, followed by *Stachybotrys chlorohalonata* was indicated by caused inhibition of micropollutant degradation through the cytochrome P450 inhibitor piperonyl butoxide. Nevertheless, biosorption dominated removal of pollutants for the other fungi. *S. rugosoannulata* also efficiently biotransformed BPA, seemingly involving cytochrome P450 catalyzed reactions, whereas biosorption was a less important removal process. By contrast, biosorption was the only BPA removal process operative in *S. chlorohalonata*. Activity of extracellular lignin-modifying enzymes was quantified by spectrophotometric 2,2'-azinobis-(3-ethylbenzothiazoline-6-sulfonic acid) ABTS assays, and laccase activity detected in *S. rugosoannulata* may have contributed to BPA removal by this strain. Elucidation of DBP degradation metabolites of *T. porosum*, *S. rugosoannulata* and *S. chlorohalonata* confirmed oxidative and hydrolytic biotransformation steps, in line with literature data. Monobutyl phthalate and phthalic acid were identified as prominent intermediates in all investigated strains and *S. rugosoannulata*, respectively.

Keywords

micropollutant, dibutyl phthalate, bisphenol A, fungi, biodegradation, biosorption, endocrine disrupting chemical

Table of content

1.	Introduction	1
1.1.	Micropollutants in the environment	1
1.2.	Phthalates	2
1.3.	Bisphenol A	3
1.4.	Biodegradation	4
1.5.	Biosorption of micropollutants	8
1.6.	Fungal inhibition and inactivation	9
1.7.	Project aims	9
2.	Materials and Methods	10
2.1.	Source of chemicals	10
2.2.	Information on fungal strains	10
2.3.	Micropollutant Removal Experiments	11
2.4.	Fungal dry mass determination	14
2.5.	Analysis of micropollutants by ultra performance liquid chromatography (UPLC) coupled with diode array detection (DAD)	14
2.6.	Calculation of micropollutant removal rates	15
2.7.	Photometrical determination of laccase and peroxidase activity	17
2.8.	Formation of DBP biotransformation products	18
2.9.	UPLC-quadrupole time-of-flight mass spectrometry (UPLC-QTOF-MS) analyses of DBP biotransformation products	18
2.10.	Statistical treatment of data	19
3.	Results	20
3.1.	Fungal biomass	20
3.2.	Comparison of alternative inhibition and inactivation methods of fungal biomass	21

3.3.	Micropollutant removal by fungal cultures	22
3.4.	Biotransformation metabolites produced from DBP in fungal cultures	35
4.	Discussion	42
4.1.	Micropollutant biotransformation efficiency by fungi	42
4.2.	Biosorption of micropollutants	45
4.3.	DBP degradation pathway based on transformation products	45
5.	Concluding remarks	48
	References	49
	Acknowledgements	54
	Appendix	I

List of Tables

Table 1 Composition of 1 l Stanier's mineral salt medium.....	13
Table 2 Mobile phase and elution profile applied for DBP quantification with UPLC analysis.....	15
Table 3 Mobile phase and elution profile applied for BPA quantification with UPLC analysis.....	15
Table 4 Reaction mix ingredients and volumes for determination of total peroxidase activity.....	17
Table 5 Mobile phase and elution profile applied for DBP metabolite separation with UPLC analysis	19
Table 6 Fungal dry biomass values after 7 days of pre-cultivation	20
Table 7 Removal rates of DBP observed in cultures of <i>T. porosum</i>	27
Table 8 Removal rates of BPA observed in cultures of <i>T. porosum</i>	27
Table 9 Removal rates of DBP observed in cultures of <i>S. rugosoannulata</i>	29
Table 10 Removal rates of BPA observed in cultures of <i>S. rugosoannulata</i>	29
Table 11 Removal rates of DBP observed in cultures of <i>S. chlorohalonata</i>	30
Table 12 Removal rates of BPA observed in cultures of <i>S. chlorohalonata</i>	30
Table 13 Removal rates of DBP observed in cultures of <i>Phoma</i> sp.	31
Table 14 Removal rates of DBP observed in cultures of <i>Ascocoryne</i> sp.	32
Table 15 Removal rates of DBP observed in cultures of <i>P. arenariae</i>	32
Table 16 Removal rates of DBP observed in cultures of <i>Acephala</i> sp.....	33
Table 17 Removal rates of DBP observed in cultures of <i>C. aquatica</i>	33
Table 18 Overview of micropollutant removal capacities, inhibitory effects of PB and biosorption by fungal isolates for DBP and BPA removal experiments.....	34
Table 19 Peak areas of DBP transformation products and their time courses detected by UPLC-QTOF-MS.	36
Table 20 Peak area of the most indicative oxidative DBP transformation products and their time course detected by UPLC-QTOF-MS	38
Table 21 Peak areas of the major hydrolytic DBP transformation products and their time courses detected by UPLC-QTOF-MS.....	39
Table 22 Peak areas of the major DBP transformation products formed by a combination of oxidative and hydrolytic processes, and their time courses detected by UPLC-QTOF-MS	40

List of Figures

Figure 1 Mode of action for endocrine disrupting chemicals.	2
Figure 2 Chemical structure of di-n-butyl phthalate (DBP).	3
Figure 3 Chemical structure of bisphenol A (BPA).	3
Figure 4 Degradation pathways of diester phthalates with linear alkyl moieties.	6
Figure 5 Compilation of possible biodegradation pathways of BPA by bacteria and fungi.	7
Figure 6 Schematic representation of fungal mycelium physiology at different scales.	8
Figure 7 Phylogenetic tree displaying relationship of fungal species used in this study.	11
Figure 8 Schematic overview of Erlenmeyer flask set-up used for each fungal strain.	13
Figure 9 Time course of DBP concentrations and laccase activity in cultures of <i>T. porosum</i> , <i>S. rugosoannulata</i> and <i>S. chlorohalonata</i>	24
Figure 10 Time course of DBP concentrations for cultures of other fungal strains and negative control..	25
Figure 11 Time course of BPA concentrations and laccase activity in cultures of <i>T. porosum</i> , <i>S. rugosoannulata</i> and <i>S. chlorohalonata</i>	26
Figure 12 Time course of peak area of DBP in cultures of <i>S. chlorohalonata</i> detected by UPLC-QTOF-MS.	40
Figure 13 Proposed DBP transformation pathway in <i>T. porosum</i> , <i>S. rugosoannulata</i> and <i>S. chlorohalonata</i>	47

Abbreviations

ABTS	2,2'-Azinobis-(3-ethylbenzothiazoline-6-sulfonic acid)
BPA	Bisphenol A
DBP	Dibutyl phthalate
min	minutes
Mn-peroxidase	Manganese peroxidase
PB	Piperonyl butoxide
UPLC-DAD	Ultra performance liquid chromatography – diode array detection
UPLC-QTOF-MS	Ultra performance liquid chromatography – quadrupole time-of-flight – mass spectrometry

1. Introduction

1.1. Micropollutants in the environment

The synthesis of organic chemicals with specialized properties suiting human needs – e.g. controlling organisms like weeds or pathogens, in technical advances, or in product development and increase of industrial process efficiency – has been very successful. The deliberate repeated release of such widely-used chemicals in addition to mayor accidents or problems related to hazardous waste management can cause large-scale contamination of the environment. Many of the organic compounds are present at trace concentrations (ng l^{-1} to $\mu\text{g l}^{-1}$) in the environment, hence the term ‘micropollutant’. It is often for the low concentrations and diverse chemical structure that these xenobiotic organic compounds are recalcitrant to removal in waste water treatment plants and subsequently released into surface waters (Luo et al., 2014). The effects caused by pollutants are often difficult to distinguish due to time offset or complexity of interactions within the ecosystem (Schwarzenbach et al., 2006). Proven and suspected detrimental impacts to living organisms include but are not limited to toxicity, carcinogenicity, teratogenicity and endocrine disruption. Further, some degradation products of pollutants are still biologically active or bare greater toxicity than the parent compounds. The pollutants also pose direct (e.g. endocrine disruption) and indirect (e.g. antibiotic resistance in pathogens; bioaccumulation of hydrophobic chemicals in body fat with biomagnification along the food chain) hazard towards human health.

As implied, micropollutants arise from different anthropogenic activities, one being the production of plastic utilized for a versatile range of products. Success and wide-spread usage of synthetic polymers, commonly named plastics, made them one of the most ubiquitous anthropogenic pollutants (Krueger et al., 2015). Though the polymeric substances are themselves not directly toxic, several chemicals used for synthesis or qualitative improvement of plastic are.

1.2. Phthalates

Phthalates, synonym for phthalate esters, are mainly used primarily as plasticizers of poly vinyl chloride (PVC – food packaging, medical devices etc.) that decrease the attractions between the polymer chains, improving its flexibility, workability and extensibility. The phthalates do not bond covalently to the polymer network, and thus leach and migrate into the environments during production, use and disposal of plastic products, resulting in its ubiquitous occurrence (Gao and Wen, 2016, Staples et al., 1997). Due to structural similarities, many phthalates are putative or proven xenoestrogens, causing endocrine disruption in wildlife and humans (Figure 1, (Bergman et al., 2013)). Endocrine disrupting agents interfere with the homeostatic balance of a spectrum of biological processes, particularly those linked with development and reproduction (Benjamin et al., 2015, Matsumoto et al., 2008, Diamanti-Kandarakis et al., 2009).

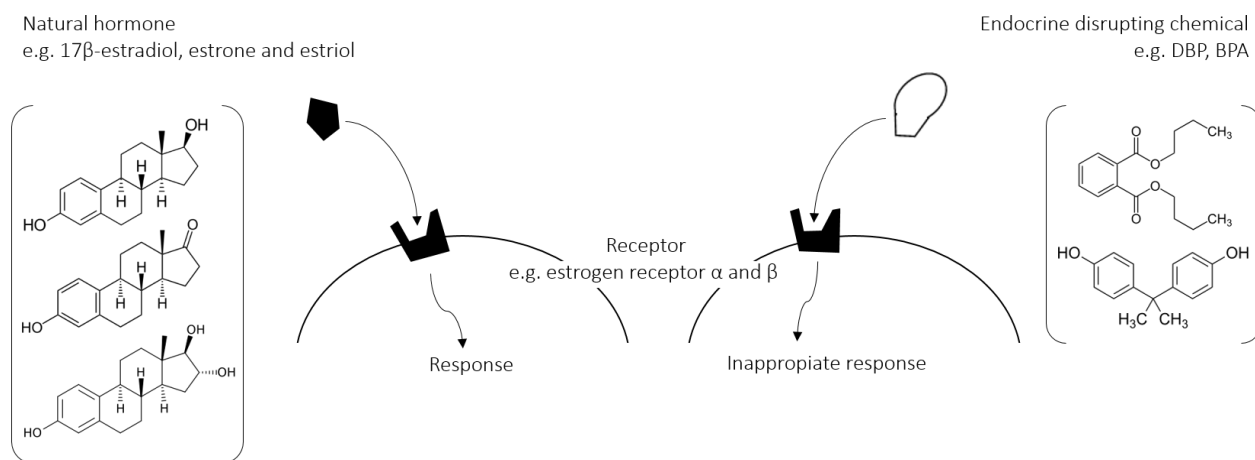


Figure 1 Mode of action for endocrine disrupting chemicals. Structural similarities of compounds to endogenous hormones such as estrogens (e.g. 17β-estradiol) allow interaction with the corresponding receptors. The resulting response is unsolicited and may lead to abnormalities in development or other hormone controlled pathways.

Structurally, all phthalates are esters or diesters of 1,2-benzenedicarboxylic acid (also called phthalic acid) with distinct alkyl or aryl moieties contributing to the hydrophobicity of the compound. Dibutyl benzene-1,2-dicarboxylate or di-n-butyl phthalate (DBP, Figure 2) is a low molecular weight phthalate ($278.35 \text{ g mol}^{-1}$, compared to a range from 194.18 to $530.82 \text{ g mol}^{-1}$, respectively of dimethyl and diisotridecyl phthalate) further used in personal care products and as solvent. DBP is a primary phthalate pollutant (Gao and Wen, 2016). Due to the low water solubility (11.2 mg l^{-1}) and high octanol-water partition coefficient ($\log K_{ow} 4.57$), DBP can readily adsorb to soil, sediment and suspended solids (Staples et al., 1997). Though it is readily degradable compared to higher molecular weight phthalates, it is pseudopersistent in the environment due to its constant anthropogenic input. Degradation is predominantly mediated by microorganisms, fungi and some algae (Benjamin et al., 2015). An overview

of studied (co-) metabolic pathways and responsible enzymes is given in the following section. Abiotic degradation processes are mainly acid or base catalyzed hydrolysis and photochemical degradation (predominantly occurring in aqueous environments) (Huang et al., 2013, Lau et al., 2005). The estimated half-life (i.e. time required for a concentration to reduce to half its initial value) is 50 to 360 days for abiotically degraded DBP (Lertsirisopon et al., 2009).

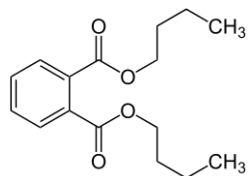


Figure 2 Chemical structure of di-n-butyl phthalate (DBP). Two butyl moieties are bond via esters to phthalic acid.

1.3. Bisphenol A

2,2-(4,4-dihydroxydiphenyl) propane, commonly bisphenol A (BPA, suffix A for acetone), is another micropollutant related to plastic production (Figure 3). BPA is predominantly used for production of polycarbonate and epoxy resins, later being incorporated into a number of industrial and consumer goods (e.g. food and beverage packaging, electronic insulation, medical catheters and implants) (Staples et al., 1998). Just as DBP, BPA is an ubiquitously present micropollutant with xenoestrogenic activity, albeit lower than that of natural estradiol (Flint et al., 2012, Ike et al., 2002). BPA is moderately water soluble (300 mg l^{-1}), however the octanol-water coefficient indicates high lipophilicity ($\log K_{OW} 3.32$, (Hansch et al., 1995, Shareef et al., 2006)). Atmospheric abiotic degradation is mainly due to photooxidation (interaction with hydroxy radicals $\text{HO}\cdot$ or other oxidants) and a half-life of 0.2 days was calculated (EC, 2003, Howard, 1989). In aqueous environment, adsorption to soils and sediments is a major sink ($\log K_{OC}$ approximately 1500, estimated from $\log K_{OW}$), while volatilization, hydrolysis and photolysis are likely to be negligible due to the physicochemical properties (EC, 2003, Howard, 1989). Biodegradation is a critical process in removal of BPA, and is reviewed in the following.

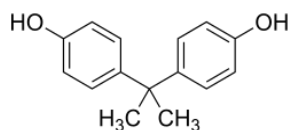


Figure 3 Chemical structure of bisphenol A (BPA).

1.4. Biodegradation

The aerobic or anaerobic degradation capacity of microorganisms including fungi, and plants alone or in collaboration is a promising pathway for remediation of organopollutants. In bioremediation living microorganisms are used to degrade environmental pollutants into benign substances or to prevent pollution. Microorganisms can act either singly or as consortium for the complete (i.e. mineralization) or partial pollutant removal (e.g. (Benjamin et al., 2015, Gu et al., 2005, Jin et al., 2014)). The organic compound can be utilized as growth substrate, in some cases even as sole source of carbon. The degradation efficiency thus relies on minimum substrate fluxes for maintenance energy. This metabolic degradation is expected to be more prominent in bacteria, and often substrate specific. In contrast, co-metabolic degradation is a consequence of unspecific enzymes, which are capable of degrading additional compounds beside the target growth substrate. Such unspecific enzymes are more common among fungi (Harms et al., 2011). Nevertheless, the organism does usually not obtain energy or carbon, thus for the organism itself co-metabolic degradation is not necessarily beneficial. Co-metabolism however provides benefits for the degraders when e.g. detoxifying compounds.

Research has focused mainly on bacterial degradation capabilities, while mycoremediation approaches are underrepresented. However, fungi have the biochemical and ecological potential to be utilized in remedial purposes. Compared to bacteria, their advantages are the previously mentioned low specificity of involved key enzymes, e.g. extracellular laccase and peroxidases and intracellular cytochrome P450 monooxygenase systems, naturally providing advantage towards growth on recalcitrant and complex organic polymeric substances like lignin; and their independence from using organopollutants as growth substrate. Further, fungi are persistent within varied and often extreme environments coupled with their intrusive and exploratory mycelial networks. This allows access to hydrophobic pollutants that tend to sorb to surfaces or accumulate in hydrophobic matrices (Harms et al., 2011). Last but not least fungi dominate the living biomass in soils, competing and co-existing with bacterial abundance, and are abundant in aqueous habitats.

In the following section, common biodegradative pathways of DBP and BPA are presented as described in literature for bacteria and fungi.

DBP biodegradation pathways

The degradation of phthalates generally consist of two processes, the primary biodegradation from phthalic diesters to monoesters and then to phthalic acid, and ultimate biodegradation from phthalic acid to complete mineralization ((Staples et al., 1997), Figure 4). The degradation controlling steps are bioavailability of phthalic diesters, depending on the length of the ester alkyl chains, and second the hydrolysis to phthalic monoesters. Accumulation of monoesters under environmentally realistic conditions is highly unlikely (Scholz, 2003). Bioavailability, and furthermore degradation itself, is affected by environmental conditions (most importantly microbial community composition and abundance, temperature, and pH) (Gao and Wen, 2016). It has been shown that the (aerobic) primary degradation conforms to first-order kinetics (de Moura Carrara et al., 2011, Peng and Li, 2012). However, concentrations far above environmentally measured pollution (i.e. greater than 2.25 mM DEP) caused inhibition of the biodegrading organisms (Navacharoen and Vangnai, 2011). Addition of substrate suitable as carbon source has been shown to significantly enhance biodegradation (e.g. (Liao et al., 2010, Yang et al., 2013b).

The primary degradation consists of different pathways all leading to phthalic acid (Figure 4). Initially, phthalate with long linear ester alkyl moieties undergo β -oxidation, which removes one ethyl group each time (Amir et al., 2005). The β -oxidation is started through hydroxylation by cytochrome P450. Then, phthalates (with shorter ester alkyl chains) are further converted by hydrolytic deesterification or oxidative O-dealkylation, which can alternatively be preceded by transesterification. Stepwise hydrolysis of phthalate to monophthalate and phthalic acid is the same under aerobic and anaerobic conditions. This deesterification is the most common one among bacteria and fungi. Alternatively, the side chains can be removed by O-dealkylation catalyzed by cytochrome P450. Transesterification is the nucleophilic substitution of an ethyl group with a methyl group in each step, producing ethyl-methyl phthalate and dimethyl phthalate (Cartwright et al., 2000). Dimethyl phthalate is then degraded to phthalic acid by hydrolysis or oxidation (O-demethylation). Exemptions to these general pathways are shown with dashed arrows in Figure 4. Low molecular weight phthalates (diethyl and dimethyl phthalate) for instance can directly be degraded into phthalic acid (Jackson et al., 1996).

The ultimate degradation of phthalic acid differs under aerobic and anaerobic conditions (Liang et al., 2008) (Figure 4). Aerobic degradation by dioxygenase, dehydrogenase and decarboxylase forms the intermediate protocatechuate (3,4-dihydroxy benzoate), followed by ring cleavage in *ortho* or *meta* position. The oxaloacetate and pyruvate (not shown) are then mineralized via the TCA cycle. By contrast, anaerobic degradation forms benzoate by carboxylation which is subsequently cleaved and degraded via

β -oxidation to acetate, carbon dioxide and dihydrogen. Furthermore, anaerobic degradation involving acyl CoA synthase over benzoyl-CoA and pimeloyl-CoA (not shown) and final β -oxidation has been reported (Benjamin et al., 2015). Spontaneous oxo-bridge formation to 1,3-isobenzofurandione followed degradation by fungal cutinase and yeast esterase. In presence of cutinase 1,3-isobenzofurandione was the major degradation product (Kim et al., 2005).

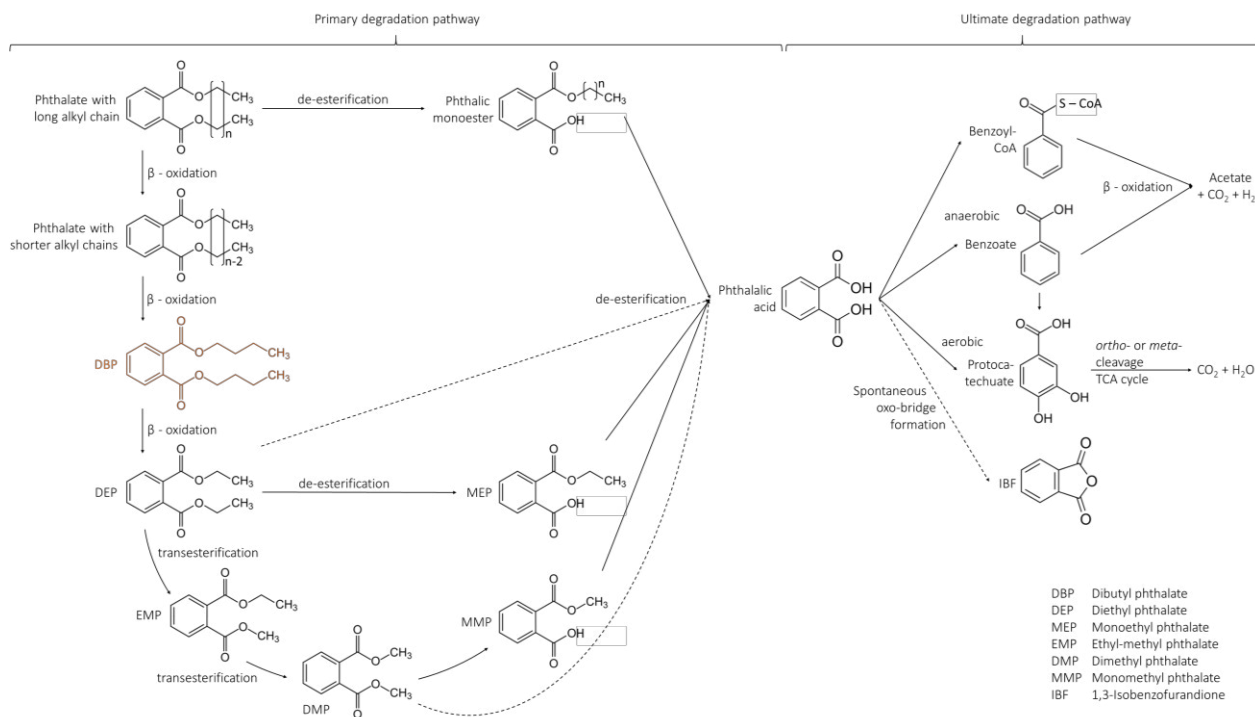


Figure 4 Degradation pathways of diester phthalates with linear alkyl moieties. The degradation can be divided in primary and ultimate degradation, where the first is the metabolic transformation from phthalate to phthalic acid and the latter completing mineralization of phthalic acid. Solid arrows indicate common pathways, while dashed arrows represent pathways of individual microorganisms.

BPA biodegradation pathways

Metabolization of BPA can be categorized into two pathways, the hydroxylation and the one electron abstraction (Figure 5). Following initial reactions, conjugate formation (glucuronides, glucosides, sulfate) is a typical phase II reaction for fungi and other eukaryotes. Morohoshi et al. (2003) showed that carbohydrate conjugation can strongly reduce the estrogenic activity of BPA. Alternatively, transformation to lower molecular weight metabolites or mineralization occurs (Chai et al., 2003, Lobos et al., 1992, Spivack et al., 1994).

Hydroxylation is catalyzed by oxidoreductases like cytochrome P450 monooxygenase or dioxygenase (Lobos et al., 1992, Sasaki et al., 2005, Spivack et al., 1994, Wang et al., 2014, Wang et al., 2013a).

Lignin-modifying enzymes like laccase and manganese-peroxidase (Mn-peroxidase), but also bacterial peroxidases, cause one electron oxidation forming phenoxy radicals, commonly followed by polymerization reactions (Sakurai et al., 2001, Uchida et al., 2001, Wang et al., 2013b). Such enzyme catalyzed polymerization is typical for the degradation of phenolic compounds and can reduce the toxic effects of BPA significantly (Ike et al., 2002).

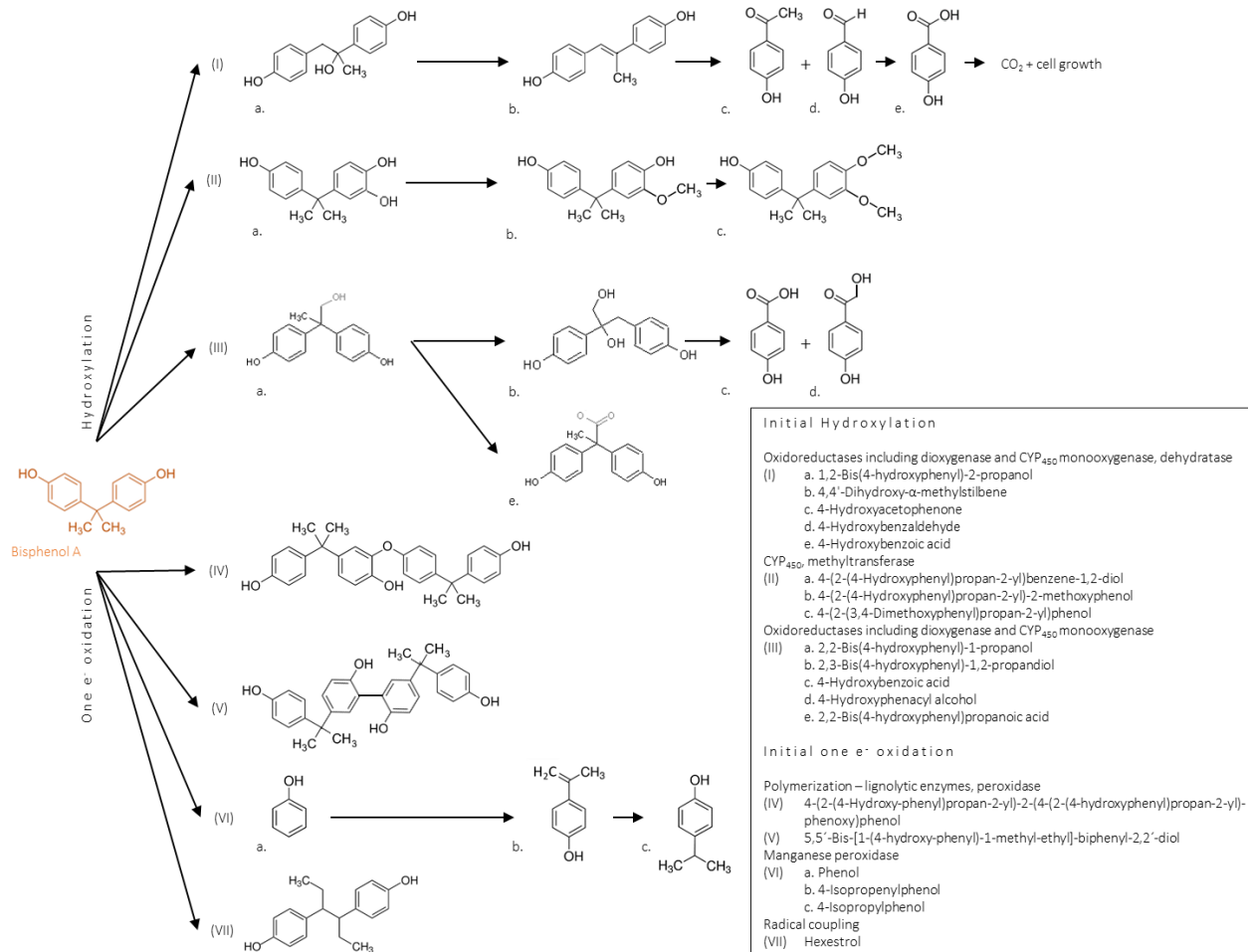


Figure 5 Compilation of possible biodegradation pathways of BPA by bacteria and fungi. Two pathways can be differentiated, namely hydroxylation and one electron (e⁻) abstraction.

1.5. Biosorption of micropollutants

Removal of organic or inorganic substances from solution by alive or dead biological material like fungal mycelium is defined as biosorption. It is a physical-chemical process including mechanisms like absorption, adsorption, ion exchange, surface complexation and precipitation (Gadd, 2009). The mycelium constitutes an extensive surface with sorption sites for nutrient uptake, exploitable for remediation of environmental pollutants (Figure 6). While the inner cell wall (chitin, β -1, 3-glucan and β -1, 6-glucan assembled into fibrous microfibrils) is relatively conserved among fungal species, the outer protein and polysaccharide moieties are species-specific (Coronado et al., 2007, Gow et al., 2017) (Figure 6C). These dynamic structures greatly influence the fungal ecology and are regulated in their composition in response to environmental or culture conditions like temperature, pH and pollutant concentrations (Gow et al., 2017). The composition of the cell wall in return affects biosorption (e.g. (Aksu and Karabayır, 2008, Kapoor and Viraraghavan, 1997)).

Moreover, biosorption has been reported to improve efficiency and type of micropollutants removed by biotransformation (Hofmann and Schlosser, 2016, Nguyen et al., 2014). The biosorptive enrichment on mycelium or extracellular polymeric substances surrounding asco- and basidiomycetous hyphae causes increased exposure to mycelium associated and intracellular enzymes enhancing degradation in addition to extracellular biocatalysts (Semple et al., 2007). On the other hand, biosorption may also decrease biotransformation in cases where binding by sorption is very strong and reduces the pollutant availability to cells.

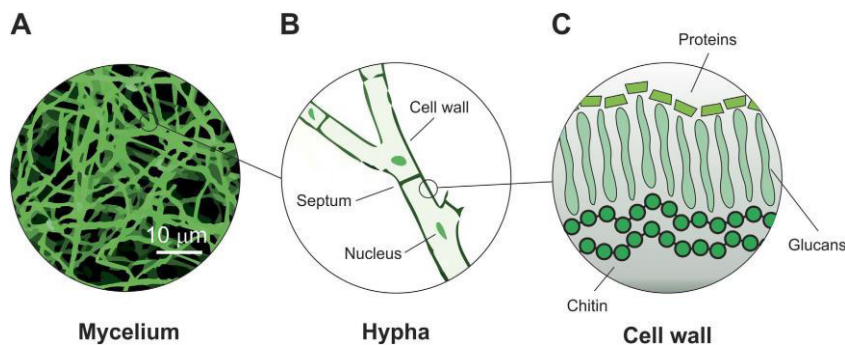


Figure 6 Schematic representation of fungal mycelium physiology at different scales (reproduced from Haneef et al. (2017) under a creative commons license; <https://creativecommons.org/licenses/by/4.0/>). (A) Optical microscopy image of a network of microfilaments. (B) A branched hyphae with cells separated by septa (cross walls). (C) Cell wall composed of layers of chitin on the cell membrane, glucans, and proteins on the outer surface (whose composition varies between species).

1.6. Fungal inhibition and inactivation

Piperonyl butoxide (PB, 5-[2-(2-Butoxyethoxy)ethoxymethyl]-6-propyl-1,3-benzodioxole) is an insecticide synergist. In the context of this study, the toxicity mechanism of cytochrome P450 inhibition is utilized (e.g. (Hodgson and Levi, 1999, Mori and Kondo, 2002, Subramanian and Yadav, 2009)) to elucidate contribution of the intracellular cytochrome P450 system towards fungal micropollutant transformation.

Sodium azide (NaN_3) is a biocide employed to determine biosorption of micropollutants to (inactive) fungal mycelia (Chauret et al., 1995, Hofmann and Schlosser, 2016, Yang et al., 2013a). The biochemical mode of action is based on disruption of the electron transport in the respiratory chain. Specifically, the azide ion irreversibly blocks the binding of oxygen to the active site of cytochrome c oxidase, and thus the regeneration of adenosine triphosphate (ATP). As a consequence the cell dies.

1.7. Project aims

The aims of this study were to **(i)** assess the potential of selected fungal isolates for biocatalytic and biosorptive removal of the micropollutants DBP and BPA, and **(ii)** increase knowledge about occurrence and distribution of phthalate and BPA degraders among and within different ecophysiological groups of fungi. Another major aim was **(iii)** to identify major enzyme classes involved in the biocatalytic removal of the target pollutants through the assessment of micropollutant removal under cytochrome P450 inhibiting conditions and concomitant monitoring of exoenzyme activities. These investigations were aided by **(iv)** the structure elucidation of DBP degradation products via mass spectrometry.

2. Materials and Methods

2.1. Source of chemicals

All chemicals were of analytical grade or gradient grade in the case of chromatography solvents, if not otherwise stated. Bisphenol A (BPA, purity 98.1%) was provided by Dr. Ehrenstorfer GmbH (Augsburg, Germany), and dibutyl phthalate (DBP, purity 99%) and piperonyl butoxide (PB) of technical grade (purity 90%) were purchased from Sigma-Aldrich (Saint Louis, MO, USA; now belonging to Merck Group, Darmstadt, Germany). 2,2'-Azinobis-(3-ethylbenzothiazoline-6-sulfonic acid) (ABTS, purity > 98%) was obtained from BioChemica AppliChem (Darmstadt, Germany). All other chemicals were purchased from Merck, Sigma-Aldrich and Th. Geyer GmbH (Renningen, Germany).

2.2. Information on fungal strains

Fungal strains used in this study belong to the culture collection of the Department of Environmental Microbiology (Helmholtz Centre for Environmental Research – UFZ, Leipzig, Germany).

The taxonomic relationship of fungal strains employed in this study is compiled in Figure 7. Both *Stropharia rugosoannulata* (DSM 11372) and *Trichosporon porosum* (JU-K-2, DSM 27593) are basidiomycetous fungi, belonging to the Agaricomycotina classes Agaricomycetes and Tremellomycetes, respectively. Six ascomycete species of the sub-divisions Leotiomyceta were included. While the strains of *Ascocoryne* (1-DS-2013-S2) and *Acephala* (JU-A-2, DSM 27592) both belong to the largest and most diverse class of *Ascomycota*, the Dothideomycetes, *Clavariopsis aquatica* (WD(A)-00-01) and *Stachybotrys chlorohalonata* (A-2008-2) are part of the sub-class Hypocreomycetidae. The strain *Paradendryphiella arenariae* (1-DS-2013-S4) and a species of *Phoma* (UHH 5-1-03) in contrast belong to Pleosporaceae.

Ecophysiologicaly, the eight fungal isolates represent wood and litter decaying fungi, soil and aquatic/marine fungi. The anamorphic yeast *T. porosum* inhabits soil, and is related to the loubieri/laibachii group of species that assimilate hemicelluloses and phenolic compounds (Middelhoven et al., 2001). *S. rugosoannulata* is a well described white rot litter-decaying fungi, but also known to attack

nematodes (Luo et al., 2006, Schlosser and Hofer, 2002). The saprobic *Phoma* sp. is a mitosporic aquatic isolate from the Saale river, Germany (Junghanns et al., 2008). The taxonomy of *Phoma* is complex, with several hundreds of described species, the majority of which are plant specific. *Ascocoryne* sp. is native to aquatic habitats (e.g. freshwater and marine sediments) and was isolated directly from a sandy beach, covered with washed up algal material (Cowan, 2017, Leinberger, 2017). The isolate *P. arenariae* originates from the same habitat, and was isolated from algae growing on a groyne (Cowan, 2017, Leinberger, 2017). The taxon is typically present on decaying marine or estuarine plants and beach sands. The aquatic hyphomycete *C. aquatica* is a species frequently observed in rivers and streams (Baldy et al., 2002, Junghanns et al., 2005, Krauss et al., 2001, Nikolcheva et al., 2003). *S. chlorohalonata* was isolated from a constructed wetland, and *Acephala* sp. was a peatland isolate (Singh et al., 2014).

All fungal strains were maintained on solid 2% malt extract (w V⁻¹) medium (pH 5.7) and incubated at 20°C.

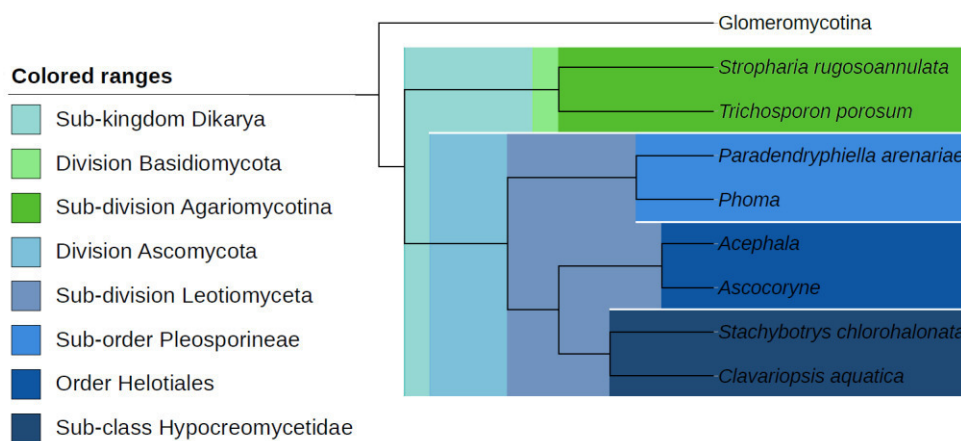


Figure 7 Phylogenetic tree displaying relationship of fungal species used in this study based on NCBI taxonomy data, generated in phyloT (<https://phylot.biobyte.de/>) and visualized with iTOL (<http://itol.embl.de/>). The fungal division Glomeromycota is shown as outgroup.

2.3. Micropollutant Removal Experiments

Pre-cultivation and micropollutant removal experiments were adapted from the method applied by Hofmann and Schlosser (2016). A schematic regarding flask set-up per fungal strain for experiments is outlined in Figure 8.

Fungal pre-cultivation

Axenic pre-cultures cultivated in 100 ml Erlenmeyer flasks containing 30 ml of a 2% (w V⁻¹) malt extract medium (pH 5.7) were established for subsequent batch tests with active and inactivated fungal cultures. Each flask was inoculated with 1 ml of a mycelial suspension added to flasks using manually cut pipette

tips. The inoculum was prepared by adding a defined number of agar cuttings accommodating mycelial growth (\varnothing 1 cm) to an equal number of ml of cultivation medium (i.e. 1 agar cutting ml^{-1}), depending on the total amount of inoculum needed. Homogenization was subsequently achieved using an Ultra-Turrax disperser (8000 min^{-1} , Model T25, IKA, Staufen, Germany) (method adapted from Junghanns et al. (2008)). Thereafter, flasks were incubated on a rotary shaker (New Brunswick™ Innova 44, Eppendorf, Hamburg, Germany) at 20°C and 120 rpm in the absence of light for 7 days (pictures of pre-cultures on day 6; Appendix Figure 1). Inactivation of three growing fungal cultures per strain occurred on day 6 of incubation by adding $150 \mu\text{l}$ of 3.08 M sodium azide (NaN_3 , Merck) resulting in a final concentration of 15.38 mM. The fungal biomass was prepared for transfer to micropollutant removal flasks by centrifugation ($7197 \times g$, 20°C , 10 min; Eppendorf centrifuges 5430R, rotor FA-45-6-30, Eppendorf, Hamburg, Germany) in 50 ml conical tubes. The supernatant was discarded and the biomass pellet washed with 30 ml synthetic mineral salts medium devoid of a source of carbon and energy (pH 6.8; Table 1 (Stanier et al., 1966)) and separated in a second centrifugation step. After discarding the supernatant the biomass pellet was ready for transfer.

Fungal micropollutant removal experiments

Micropollutants, $150 \mu\text{l}$ of a 12.5 mM stock solution in methanol (Carl Roth GmbH & Co. KG, Karlsruhe, Germany), containing 10% (w V^{-1}) Tween 80 (Merck), were added to 100 ml Erlenmeyer flasks containing 30 ml of the aforementioned mineral salt medium to yield a final concentration of $62.5 \mu\text{M}$ (modified from (Jahangiri et al., 2017, Junghanns et al., 2005)). Tween 80 was included in order to improve the aqueous solubility of the micropollutants in the culture. Furthermore, $150 \mu\text{l}$ of methanol containing 10% Tween 80, with or without 0.2 M cytochrome P450 inhibitor PB (resulting in a final concentration of 1 mM) were added to the active flasks. The NaN_3 inactivated flasks received the same addition of $150 \mu\text{l}$ of methanol containing 10% Tween 80 and an additional $150 \mu\text{l}$ 3.08 M NaN_3 (final concentration of 15.38 mM). These inactivated flasks were utilized to determine the contribution of biosorption to total micropollutant removal. Thus the concentrations corresponded to 1% (V V^{-1}) methanol and 0.1% (w V^{-1}) Tween 80 in all flasks.

Screening of BPA removal was performed for the fungal strains *T. porosum*, *S. rugosoannulata* and *S. chlorohalonata*.

Screening of DBP removal was carried out for all the fungal strains. Two variations of the previously described inactivation methods were included. Namely, $150 \mu\text{l}$ 1 M PB (resulting in a final concentration of 5 mM) in methanol containing 10% Tween 80, or $150 \mu\text{l}$ of methanol containing 10% Tween 80 and

150 μl NaN_3 (final concentration of 3.08 M) were added to the active flasks. Further, moist heat sterilization (121°C, 2.4 bar, 20 min) on day 7 before biomass transfer was tested as inactivation method.

Additionally, negative controls (i.e. Erlenmeyer flasks with micropollutant, cytochrome P450 enzyme inhibitor and NaN_3 in mineral salt medium as described before, but without fungal biomass) for both DBP and BPA experiments were included.

All flasks were shaken on a horizontal shaker (GFL, Burgwedel, Germany) at 90 strokes min^{-1} and room temperature for 2 h prior to biomass addition. Micropollutant-containing fungal cultures were incubated on a rotary shaker at 120 rpm and 20°C in the dark for 14 days. Triplicate experiments were always performed.

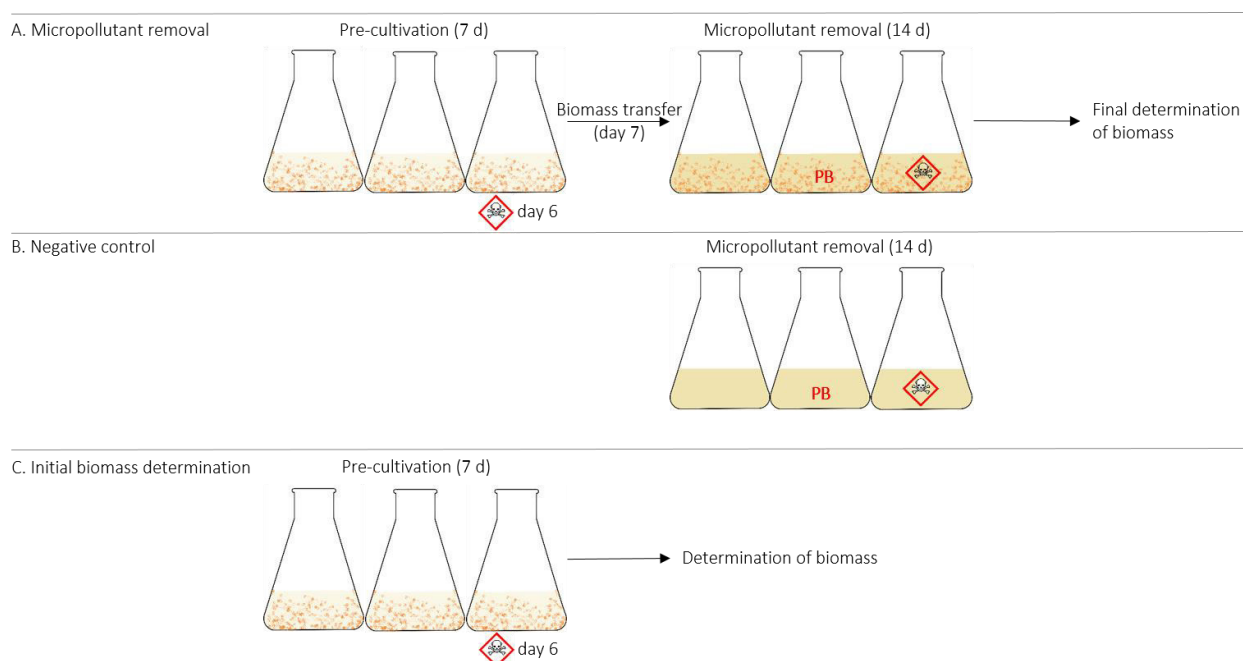


Figure 8 Schematic overview of Erlenmeyer flask set-up used for each fungal strain and micropollutant, where one flask represents a triplicate. The GHS toxicity symbol signifies NaN_3 . A pre-cultivation of fungal biomass in 2% malt extract medium over 7 days (inactivation with NaN_3 on day 6) was followed by biomass transfer to mineral salt medium with micropollutants, cytochrome P450 inhibitor PB and NaN_3 . The fungal cultures were again incubated for 14 days. After finalization of the cultivation period, fungal biomass was determined. Experiment A was always carried out in conjunction with a negative control (B), excluding fungal biomass, and (C) additional Erlenmeyer flasks in pre-cultivation for determination of the initial fungal biomass (i.e. at the moment of biomass transfer to micropollutant removal flasks).

Table 1 Composition of 1 l Stanier's mineral salt medium

Volume	Substance
40 ml	$\text{Na}_2\text{HPO}_4 + \text{KH}_2\text{PO}_4$ buffer (1 M, pH 6.8)
20 ml	Hutner's vitamin-free mineral base (as described by Cohen-Bazire <i>et al.</i> (1957))
1.0 g	$(\text{NH}_4)_2\text{SO}_4$
to 1 l	Deionized water

Sampling procedure

Sampling was carried out prior to biomass addition (0 h) and after 1.5 h, 3.5 h, 1 day, 2 days, 5 days, 9 days and 14 days. For the determination of micropollutant concentrations via UPLC, 500 µl supernatant was removed, mixed with an equal volume of methanol and stored in 1.5 ml Eppendorf tubes. A volume of 200 µl supernatant was taken at each time point for determination of enzyme activity. Sampling was carried out under sterile conditions and all samples were stored at -20°C until analysis.

2.4. Fungal dry mass determination

Fungal biomass was pre-cultivated and inactivated (NaN₃ addition on day 6, or steam heat inactivation on day 7) as for micropollutant removal experiments (Figure 8C). Fungal biomass was harvested on the same day as transfer of biomass to micropollutant removal flasks by sterile filtration over washed, pre-dried and pre-weighed Whatman no. 1 paper filters (GE Healthcare, Freiburg, Germany) employing a vacuum pump. Flasks were rinsed with deionized water to ensure collection of all available biomass. Filters and biomass were dried overnight at 80°C, followed by subsequent weighing (G-semi-microscale R180D, Sartorius, Göttingen, Germany). Biomass was measured in the same way in the removal flasks at the end of the 14-day incubation period.

2.5. Analysis of micropollutants by ultra performance liquid chromatography (UPLC) coupled with diode array detection (DAD)

Samples were prepared for UPLC analysis by thawing and subsequent centrifugation at about 20800 x g, 4°C for 10 min (Eppendorf centrifuge 5430R, rotor type FA-45-30-11, Eppendorf, Hamburg, Germany) to ensure biomass free supernatant. All possible supernatant was transferred to 1.5 ml glass vials. Samples were analyzed by an Aquity™ UPLC system (Waters, Eschborn, Germany) via injection of 3.3 µl aliquots of sample, operating at a column temperature of 40°C (Aquity™ UPLC BEH C18 column; 1.7 µm particle size; 2.1 x 50 mm; Waters). The elution gradients (0.5 ml min⁻¹ flow rate) employed are outlined in Table 2. The mobile phase solvents were A – 10% methanol in deionized water (Q-Gard 2, Millipore, Schwalbach, Germany), B – 100% methanol, both acidified to pH 3.0 with 0.1% (V V⁻¹) formic acid. Compound detection was carried out by an Aquity™ eλ photodiode array detector set to wavelength 278 nm. Representative examples of chromatograms (at 278 nm wavelength) and characteristic micropollutant and PB spectra (from 230 to 390 nm wavelength) are included in Appendix Figures 2 and 3, respectively. Peak integration (ApexTrack Algorithm) for subsequent micropollutant quantification was performed using peak areas (peak height in case of DPB quantification in *S. chlorohalonata*, Appendix

Figure 5). Automatic detection of peak shoulders and application of Gaussian skim (within the UPLC software Empower, Waters) was applied for peak area correction, necessary where target peaks were incompletely separated from other non-target peaks (Appendix Figure 4). Micropollutant concentrations were always measured against external standards (calibration range micropollutants 7.8125 - 125 μM , PB 62.5 - 2000 μM – higher concentrations of PB were not included to reduce retention in the UPLC system).

*Table 2 Ratio of solvents ($V V^{-1}$) served as mobile phase and elution profile applied for **DBP** quantification with UPLC analysis*

Description	Solvent A in %	Solvent B in %	Time period in min
Isocratic	70	30	0 - 0.14
Linear increase of B	65	35	0.14 - 5
Linear increase of B	0.1	99.9	5 - 5.5
Isocratic	0.1	99.9	5.5 - 8
Linear increase of A	70	30	8 - 8.2
Isocratic	70	30	8.2 - 8.5

*Table 3 Ratio of solvents ($V V^{-1}$) served as mobile phase and elution profile applied for **BPA** quantification with UPLC analysis*

Description	Solvent A in %	Solvent B in %	Time period in min
Isocratic	80	20	0 - 0.14
Linear increase of B	0.1	99.9	0.14 - 2.8
Isocratic	0.1	99.9	2.8 - 3.2
Linear increase of A	80	20	3.2 - 3.25
Isocratic	80	20	3.25 - 3.5

2.6. Calculation of micropollutant removal rates

Respective micropollutant removal rates were determined from the UPLC results for each fungal strain. Data of pollutant concentrations versus time was fitted using non-linear regression (Equation 2) in OriginPro software (2018 95G b9.5.1.195, OriginLab Corporation, Northampton, MA, USA) assuming pseudo first order kinetics following equation 1.

$$v_t = c_t \cdot k' \quad \text{Equation 1}$$

where the removal rate v_t ($\mu\text{M h}^{-1}$) at a given time point t in is directly proportional to the micropollutant concentration c_t (μM) at time point t and k' (h^{-1}) represents the apparent first-order decay constant. Replicate data was fitted by internally combining all data into one concatenated dataset (i.e. triplicates were fitted simultaneously resulting in one regression function).

$$C_t = C_a + C_s \cdot e^{-k' \cdot t}$$

Equation 2

in the exponential fit function c_a (μM) represents a bottom asymptote micropollutant concentration approached at infinite time where micropollutant removal was incomplete, c_s corresponds to the removal rate-governing micropollutant concentration at $t = 0$ (μM) (with the sum of c_a and c_s yielding the initial micropollutant concentration), and t is the time of incubation in presence of micropollutant (h). Where micropollutant removal was complete within the duration of the experiment, c_a was set to $0 \mu\text{M}$.

The initial (maximal) removal rates at $t = 0$ were obtained by multiplying the respective c_s and k' values. By normalization the initial removal rates using the initial biomass (g) values of active or inactive fungal cultures, the specific initial rate values ($\mu\text{M h}^{-1} \text{g}^{-1}$) were achieved. Not for all data a good exponential regression fit was obtained (coefficient of determination (R^2) value < 0.9), or initial removal rates were artificially high due to a steep curve cut by a bottom asymptote. Therefore, additional removal rates based on reduction of micropollutant concentration over selected time periods, normalized by the initial biomass, were calculated according to equation 3.

$$(c_{t_0} - c_t) / (t_0 - t_{ct}) / \text{biomass}$$

Equation 3

where c_{t_0} (μM) corresponds to the micropollutant concentration at t_0 ($t = 0$), and c_t to the micropollutant concentration at t_{ct} (3.5 h, 24 h, 48 h or 336 h). The latter removal rates were calculated per replicate and reported as mean and standard deviation of triplicates (where not indicated otherwise). A positive difference between the specific (initial) removal rates of active or PB inhibited and inactive fungal cultures indicates the contribution of enzymatic transformation to the micropollutant removal. These specific (initial) rates of biological removal will be referred to as active and PB (inhibited) biotransformation further on.

2.7. Photometrical determination of laccase and peroxidase activity

Samples from the DBP and BPA removal experiments with fungal cultures of *T. porosum*, *S. rugosoannulata* and *S. chlorohalonata* and representative samples from the negative controls were prepared for exoenzyme activity assays by thawing and subsequent centrifugation at 20817 x g, 4°C for 10 min (Eppendorf centrifuge 5430R, rotor type FA-45-30-11, Eppendorf, Hamburg, Germany) to ensure biomass free supernatant. Laccase activity was determined following the oxidation of 2 mM ABTS to the blue ABTS^{•+} radical in 0.1 M citrate phosphate buffer (pH 4.0) (Johannes and Majcherczyk, 2000, McIlvaine, 1921). Mn-dependent and Mn-independent peroxidase type activities were determined in four reactions (Table 4) by oxidation of 2 mM ABTS in Na-Malonate buffer (pH 4.5) in presence and absence of H₂O₂ and Mn²⁺ (Liers et al., 2011).

Table 4 Reaction mix ingredients and volumes for determination of total peroxidase activity (reaction D - C), Mn-independent peroxidase (reaction B - A) and Mn-dependent peroxidase activity (total peroxidase - Mn-independent peroxidase activity)

Reaction mix	Mn-dependent peroxidase			
	Mn-independent peroxidase		All peroxidases	
	A. Laccase	B. Laccase and Mn-independent peroxidase	C. Laccase	D. Laccase and All peroxidases
Sample	20	20	20	20
ABTS – 2 mM	20	20	20	20
H ₂ O ₂ – 100 µM	-	20	-	20
MnCl ₂ – 200 µM	-	-	20	20
Na-EDTA – 1 mM	20	20	-	-
Aqua dest.	40	20	40	20
Na-Malonate buffer – 50 mM	100	100	100	100
Total reaction	200	200	200	200

Assays were carried out on 96-well plates and absorbance at 420 nm was measured over 6 min in a GENiosPlus microplate reader (Tecan, Männedorf, Switzerland) (a picture is given as example in Appendix Figure 6). ABTS and H₂O₂ were only added immediately before the start of the run. From the maximum slope of the resulting curves ΔE (change in absorption per minute), the respective exoenzyme activity A_V (in U l⁻¹, where 1 U is the international unit defined as the amount of exoenzyme capable of oxidizing 1 µmol ABTS min⁻¹) was calculated using equation 4.

$$A_V = \Delta E / \epsilon_{420} \cdot V_G / V_P \cdot 1 / D \quad \text{Equation 4}$$

where ϵ_{420} is the extinction coefficient for ABTS at 420 nm (36 mM⁻¹ cm⁻¹), V_G is total reaction volume (200 µl), V_P sample volume (20 µl), and D is optical thickness (0.5925 cm). All absorbances were corrected against a blank well of equal volume (sample component substituted by respective buffer).

2.8. Formation of DBP biotransformation products

In a follow-up experiment, formation of DBP biotransformation products was studied. If not described differently, the same pre-cultivation and micropollutant removal method and sampling procedure was applied as for the micropollutant removal experiments. From a 25 mM DBP stock solution in methanol, 300 μl was transferred to 100 ml Erlenmeyer flasks containing 30 ml mineral salts medium, to yield a final concentration of 250 μM . Tween 80 was omitted in the stock solutions. After addition of methanol, PB and methanol and NaN_3 the final methanol concentration was the same in all flasks (1.5% (V V^{-1})). Sampling of DBP removal flasks was carried out prior to biomass addition (0 h) and at further time points of 3.5 h, 2 days, 5 days and 9 days. Fungal biomass was not determined and no enzyme activity samples were taken.

2.9. UPLC-quadrupole time-of-flight mass spectrometry (UPLC-QTOF-MS) analyses of DBP biotransformation products

The method for DBP metabolite analysis was adapted from Jahangiri et al. (2017). Analysis was performed with high mass resolution mass spectrometry using a Waters AcquityTM UPLC system connected to a XEVO XS QTOF-mass spectrometer equipped with an electrospray ionization source (Waters, Eschborn, Germany). Separation of analytes was achieved using an Acquity HSS-T3-column (100 x 2.1 mm, particle size 1.7 μm , Waters), at a column temperature set to 45°C. Eluent A consisted of deionized water (Q-Gard 2, Millipore, Schwalbach, Germany) and eluent B of methanol, both acidified with 0.1% formic acid. The elution gradient is outlined in Table 5. A flow rate of 450 $\mu\text{L min}^{-1}$ was applied, and 10 μL of each sample were injected for analysis. Ionization source conditions were as followed: the capillary voltage was set to 0.7 kV and operated at 140°C. The sampling cone voltage was set to 20 V, source offset at 50 V. Nitrogen and argon were used as cone and collision gases. The desolvation temperature was 550 °C and the gas flow 950 L h^{-1} . To ensure accuracy during MS analysis, leucine enkephalin was infused via the reference probe as the lockspray. The samples were ordered for the measurement so that first one replicate for all sampling times, then the second replicate was measured (the third replicate was not measured). A caffeine standard was used after every tenth sample and used to normalize the target peak areas to reduce the tailing. MS data were collected from m/z 50 to m/z 1200 in negative and positive centroid mode with a 0.15 s scan time. Two sets of data were collected in parallel using MS^E acquisition. One dataset contained low-collision energy data (4 eV, MS; effectively the accurate mass of precursors) and the second dataset elevated-collision-energy data (15-35 eV, MS^E ; fragmentation mode). High resolution data were processed with MassLynx 4.1 software (Waters). A mass resolution of 20000

was applied with a mass precision of approximately 5 ppm. The identification was done by non-target screening for transformation products by using multivariate statistics by MarkerLynx and the peak areas were integrated by TargetLynx. The tentative chemical structures of DBP metabolites were not confirmed experimentally but were proposed upon detected masses, interpretation of fragmentation (i.e. favorable interactions of fragments).

Table 5 Ratio of solvents served as mobile phase and elution profile applied for DBP metabolite separation with UPLC analysis, prior to electrospray ionization and QTOF-MS

Description	Solvent A in %	Solvent B in %	Time period in min
Isocratic	98	2	0 - 0.25
Linear increase of B	1	99.9	0.25 - 12.25
Isocratic	1	99.9	12.25 - 15
Linear increase of A	2	98	15 - 15.1
Isocratic	2	98	15.1 - 17

2.10. Statistical treatment of data

Independent two-sample student's t-tests (two-sided, for equal or unequal variances, dependent on the outcome of the preceding F-test) were performed in Excel 2013 (Microsoft Corporation) to compare biomass of fungal strains employed in the BPA and DBP experiments ($\alpha = 0.05$).

Where data is presented as means \pm standard errors from triplicate cultures, Doerffel's propagation of uncertainty (Doerffel, 1966) was used to calculate the associated errors. Dependent on the nature of calculation, the appropriate form of equation 5 was chosen (where σ_x is the associated standard deviation of value x etc.).

$$\begin{aligned} \text{for } z = x + y \text{ and } z = x - y, & \quad \sigma_z^2 = \sigma_x^2 + \sigma_y^2 \\ \text{for } z = x \cdot y \text{ and } z = x / y, & \quad (\sigma_z / z)^2 = (\sigma_x / x)^2 + (\sigma_y / y)^2 \end{aligned} \quad \text{Equation 5}$$

3. Results

3.1. Fungal biomass

Previous studies on fungal growth behavior suggested a pre-cultivation duration for 7 days, as the stationary phase of growth was reached at similar times for all fungal strains employed (Hofmann and Schlosser, 2016, Cowan, 2017, Leinberger, 2017). Nevertheless, fungal biomass varied with species, and initial fungal dry biomass values are presented in Table 6. Statistical tests comparing fungal biomass in dibutyl phthalate (DBP) and bisphenol A (BPA) experiments revealed significant differences for *T. porosum* and *S. chlorohalonata* (though for the later the variances were statistically equal). For *S. rugosoannulata* the biomass did not differ between the experiments. Results of final fungal dry biomass are presented in Appendix Table 1, however some biomass was lost each sampling time for UPLC analysis and exoenzyme assays. Increases of biomass during the removal experiment was only observed in some cultures of *S. rugosoannulata*, and species of the genera *Phoma* and *Acephala*, but were not statistically significant. Significant reductions in biomass were affecting most fungal cultures (see Appendix Table 1).

		Initial fungal dry biomass weight [g]							
		<i>T. porosum</i>	<i>S. rugosoannulata</i>	<i>S. chlorohalonata</i>	<i>Phoma</i> sp.	<i>Ascocoryne</i> sp.	<i>P. arenariae</i>	<i>C. aquatica</i>	<i>Acephala</i> sp.
Active	DBP	0.249 ± 0.011	0.104 ± 0.007	0.217 ± 0.017	0.337 ± 0.038	0.069 ± 0.008	0.262 ± 0.020	0.081 ± 0.004	0.264 ± 0.007
	BPA	0.087 ± 0.004	0.041 ± 0.003	0.183 ± 0.040	-	-	-	-	-
NaN ₃ inactivated	DBP	0.203 ± 0.058	0.068 ± 0.020	0.199 ± 0.008	0.335 ± 0.026	0.037 ± 0.001	0.183 ± 0.004	0.047 ± 0.009	0.240 ± 0.007
	BPA	0.078 ± 0.005	0.069 ± 0.012	0.141 ± 0.004	-	-	-	-	-
Heat inactivated	DBP	-	0.059 ± 0.009	0.156 ± 0.028	-	-	-	0.054 ± 0.004	0.223 ± 0.004

Table 6 Fungal dry biomass values (g) after 7 days of pre-cultivation and, where applicable, inactivation by NaN₃ or moist heat. Biomass was determined in triplicates for each strain and experiment. Values of alternative inhibition method are presented in italic letters

3.2. Comparison of alternative inhibition and inactivation methods of fungal biomass

As different inactivation methods are described in literature, alternatives were tested to choose from. Inactivation with sodium azide (NaN_3) only in micropollutant removal flasks differed in effectiveness with regard to fungal strains (comparison of removal rates implied by exponential regression fitting were excluded due to the poor fits, Appendix Figure 10, Tables 2 to 9). In cultures of *T. porosum*, *Phoma* sp., *S. rugosoannulata* and *C. aquatica* DBP removal was more strongly inhibited in double NaN_3 inactivated cultures. However, the difference in inhibition was only significant (student's t-test) for *C. aquatica*. By contrast, in cultures of *P. arenariae*, *S. chlorohalonata*, *Ascocoryne* sp. and *Acephala* sp., inhibition only in micropollutant removal flasks was as effective – in the range of standard deviation – as NaN_3 inactivation on two subsequent days.

Moist heat inactivation (not performed for *T. porosum* and *Phoma* sp.) had stronger – significantly stronger cultures of *Ascocoryne* sp. – to similarly strong inhibitory effect on DBP removal as double NaN_3 inactivation in most fungal cultures (Appendix Figure 10, Tables 2 to 9). Exceptions were weaker inhibition by heat inactivation in cultures of *C. aquatica* and partly *S. rugosoannulata*. However, moist heat inactivation affected fungal biomass optically, and an alteration of the biomass surface and thus sorption of pollutants can not be excluded. For this reason, and because of the trend of stronger inhibition of DBP removal by double NaN_3 inactivation, the NaN_3 inactivation on two subsequent days was chosen as the method of choice (from now on referred to as NaN_3 inactivation).

The biotransformation rates of 5 mM piperonyl butoxide (PB) inhibited strains did not differ from biotransformation rates of 1 mM PB inhibited strains, thus indicating the same trends of cytochrome P450 contribution to degradation. However, when 5 mM PB was added from the stock solution, precipitation was observed (since the concentration was above the aqueous solubility of 14.3 mg l⁻¹ at 25°C (Tomlin, 2009)). Thus, the initial PB concentration was lower than the nominal 5 mM (Appendix Figure 11), but re-dissolving in equilibrium with sorption and transformation of PB is likely. Because of this uncertainty, cytochrome P450 enzyme inhibition with 1 mM was chosen as the standard methods of choice (in the following referred to as PB inhibited).

3.3. Micropollutant removal by fungal cultures

DBP and BPA were removed to varying degrees from the fungal culture supernatants by different fungal strains (Figures 9 to 11). The PB concentration decreased over time in all fungal cultures (except *T. porosum* in the BPA experiment) to varying degree (Appendix Figures 11 and 12). However, only in cultures of *S. rugosoannulata* a complete disappearance was observed. In the fungal biomass free negative controls, the micropollutant and PB concentrations remained constant over the duration of the experiment, and no exoenzyme activity was detected (Figures 10 and 11, Appendix Figures 11 and 12).

DBP removal

In active fungal cultures, the DBP concentration had decreased from $53 \pm 8 \mu\text{M}$ (0 h) to values between about $31 \mu\text{M}$ and below the quantification limit after 3.5 h of incubation, corresponding to relative removals (i.e. relative to the actually quantified initial concentration) of approximately 36 to 100% (Figures 9 and 10). With exception of *S. chlorohalonata* (approximately 44% of initially quantified concentration remaining) DBP was completely removed by all active fungal cultures at the latest after 14 days. In the PB inhibited cultures, i.e. micropollutant removal not by cytochrome P450, the DBP concentrations were reduced from $59 \pm 8 \mu\text{M}$ (0 h) to between 51 and $9 \mu\text{M}$, corresponding to a relative reduction of 21 to 81% after 3.5 h. Similarly, the initially quantified DBP concentration was reduced between 22 to 94% in NaN_3 inactivated fungal cultures after 3.5 h of incubation, suggesting that the reduction of pollutant concentration occurred mainly due to biosorption. Comparison of DBP concentrations for active or PB inhibited and NaN_3 inactivated fungal cultures revealed differences in contribution of biotransformation to the total removal (biosorption and biotransformation) dependent on the fungal strain (Tables 7, 9, 11, and 13 to 17). In the case of *Acephala* sp., complete disappearance of DBP after 2 days of incubation in NaN_3 inactivated cultures indicated pollutant removal dominated by sorption onto the fungal biomass (Figure 10). For all other NaN_3 inactivated cultures, the concentrations tended to level off over the duration of the experiment, possibly because sorption equilibria were reached. Only about 12% of the initially measured DBP concentration had finally been removed by NaN_3 inactivated *S. rugosoannulata* cultures, suggesting that for this fungal isolate biosorption was negligible.

Extracellular laccase activities, which were concomitantly monitored with pollutant concentrations in supernatants of *S. rugosoannulata* increased continuously in active and PB inhibited, but not NaN_3 inactivated cultures (Appendix Table 10). At the end of the incubation, values of $103 \pm 19 \text{ U l}^{-1}$ and $23 \pm 10 \text{ U l}^{-1}$ respectively for active and PB inhibited *S. rugosoannulata* cultures were recorded (Figure 9). By contrast, laccase activities in cultures of *S. chlorohalonata* and *T. porosum*, and Mn-dependent and

independent peroxidase in all three fungal cultures did not increase and remained far below relevant levels for contribution to enzymatic degradation (i.e. $< 5 \text{ U l}^{-1}$) (Appendix Table 10).

BPA removal

Compared to DBP, removal of BPA was initially slower with reduction from $47 \pm 6 \mu\text{M}$ (0 h) to about 42, 24 and $23 \mu\text{M}$ respectively in active cultures of *T. porosum*, *S. rugosoannulata* and *S. chlorohalonata* after 3.5 h of incubation, corresponding to relative removal of approximately 1, 49 and 53% (Figure 11). Complete degradation was achieved after 24 h in active cultures of *S. rugosoannulata*. In active cultures of *T. porosum* and *S. chlorohalonata*, respectively 1 and 58% of the initially quantified BPA concentration were removed by the end of the cultivation. In PB inhibited cultures of *S. rugosoannulata* the BPA concentration decreased 31% from $52 \mu\text{M}$ (0 h) to $36 \mu\text{M}$ after 3.5 h. As in the active cultures, BPA was completely removed after 24 h. The removal of BPA in cultures of *S. chlorohalonata* with PB inhibited cytochrome P450 system was initially faster, after 3.5 h a concentration of about $30 \mu\text{M}$ was measured, corresponding to a decrease of 45% from initially $53 \pm 2 \mu\text{M}$. However, only 50% of the initial concentration was removed at the end of the experiment. In NaN_3 inactivated fungal cultures, 19 and 49% of the initial BPA concentration had been removed by biosorption after 3.5 h of incubation respectively for *S. rugosoannulata* and *S. chlorohalonata*, and a level off was observed with respectively 64 and 51% of the initial concentration remaining after the end of cultivation. In comparison, for the PB inhibited and inactivated *T. porosum* cultures the BPA concentration did not decrease over time. The sample taken after 3.5 h of incubation of PB inhibited cultures was lost, but interpolation from the preceding and following sampling time indicates a reduction in concentration in the range of 1 to $3 \mu\text{M}$, and a measured increase of 4% of the initial concentration of $51 \mu\text{M}$ at the end of the incubation period. In the inactivated *T. porosum* cultures a measured increase of $2 \mu\text{M}$ after 3.5 h from initially $46 \mu\text{M}$, and a decrease of $2 \mu\text{M}$ over the whole duration of the experiment was observed.

As in the DBP removal experiment, extracellular enzyme activity was only measurable for laccase in active and PB inhibited cultures of *S. rugosoannulata* (Figure 11). A continuous increase to a final laccase activity of $51 \pm 36 \text{ U l}^{-1}$ and $67 \pm 87 \text{ U l}^{-1}$ respectively for active and PB inhibited cultures was recorded (Appendix Table 11).

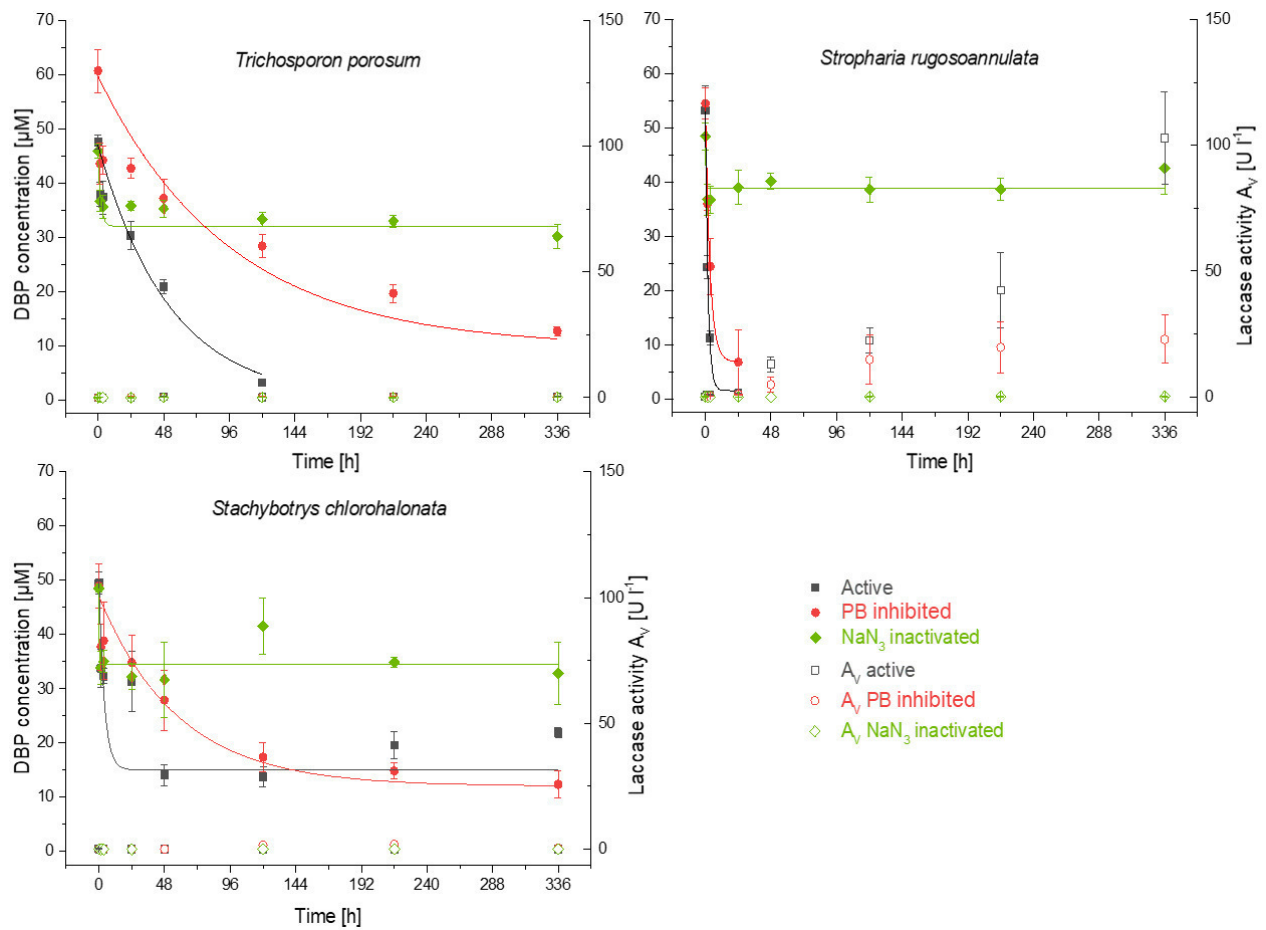


Figure 9 Time course of DBP concentrations (filled symbols) and laccase activity (open symbols) for active (black squares), PB inhibited (red circles) and NaN₃ inactivated cultures (green diamonds) for *T. porosum*, *S. rugosoannulata* and *S. chlorohalonata*. The corresponding solid lines arise from data fitting of measured micropollutant concentration by exponential regression. Symbols represent means \pm standard deviations from triplicate cultures.

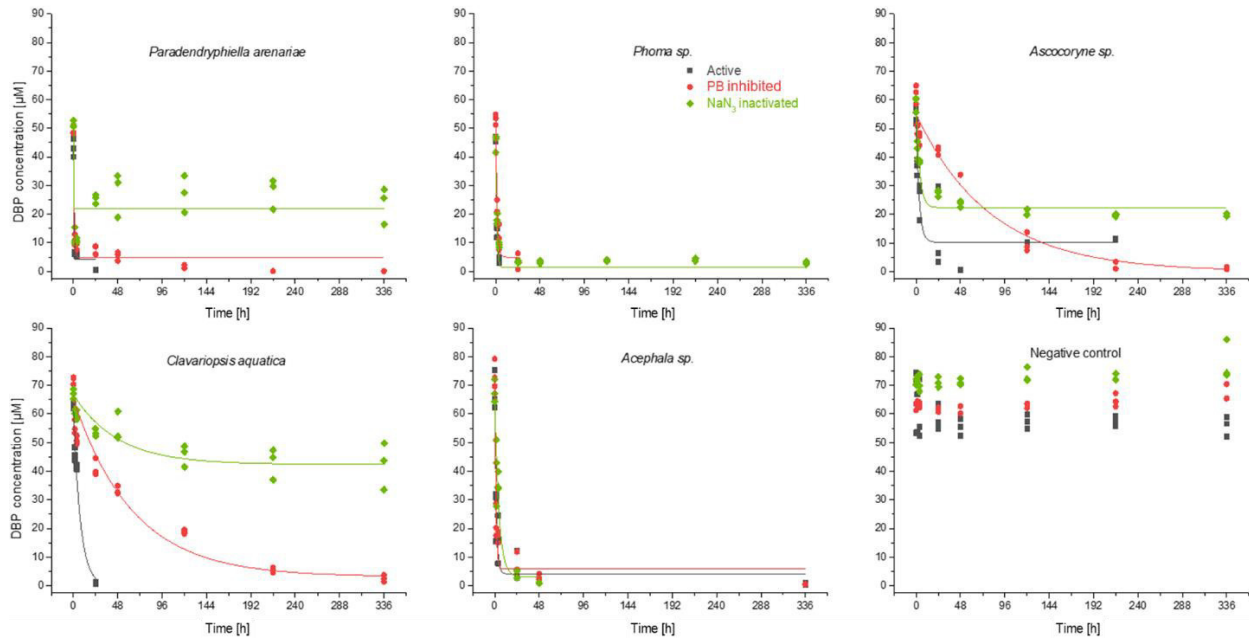


Figure 10 Time course of **DBP** concentrations for active (black squares), PB inhibited (red circles) and NaN₃ inactivated cultures (green diamonds) for other fungal strains and negative control. The corresponding solid lines arise from data fitting of measured micropollutant concentration by exponential regression.

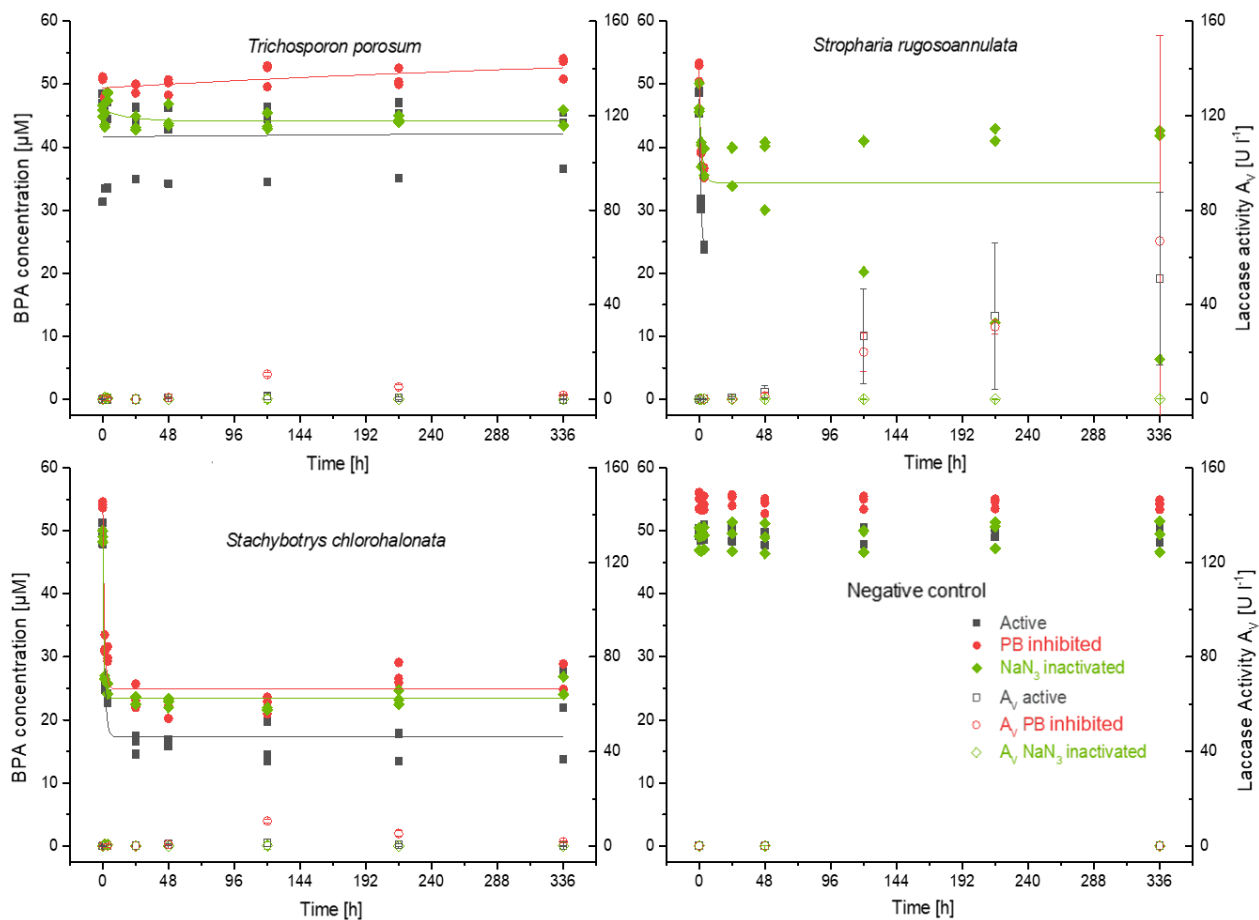


Figure 11 Time course of **BPA** concentrations (filled symbols) and laccase activity (open symbols) for active (black squares), PB inhibited (red circles) and NaN_3 inactivated cultures (green diamonds) for *T. porosum*, *S. rugosoannulata* and *S. chlorohalonata*. The corresponding solid lines arise from data fitting of measured micropollutant concentration by exponential regression.

In the following sections, results will be presented in more detail with regard to each fungal strain.

T. porosum

In both active and cytochrome P450 inhibited cultures the DBP biotransformation rates were low (Table 7). Absolute removal indicated better (i.e. complete) degradation of DBP with cytochrome P450. After 48 h of incubation an inhibition of approximately 20% in PB inactivated cultures was witnessed, however the standard deviation was high in relation to the low removal rates. Sorption to biomass rapidly attained its equilibrium, and dominated removal within the first hours of incubation. As previously mentioned, removal of BPA was negligible (Figure 11, Table 8).

Table 7 Initial and specific (initial) removal rates of DBP observed with active, PB inhibited and NaN₃ inactivated cultures of *T. porosum*. Further, the absolute DBP removal as recorded by the end of cultivation is shown

Removal rate ¹	<i>T. porosum</i>				
	Active	PB inhibited	NaN ₃ inactivated	Biotransformation ²	
				Active	PB
Initial rate (μM h ⁻¹)	0.70 ± 0.08	[§] 0.52 ± 0.09	[§] 9.94 ± 2.31		
Specific Initial rate (μM h ⁻¹ g ⁻¹)	2.82 ± 0.34	[§] 2.08 ± 0.37	[§] 48.93 ± 18.03	n.a.	
Specific 3.5 h rate (μM h ⁻¹ g ⁻¹)	11.67 ± 0.42	18.83 ± 0.11	14.41 ± 0.02	0	4.43
Specific 24 h rate (μM h ⁻¹ g ⁻¹)	2.88 ± 0.77	3.00 ± 0.86	2.08 ± 0.15	0.79	0.91
Specific 48 h rate (μM h ⁻¹ g ⁻¹)	2.23 ± 0.25	1.96 ± 0.33	1.09 ± 0.19	1.14	0.87
Specific overall rate (μM h ⁻¹ g ⁻¹)	0.57 ± 0.99	0.57 ± 2.54	0.23 ± 1.56	0.34	0.34
Absolute removal (μM)	47.53 (100%)	47.95 (79%)	15.74 (34%)		

¹ Initial and specific initial removal rates obtained by exponential regression fit, and manually calculated specific removal rates for different time points, and the whole cultivation period. ² Calculated as the difference between the rates of active or PB inhibited and NaN₃ inactivated cultures. [§] indicates non-linear regression fitting with a R² < 0.9 and therefore not considered as accurate (n.a.) and not used for calculation of biotransformation.

Table 8 Initial and specific (initial) removal rates of BPA observed with active, PB inhibited and NaN₃ inactivated cultures of *T. porosum*. Further, the absolute DBP removal as recorded by the end of cultivation is shown

Removal rate ¹	<i>T. porosum</i>				
	Active	PB inhibited	NaN ₃ inactivated	Biotransformation ²	
				Active	PB
Initial rate (μM h ⁻¹)	[§] -0.00 ± 0.33	[§] -0.01 ± 0.05	[§] 0.11 ± 0.18		
Specific Initial rate (μM h ⁻¹ g ⁻¹)	[§] -0.02 ± 3.87	[§] -0.15 ± 0.62	[§] 1.38 ± 2.25	n.a.	
Specific 3.5 h rate (μM h ⁻¹ g ⁻¹)	1.86 ± 55.75	-	-8.93 ± 0.26	0	-
Specific 24 h rate (μM h ⁻¹ g ⁻¹)	0.25 ± 636.81	0.69 ± 15.26	1.16 ± 3.57	0	0
Specific 48 h rate (μM h ⁻¹ g ⁻¹)	0.29 ± 251.04	0.29 ± 71.34	0.29 ± 64.64	0	0
Specific overall rate (μM h ⁻¹ g ⁻¹)	0.01 ± 40031.89	-0.06 ± 304.19	0.06 ± 162.19	0	0
Absolute removal (μM)	0.29 (1%)	-1.88 (-4%)	1.53 (3%)		

¹ Initial and specific initial removal rates obtained by exponential regression fit, and manually calculated specific removal rates for different time points, and the whole cultivation period. ² Calculated as the difference between the rates of active or PB inhibited and NaN₃ inactivated cultures. [§] indicates non-linear regression fitting with a R² < 0.9 and therefore not considered as accurate (n.a.) and not used for calculation of biotransformation.

S. rugosoannulata

Removal of both micropollutants was complete in active and cytochrome P450 inhibited cultures of *S. rugosoannulata* after 24 and 3.5 h, for DBP and BPA, respectively (Figure 9 and 11). A sorption equilibrium was reached within the first hours of incubation for both compounds, restricting the biosorption to 12 and 36% for DBP and BPA, respectively. The variance of BPA concentration in NaN_3 inhibited cultures increased over time, possibly due to incomplete inactivation of one replicate (as the other two had small variance and revealed a clear bottom asymptote). Regardless, the importance of biotransformation was obvious for removal of both organopollutants. However, the inhibitory effect of PB on cytochrome P450 was likely limited due to removal of the same (Appendix Figures 11 and 12). Nevertheless, comparison of biotransformation rates indicated relevant contribution of cytochrome P450 enzymes of initially 55 and 40% for DBP and BPA, respectively (Table 9 and 10).

After 24 and 3.5 h of incubation, the spectra measured at typical retention times for DBP and BPA changed and did not anymore resemble characteristic absorption maxima of DBP and BPA, indicating biotransformation. The peak area of that non-target compound increased slowly until the end of the incubation.

Table 9 Initial and specific (initial) removal rates of DBP observed with active, PB inhibited and NaN₃ inactivated cultures of *S. rugosoannulata*. Further, the absolute DBP removal as recorded by the end of cultivation is shown

Removal rate ¹	<i>S. rugosoannulata</i>					
	Active	PB inhibited	NaN ₃ inactivated	Biotransformation ²		
				Active	PB	
Initial rate (μM h ⁻¹)	26.41 ± 2.67	14.85 ± 2.15	§17339.30 ± 3505.25			
Specific Initial rate (μM h ⁻¹ g ⁻¹)	253.68 ± 30.53	142.65 ± 22.61	§292992.64 ± 74331.03			n.a.
Specific 3.5 h rate (μM h ⁻¹ g ⁻¹)	115.11 ± 0.01	82.41 ± 0.01	56.53 ± 0.00	58.58	25.88	
Specific 24 h rate (μM h ⁻¹ g ⁻¹)	20.88 ± 0.06	19.08 ± 0.12	6.63 ± 0.06	14.25	12.45	
Specific 48 h rate (μM h ⁻¹ g ⁻¹)	10.65 ± 0.12	10.90 ± 0.07	2.92 ± 0.27	7.73	7.98	
Specific overall rate (μM h ⁻¹ g ⁻¹)	1.52 ± 0.87	1.56 ± 0.52	0.30 ± 8.58	1.23	1.26	
Absolute removal (μM)	53.24 (100%)	54.48 (100%)	5.87 (12%)			

¹Initial and specific initial removal rates obtained by exponential regression fit, and manually calculated specific removal rates for different time points, and the whole cultivation period. ²Calculated as the difference between the rates of active or PB inhibited and NaN₃ inactivated cultures. § indicates non-linear regression fitting with a R² < 0.9 and therefore not considered as accurate (n.a.) and not used for calculation of biotransformation.

Table 10 Initial and specific (initial) removal rates of BPA observed with active, PB inhibited and NaN₃ inactivated cultures of *S. rugosoannulata*. Further, the absolute DBP removal as recorded by the end of cultivation is shown

Removal rate ¹	<i>S. rugosoannulata</i>					
	Active	PB inhibited	NaN ₃ inactivated	Biotransformation ²		
				Active	PB	
Initial rate (μM h ⁻¹)	17.80 ± 3.20	16.94 ± 3.20	§5.71 ± 7.06			
Specific Initial rate (μM h ⁻¹ g ⁻¹)	437.60 ± 86.49	416.43 ± 89.94	§83.29 ± 103.51			n.a.
Specific 3.5 h rate (μM h ⁻¹ g ⁻¹)	164.86 ± 0.01	113.01 ± 0.00	37.22 ± 0.04	127.64	75.79	
Specific 24 h rate (μM h ⁻¹ g ⁻¹)	48.75 ± 0.01	53.51 ± 0.01	5.72 ± 0.31	43.03	47.79	
Specific 48 h rate (μM h ⁻¹ g ⁻¹)	24.38 ± 0.02	26.76 ± 0.01	3.13 ± 0.89	21.24	33.63	
Specific overall rate (μM h ⁻¹ g ⁻¹)	3.48 ± 0.15	3.82 ± 0.10	0.74 ± 9.05	2.74	3.08	
Absolute removal (μM)	47.59 (100%)	52.24 (100%)	17.02 (36%)			

¹Initial and specific initial removal rates obtained by exponential regression fit, and manually calculated specific removal rates for different time points, and the whole cultivation period. ²Calculated as the difference between the rates of active or PB inhibited and NaN₃ inactivated cultures. § indicates non-linear regression fitting with a R² < 0.9 and therefore not considered as accurate (n.a.) and not used for calculation of biotransformation.

S. chlorohalonata

In comparison with all the other fungal strains, cultures of *S. chlorohalonata* exhibited the least removal of micropollutants (ignoring BPA removal by *T. porosum*), with 56 and 58% of the initial concentration being removed by the end of the experiment for DBP and BPA, respectively (Table 11 and 12). After 48 h some biotransformation occurred which was completely catalyzed by cytochrome P450. However, biosorption was the primary removal process observed over the complete time course, even more so for BPA than DBP.

Table 11 Initial and specific (initial) removal rates of **DBP** observed with active, PB inhibited and NaN_3 inactivated cultures of *S. chlorohalonata*. Further, the absolute DBP removal as recorded by the end of cultivation is shown

Removal rate ¹	<i>S. chlorohalonata</i>							
	Active		PB inhibited		NaN_3 inactivated		Biotransformation ²	
							Active	PB
Initial rate ($\mu\text{M h}^{-1}$)	§10.85	± 2.54	§0.84	± 0.16	§6649.66	± 2265.64		
Specific Initial rate ($\mu\text{M h}^{-1} \text{g}^{-1}$)	§50.09	± 12.34	§3.88	± 0.81	§42745.20	± 16486.83	n.a.	
Specific 3.5 h rate ($\mu\text{M h}^{-1} \text{g}^{-1}$)	22.67	± 0.02	13.30	± 0.31	24.71	± 0.02	0	0
Specific 24 h rate ($\mu\text{M h}^{-1} \text{g}^{-1}$)	3.50	± 0.74	2.71	± 0.38	4.35	± 0.14	0	0
Specific 48 h rate ($\mu\text{M h}^{-1} \text{g}^{-1}$)	3.41	± 0.08	2.03	± 0.84	2.26	± 0.90	1.15	0
Specific overall rate ($\mu\text{M h}^{-1} \text{g}^{-1}$)	0.38	± 1.40	0.50	± 1.21	0.30	± 5.92	0.08	0.20
Absolute removal (μM)	27.61 (56%)		36.54 (75%)		15.64 (32%)			

¹ Initial and specific initial removal rates obtained by exponential regression fit, and manually calculated specific removal rates for different time points, and the whole cultivation period. ² Calculated as the difference between the rates of active or PB inhibited and NaN_3 inactivated cultures. § indicates non-linear regression fitting with a $R^2 < 0.9$ and therefore not considered as accurate (n.a.) and not used for calculation of biotransformation.

Table 12 Initial and specific (initial) removal rates of **BPA** observed with active, PB inhibited and NaN_3 inactivated cultures of *S. chlorohalonata*. Further, the absolute DBP removal as recorded by the end of cultivation is shown

Removal rate ¹	<i>S. chlorohalonata</i>							
	Active		PB inhibited		NaN_3 inactivated		Biotransformation ²	
							Active	PB
Initial rate ($\mu\text{M h}^{-1}$)	23.91	± 4.74	23.40	± 4.17	34.40	± 4.35		
Specific Initial rate ($\mu\text{M h}^{-1} \text{g}^{-1}$)	130.57	± 38.48	127.79	± 36.00	243.20	± 31.45	0	0
Specific 3.5 h rate ($\mu\text{M h}^{-1} \text{g}^{-1}$)	41.28	± 0.00	37.77	± 0.00	48.90	± 0.02	0	0
Specific 24 h rate ($\mu\text{M h}^{-1} \text{g}^{-1}$)	7.72	± 0.01	7.04	± 0.03	7.72	± 0.08	0	0
Specific 48 h rate ($\mu\text{M h}^{-1} \text{g}^{-1}$)	3.86	± 0.04	3.76	± 0.03	3.93	± 0.09	0	0
Specific overall rate ($\mu\text{M h}^{-1} \text{g}^{-1}$)	0.47	± 1.86	0.44	± 0.76	0.51	± 2.75	0	0
Absolute removal (μM)	28.85 (58%)		26.94 (50%)		24.17 (49%)			

¹ Initial and specific initial removal rates obtained by exponential regression fit, and manually calculated specific removal rates for different time points, and the whole cultivation period. ² Calculated as the difference between the rates of active or PB inhibited and NaN_3 inactivated cultures.

Other fungal strains

The other fungal strains were only tested for DBP removal and are compared ahead. With exception of degradation by *C. aquatica*, biosorption was largely responsible for overall DBP removal. Absolute biosorptive removal by *Phoma* sp. and *Acephala* sp. was high (94 and 100%, respectively), however biomass normalized active and PB inhibited removal rates indicated additionally enzymatic degradation especially over the first hours (Tables 13 and 16). In the case of active and PB inhibited cultures of *Phoma* sp., biosorption and initial contribution of biotransformation combined resulted in complete removal of DBP after 3.5 and 24 h, respectively. Inhibition of biotransformation of approximately 6% after 3.5 h indicated minor but perceptible contribution by cytochrome P450. PB did not have an inhibitory effect on biotransformation in *Acephala* sp. Regarding *Ascocoryne* sp., only after normalization of removal rate with the initial biomass the absolute dominance of biosorption became obvious (i.e. biosorption accountable for all micropollutant removal) (Table 14). Similarly, biosorption was the dominant process observed in *P. arenariae*, though minor contribution of biotransformation was witnessed (Table 15). After 24 h an inhibition of about 25% implied involvement of cytochrome P450 in degradation by *P. arenariae*. In contrast, removal rates of cultures from *C. aquatica* indicated removal by biotransformation to be more important than by biosorption (Table 17). Cytochrome P450 was in part responsible for enzymatic degradation, with approximately 75% inhibition of biotransformation by PB 24 h after start of cultivation. At preceding and following sampling times (i.e. 3.5 and 48 h), inhibition in the range of 5 to 55% was still significant.

Table 13 Initial and specific (initial) removal rates of DBP observed with active, PB inhibited and NaN₃ inactivated cultures of Phoma sp. Further, the absolute DBP removal as recorded by the end of cultivation is shown

Removal rate ¹	<i>Phoma</i> sp.				
	Active	PB inhibited	NaN ₃ inactivated	Biotransformation ²	
				Active	PB
Initial rate (μM h ⁻¹)	37.20 ± 3.98	32.67 ± 5.27	32.89 ± 2.24		
Specific Initial rate (μM h ⁻¹ g ⁻¹)	110.28 ± 17.09	96.85 ± 19.02	98.17 ± 10.20	12.12	0
Specific 3.5 h rate (μM h ⁻¹ g ⁻¹)	35.39 ± 0.00	35.00 ± 0.02	30.41 ± 0.03	4.99	4.60
Specific 24 h rate (μM h ⁻¹ g ⁻¹)	5.67 ± 0.03	6.11 ± 0.03	5.19 ± 0.17	0.48	0.92
Specific 48 h rate (μM h ⁻¹ g ⁻¹)	2.83 ± 0.06	3.28 ± 0.10	2.59 ± 0.29	0.24	0.69
Specific overall rate (μM h ⁻¹ g ⁻¹)	0.40 ± 0.45	0.47 ± 0.67	0.37 ± 2.12	0.03	0.09
Absolute removal (μM)	45.89 (100%)	53.14 (100%)	42.13 (94%)		

¹ Initial and specific initial removal rates obtained by exponential regression fit, and manually calculated specific removal rates for different time points, and the whole cultivation period. ² Calculated as the difference between the rates of active or PB inhibited and NaN₃ inactivated cultures.

Table 14 Initial and specific (initial) removal rates of DBP observed with active, PB inhibited and NaN₃ inactivated cultures of *Ascocoryne* sp. Further, the absolute DBP removal as recorded by the end of cultivation is shown

Removal rate ¹	<i>Ascocoryne</i> sp.					
	Active	PB inhibited	NaN ₃ inactivated	Biotransformation ²		
				Active	PB	
Initial rate (μM h ⁻¹)	[§] 13.66 ± 3.66	0.68 ± 0.07	9.34 ± 1.71			
Specific Initial rate (μM h ⁻¹ g ⁻¹)	[§] 197.42 ± 57.18	9.83 ± 1.47	254.97 ± 47.84	n.a.	0	
Specific 3.5 h rate (μM h ⁻¹ g ⁻¹)	118.38 ± 0.01	64.39 ± 0.01	158.70 ± 0.02	0	0	
Specific 24 h rate (μM h ⁻¹ g ⁻¹)	24.62 ± 0.10	11.96 ± 0.07	35.71 ± 0.04	0	0	
Specific 48 h rate (μM h ⁻¹ g ⁻¹)	16.21 ± 0.03	8.51 ± 0.12	19.97 ± 0.06	0	0	
Specific overall rate (μM h ⁻¹ g ⁻¹)	2.32 ± 0.21	2.62 ± 0.16	3.16 ± 0.46	0	0	
Absolute removal (μM)	54.00 (100%)	60.99 (98%)	38.90 (66%)			

¹ Initial and specific initial removal rates obtained by exponential regression fit, and manually calculated specific removal rates for different time points, and the whole cultivation period. ² Calculated as the difference between the rates of active or PB inhibited and NaN₃ inactivated cultures. [§] indicates non-linear regression fitting with a R² < 0.9 and therefore not considered as accurate (n.a.) and not used for calculation of biotransformation.

Table 15 Initial and specific (initial) removal rates of DBP observed with active, PB inhibited and NaN₃ inactivated cultures of *P. arenariae*. Further, the absolute DBP removal as recorded by the end of cultivation is shown

Removal rate ¹	<i>P. arenariae</i>					
	Active	PB inhibited	NaN ₃ inactivated	Biotransformation ²		
				Active	PB	
Initial rate (μM h ⁻¹)	62.19 ± 16.38	51.69 ± 8.41	[§] 350454.91 ± 112084.21			
Specific Initial rate (μM h ⁻¹ g ⁻¹)	237.46 ± 65.23	197.38 ± 35.61	[§] 1918650.33 ± 615358.61	n.a.		
Specific 3.5 h rate (μM h ⁻¹ g ⁻¹)	40.59 ± 0.02	43.44 ± 0.01	63.53 ± 0.01	0	0	
Specific 24 h rate (μM h ⁻¹ g ⁻¹)	6.83 ± 0.13	6.59 ± 0.06	5.96 ± 0.25	0.87	0.64	
Specific 48 h rate (μM h ⁻¹ g ⁻¹)	3.43 ± 0.28	3.49 ± 0.10	2.70 ± 4.55	0.72	0.78	
Specific overall rate (μM h ⁻¹ g ⁻¹)	0.49 ± 1.97	0.56 ± 0.77	0.45 ± 18.24	0.04	0.10	
Absolute removal (μM)	43.08 (100%)	49.23 (100%)	27.90 (54%)			

¹ Initial and specific initial removal rates obtained by exponential regression fit, and manually calculated specific removal rates for different time points, and the whole cultivation period. ² Calculated as the difference between the rates of active or PB inhibited and NaN₃ inactivated cultures. [§] indicates non-linear regression fitting with a R² < 0.9 and therefore not considered as accurate (n.a.) and not used for calculation of biotransformation.

Table 16 Initial and specific (initial) removal rates of DBP observed with active, PB inhibited and NaN₃ inactivated cultures of *Acephala* sp. Further, the absolute DBP removal as recorded by the end of cultivation is shown

Removal rate ¹	<i>Acephala</i> sp.					
	Active	PB inhibited	NaN ₃ inactivated	Biotransformation		
				Active	PB	
Initial rate (μM h ⁻¹)	38.20 ± 7.33	55.19 ± 8.69	13.78 ± 1.85			
Specific Initial rate (μM h ⁻¹ g ⁻¹)	144.50 ± 27.99	208.79 ± 33.32	61.77 ± 8.38	82.73	147.02	
Specific 3.5 h rate (μM h ⁻¹ g ⁻¹)	55.54 ± 0.04	61.30 ± 0.03	40.74 ± 0.05	14.80	20.56	
Specific 24 h rate (μM h ⁻¹ g ⁻¹)	9.65 ± 0.12	10.48 ± 0.07	11.86 ± 0.20	0	0	
Specific 48 h rate (μM h ⁻¹ g ⁻¹)	5.28 ± 0.80	5.59 ± 0.36	6.28 ± 0.45	0	0	
Specific overall rate (μM h ⁻¹ g ⁻¹)	0.75 ± 4.84	0.83 ± 3.05	0.90 ± 3.47	0	0	
Absolute removal (μM)	67.04 (99%)	73.51 (100%)	67.86 (100%)			

¹Initial and specific initial removal rates obtained by exponential regression fit, and manually calculated specific removal rates for different time points, and the whole cultivation period. ²Calculated as the difference between the rates of active or PB inhibited and NaN₃ inactivated cultures.

Table 17 Initial and specific (initial) removal rates of DBP observed with active, PB inhibited and NaN₃ inactivated cultures of *C. aquatica*. Further, the absolute DBP removal as recorded by the end of cultivation is shown

Removal rate ¹	<i>C. aquatica</i>					
	Active	PB inhibited	NaN ₃ inactivated	Biotransformation ²		
				Active	PB	
Initial rate (μM h ⁻¹)	8.08 ± 0.98	0.96 ± 0.11	[§] 0.51 ± 0.11			
Specific Initial rate (μM h ⁻¹ g ⁻¹)	99.31 ± 13.01	11.83 ± 1.43	[§] 9.50 ± 2.10	n.a.		
Specific 3.5 h rate (μM h ⁻¹ g ⁻¹)	75.62 ± 0.01	73.54 ± 0.01	39.83 ± 0.02	35.79	33.71	
Specific 24 h rate (μM h ⁻¹ g ⁻¹)	31.81 ± 0.01	15.74 ± 0.09	10.57 ± 0.05	21.25	5.18	
Specific 48 h rate (μM h ⁻¹ g ⁻¹)	16.08 ± 0.02	9.88 ± 0.05	4.71 ± 1.01	11.36	5.17	
Specific overall rate (μM h ⁻¹ g ⁻¹)	2.30 ± 0.11	2.53 ± 0.07	1.37 ± 2.93	0.92	1.16	
Absolute removal (μM)	62.78 (100%)	69.28 (97%)	24.73 (37%)			

¹Initial and specific initial removal rates obtained by exponential regression fit, and manually calculated specific removal rates for different time points, and the whole cultivation period. ²Calculated as the difference between the rates of active or PB inhibited and NaN₃ inactivated cultures. [§] indicates non-linear regression fitting with a R² < 0.9 and therefore not considered as accurate (n.a.) and not used for calculation of biotransformation.

Overview of Micropollutant Removal Capacities, Biosorption and Cytochrome P450 Inhibition Effects

Based upon the incidence and magnitude of biotransformation rates observed for micropollutant removal experiments, the degree of active biological removal in regard to individual fungal strains was proposed for DBP and BPA. The degree of biosorption and the effect of cytochrome P450 inhibition was evaluated the same way. A qualitative ranking of fungal isolates concerning micropollutant biotransformation, biosorption and inhibition of biotransformation by PB is represented in Table 18.

Table 18 Overview of micropollutant removal capacities, inhibitory effects of PB and biosorption by fungal isolates for DBP and BPA removal experiments

		Qualitative ranking of fungal isolates
Biotransformation	DBP	<i>S. rugosoannulata</i> > <i>C. aquatica</i> >> <i>Acephala</i> sp. > <i>Phoma</i> sp. > <i>T. porosum</i> > <i>P. arenariae</i> > <i>S. chlorohalonata</i> >> <i>Ascocoryne</i> sp.
	BPA	<i>S. rugosoannulata</i> >> (<i>T. porosum</i>) > <i>S. chlorohalonata</i>
Inhibition of biotransformation by PB	DBP	<i>S. rugosoannulata</i> > <i>C. aquatica</i> >> <i>S. chlorohalonata</i> > <i>P. arenariae</i> > <i>T. porosum</i> > <i>Phoma</i> sp. >> <i>Ascocoryne</i> sp. > <i>Acephala</i> sp.
	BPA	<i>S. rugosoannulata</i> >> <i>S. chlorohalonata</i> > (<i>T. porosum</i>)
Biosorption	DBP	<i>Acephala</i> sp. > <i>Ascocoryne</i> sp. >> <i>Phoma</i> sp. > <i>P. arenariae</i> > <i>T. porosum</i> > <i>S. chlorohalonata</i> >> <i>C. aquatica</i> > <i>S. rugosoannulata</i>
	BPA	<i>S. chlorohalonata</i> > (<i>T. porosum</i>) >> <i>S. rugosoannulata</i>

3.4. Biotransformation metabolites produced from DBP in fungal cultures

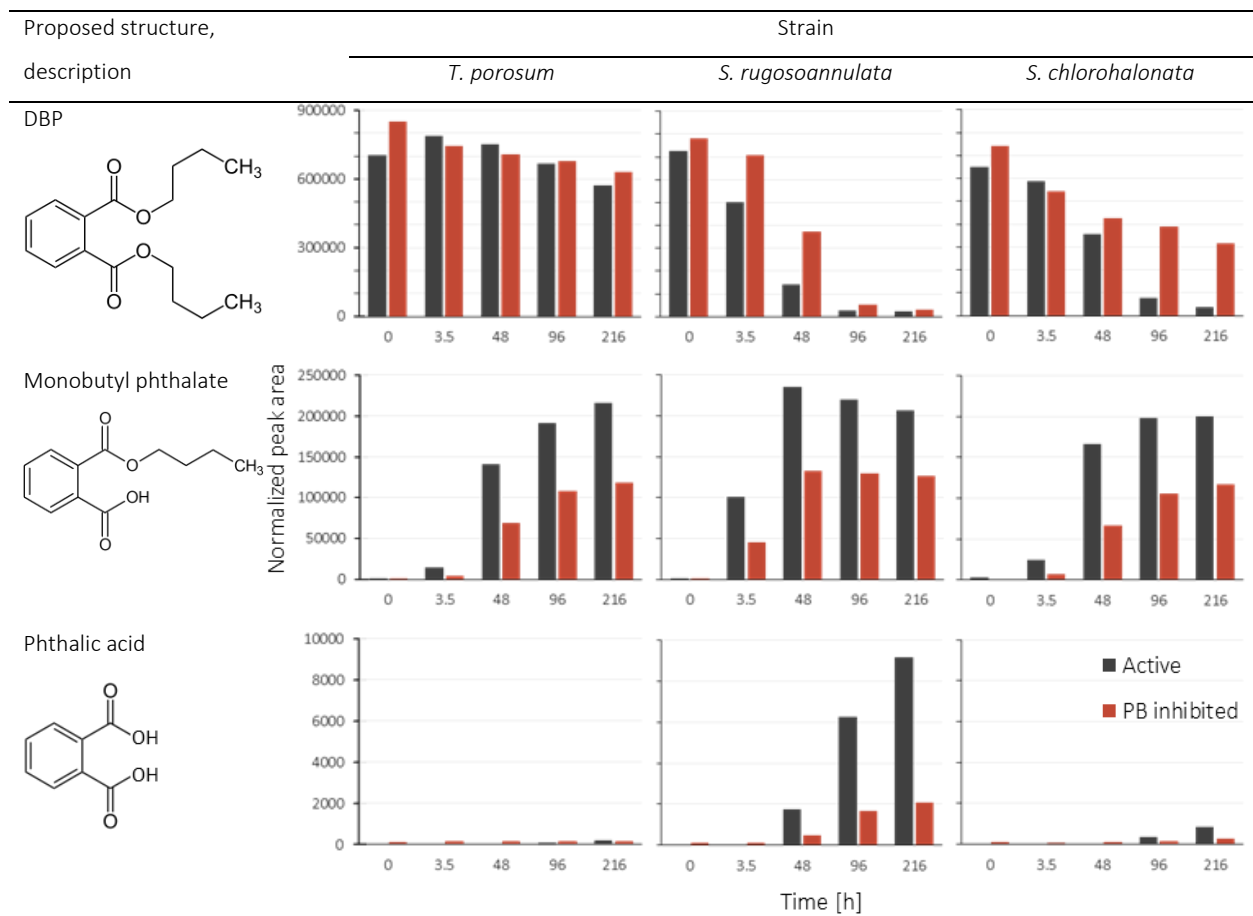
Focus in this study was on the analysis of DBP biotransformation products resulting from metabolism in cultures of *T. porosum*, *S. rugosoannulata* and *S. chlorohalonata* utilizing UPLC-QTOF-MS. To elucidate the oxidative contributions by cytochrome P450 the inhibitor PB was employed. The higher concentration of DBP – intended to increase the concentration and hence to improve the detection of biotransformation products – lead to its partial separation as non-aqueous phase liquid (NAPL) on the surface of the growth medium after 24 hours of cultivation. However, formed DBP metabolites were assumed to be less hydrophobic and thus sufficiently detectable in aqueous samples of the culture supernatant.

The following reported peak areas of detected biotransformation products can not directly be related to the concentration of those compounds. Nevertheless, differences in peak area were considered to provide a rough indication of the respective metabolite amount and changes in amount with time. A representative base peak chromatogram at start (0 h) and end (216 h) of the experiment, and a summary of DBP biotransformation products can be found in Appendix Figures 7 and 8, and Appendix Table 12, respectively.

DBP and central intermediates of the DBP degradation process (Figure 4), namely monobutyl phthalate and phthalic acid, are reported in Table 19. Transformation products resulting from oxidative degradation, including those likely catalyzed by cytochrome P450 are presented in Table 20. In contrast, DBP metabolites indicative for ester hydrolysis or transesterification as the initial breakdown step are reported in Table 21. However, alkyl chain shortening through β -oxidation or O-dealkylation could also be accountable for such reactions. Transformation products formed by a combination of oxidative and hydrolytic processes are presented in Table 22.

An apparent inhibitory effect was witnessed to some extent also in formation of presumably hydrolytic metabolites including monobutyl phthalate and phthalic acid for all fungi. However, revising the raw data revealed matrix interference in samples of cytochrome P450 inhibited cultures caused by PB that affected potential target peaks (i.e. those corresponding to retention times in between approximately 6 to 9 minutes) (Appendix Figure 9). There is uncertainty with regard to the effects on individual analytes since ionization is concentration dependent and competitive – thus expected to vary for each sample. The peak area of DBP can be assumed to be unaffected for the late elution from the column (i.e. high retention time).

Table 19 Caffeine standard normalized peak areas of DBP and central DBP transformation products and their time courses detected by UPLC-QTOF-MS. Active fungal cultures contained 250 μM of DBP, cytochrome P450 inhibited cultures 250 μM DBP and 1 mM PB. Tentative structures reported were not experimentally determined but were proposed upon detected masses, interpretation of fragmentation and favorable interactions



T. porosum

Degradation of DBP by *T. porosum* was slower than in the preceding removal experiment (compare Figure 9). Inhibition of cytochrome P450 did not have an unambiguous inhibitory effect on DBP metabolism, as the trend in DBP removal witnessed for active and PB inhibited cultures was similar (Table 19). Transformation products including those formed oxidation were absent (Table 20), and no substantial amounts of metabolites of combined oxidative and hydrolytic processes were observed (Table 22). Instead, DBP degradation by *T. porosum* as indicated by formation of monobutyl phthalate and hydrolytic transformation products have to be considered to be hydrolytic (Table 21). However, degradation by *T. porosum* did not yield phthalic acid (Table 19).

S. rugosoannulata

In cultures of *S. rugosoannulata* an almost complete removal of DBP was observed after 96 h for both active and cytochrome P450 inhibited cultures (Table 19). However, the decrease in normalized peak area of DBP was slower in PB inhibited cultures, thus increasingly indicating the involvement of cytochrome P450 catalyzed oxidation steps. Further evidence for cytochrome P450 catalyzed oxidation is present in Table 20. In all cases, the isomers of the oxidative metabolite are absent or show a considerable reduction in their amount for inhibited flasks. The low levels of oxidative transformation products in PB inhibited cultures at later sampling times (i.e. after 48 h) may be explained by the concomitant degradation of PB as witnessed in the DBP removal experiment (Appendix Figure 11). This might also be the reason for similar DBP removal observed at the end of the experiment by active and PB inhibited cultures. The oxidative transformation product is further degraded as the reduction in normalized peak areas indicates, with the maxima observed in the samples taken 48 and 96 h after incubation (Table 20). Similarly, monobutyl phthalate and the hydrolytic metabolite “DBP-C₄H₈-C₂H₄” reached their respective highest amount after 48 and 96 h and then decreased, while the hydrolytic metabolite “DBP-C₄H₈-C₃H₆” and phthalic acid increased over time (Tables 19 and 21). Three major isomeric transformation products formed by combined oxidative and hydrolytic processes were detected, two of which showed decreasing peak areas towards the end of the experiment, indicative for further degradation (Table 22). By contrast, the metabolite “DBP+O-C₄H₈” accumulated over time.

Table 20 Caffeine standard normalized peak area of the most indicative oxidative DBP transformation products and their time course detected by UPLC-QTOF-MS. Active fungal cultures contained 250 μM of DBP, cytochrome P450 inhibited cultures 250 μM DBP and 1 mM PB. Tentative structures reported were not experimentally determined but were proposed upon detected masses, interpretation of fragmentation and favorable interactions. Peaks recorded with the same m/z are considered as isomeric and are indicated by (I), (II) etc

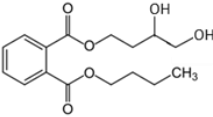
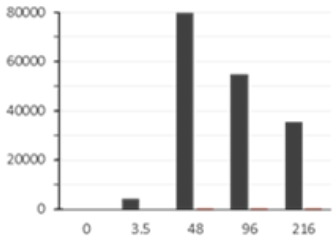
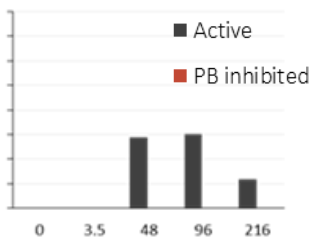
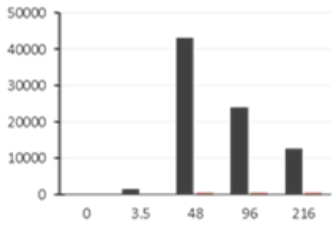
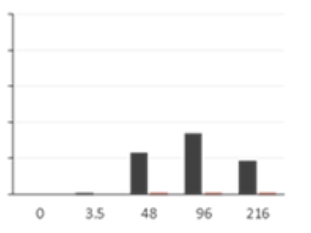
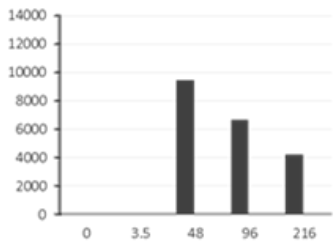
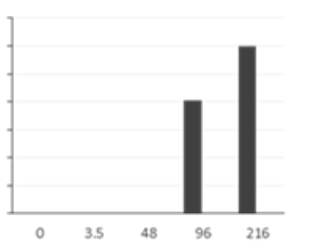
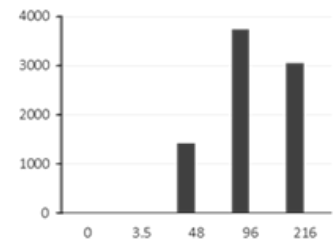
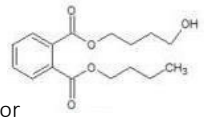
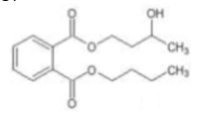
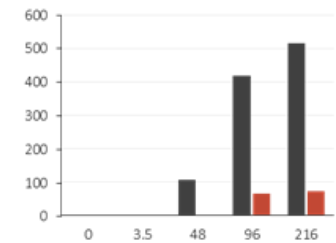
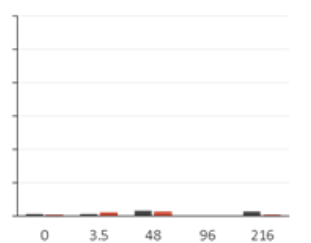
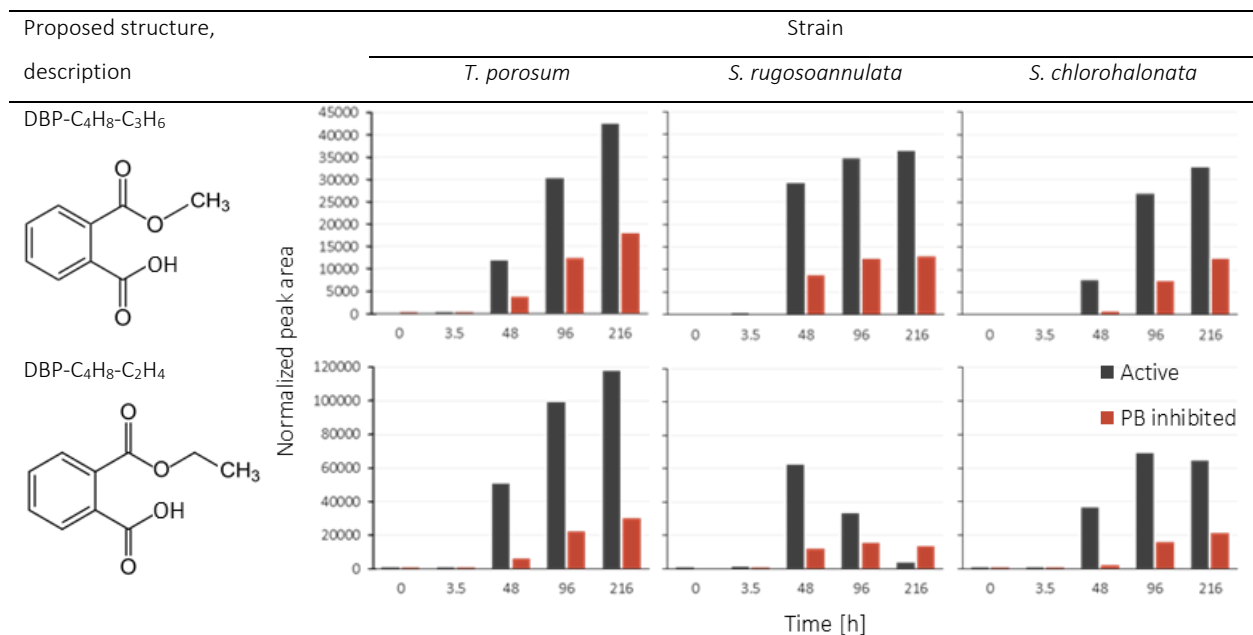
Proposed structure, description	Strain		
	<i>T. porosum</i>	<i>S. rugosoannulata</i>	<i>S. chlorohalonata</i>
DBP+2O (I) 	not detected		
(II)	not detected		
(III)	not detected		
(IV)	not detected		not detected
DBP+O  or 	not detected		

Table 21 Caffeine standard normalized peak areas of the major hydrolytic DBP transformation products and their time courses detected by UPLC-QTOF-MS. Active fungal cultures contained 250 μ M of DBP, cytochrome P450 inhibited cultures 250 μ M DBP and 1 mM PB. Tentative structures reported were not experimentally determined but were proposed upon detected masses, interpretation of fragmentation and favorable interactions



S. chlorohalonata

S. chlorohalonata exhibited greater removal of DBP than in the preceding experiment (Table 19, compare Figure 9). Though not corrected for the fungal dry biomass, results presented in Figure 12 indicate biotransformation, not biosorption (measured in NaN₃ inactivated cultures) to be a major removal process, contrasting to previous results (compare to Table 11). In active fungal cultures, the initial DBP amount was decreased significantly by the end of the incubation, whereas PB inhibited cultures had comparably lower removal indicating contribution of cytochrome P450 to degradation (Table 19). Supportive evidence is provided by the absence of oxidative transformation product in the presence of PB (Table 20). In active cultures, three isomeric oxidation products were detected, two of them with later and lower peak area maximum compared to *S. rugosoannulata*. The third isomer of the oxidative metabolite was higher in amount and increased over the last two sampling times (Table 20). Hydrolytic metabolites including monobutyl phthalate increased in normalized peak area over time, though less than in cultures of *T. porosum* (Table 21). Further, phthalic acid production was very low and only considerable after 96 h. Compared to metabolites formed by combined oxidative and hydrolytic processes by *S. rugosoannulata*, in active cultures of *S. chlorohalonata* more “DBP-C₃H₆+O” was produced (Table 22). Other (isomeric) transformation products were detected in comparably lower amounts.

Table 22 Caffeine standard normalized peak areas of the major DBP transformation products formed by a combination of oxidative and hydrolytic processes, and their time courses detected by UPLC-QTOF-MS. Active fungal cultures contained 250 μM of DBP, cytochrome P450 inhibited cultures 250 μM DBP and 1 mM PB. Tentative structures reported were not experimentally determined but were proposed upon detected masses, interpretation of fragmentation and favorable interactions. Peaks recorded with the same m/z are considered as isomeric and are indicated by (I), (II) etc →

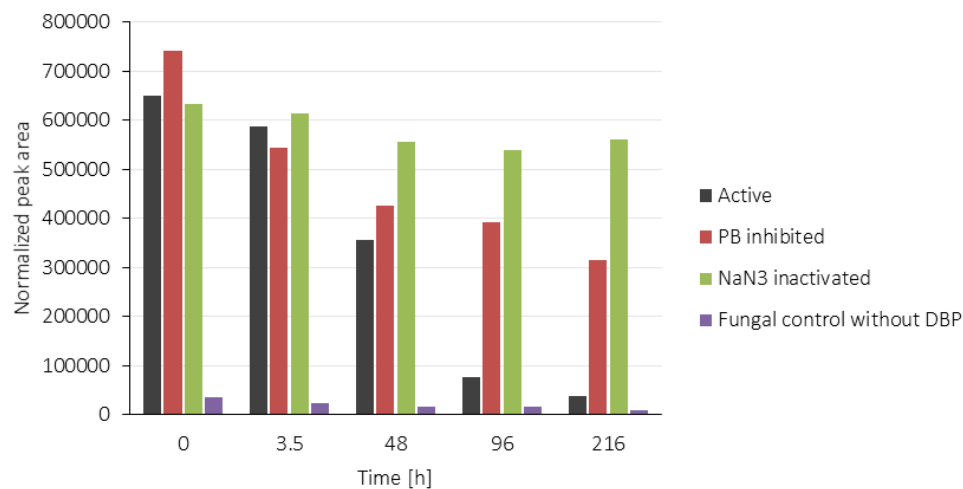
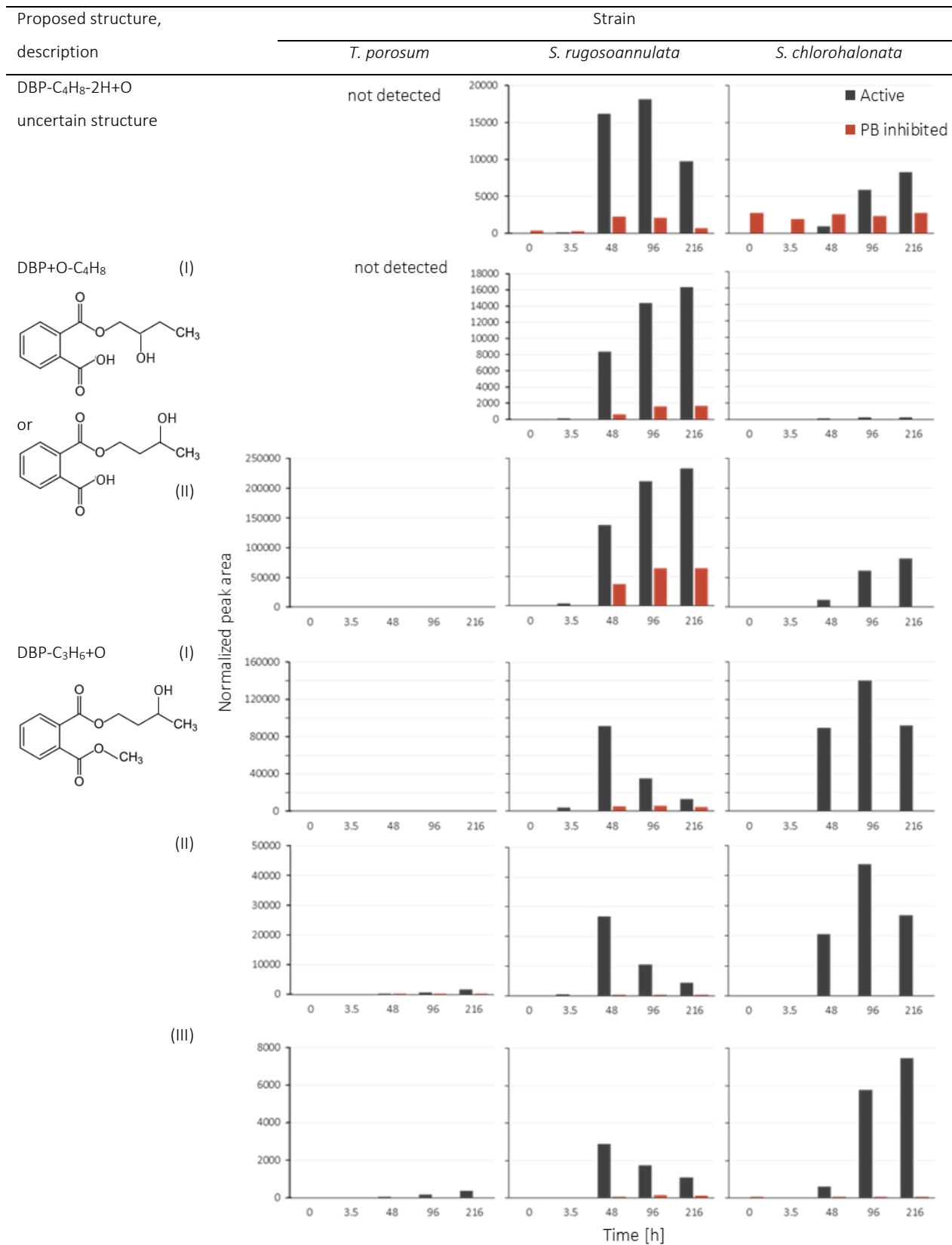


Figure 12 Time course of caffeine standard normalized peak area of DBP in cultures of *S. chlorohalonata* detected by UPLC-QTOF-MS. Active fungal cultures contained 250 μM of DBP, cytochrome P450 inhibited cultures 250 μM DBP and 1 mM PB, NaN_3 inactivated cultures contained 250 μM DBP and 15.38 mM NaN_3 , and the control for fungal exudates contained only biomass.



4. Discussion

4.1. Micropollutant biotransformation efficiency by fungi

A major aim of this study was the determination of biocatalytical degradation efficiencies of individual strains and comparison of the removal capacities among tested fungi. Biotransformation was witnessed for both micropollutants to a similar extent, however individual strains exhibited wide differences in biodegradation efficiency. Biosorption (as discussed in the next section) interfered with biotransformation, thus hampering the direct determination of biocatalytic degradation rates.

Biotransformation of dibutyl phthalate (DBP) and bisphenol A (BPA) was most efficient for *S. rugosoannulata* (Tables 9 and 10). No literature was found regarding phthalate degradation by this species. Through the formation of polymers catalyzed by lignin-modifying enzymes the estrogenicity of BPA is reduced (Kabiersch et al., 2011). In cultures of *S. rugosoannulata* the estrogenicity was reduced significantly, though temporarily re-emerged likely due to formation of ring fission products (the BPA concentration course itself was not quantified in the study by Kabiersch et al. (2011)). Both Mn-peroxidase and laccase activities were detected before BPA addition, but decreased temporarily after BPA addition and then recovered and increased to rather weak to moderate exoenzyme activities not exceeding 55 U l^{-1} (which was above the pollutant free fungal control levels in case of laccase) (Kabiersch et al., 2011). In the present study, the laccase activity was detectable after 24 h of incubation and increased thereafter. After the same cultivation time, laccase activity was approximately 5-fold higher than in the aforementioned study by Kabiersch et al. (2011), but no appreciable Mn-peroxidase activity was detected (Figures 9 and 11). Thus, although the laccase activity was initially low, laccase may have contributed to BPA removal by this strain.

For the basidiomycetous yeast *T. porosum*, no literature on DBP or BPA removal was found. The co-cultivation of *Trichosporon cutaneum* and *Aspergillus awamori* immobilized on modified polyamide beads was reported to completely remove BPA applied at a more than an order of magnitude higher concentration (about 1.3 mM) than that of the present study, though the authors did not distinguish

biosorption and biotransformation (Yordanova et al., 2013). Furthermore, no removal of the high molecular weight phthalate dioctyl phthalate ($\log K_{ow} = 8.10$) was observed in cultures of *T. porosum* (Sabev et al., 2006). In the present study, biotransformation (and biosorption) was detected for the lower molecular weight phthalate DBP. The reason is likely the higher bioavailability due to comparably lower hydrophobicity and a potentially decreased steric hindrance for compound-enzyme interaction due to smaller molecule size. There was little evidence for contribution of cytochrome P450 to DBP degradation (Table 7). Results for BPA removal were assumed to be affected by the significantly lower initial fungal dry biomass (Appendix Table 1), and thus not discussed further.

No reports of successful DBP or BPA removal by *S. chlorohalonata* were found in the literature search. In the present study limited biocatalytic DBP degradation was witnessed, however significant biosorption occurred for both micropollutants (Tables 11 and 12).

Phoma sp. has been shown to completely degrade a mixture of endocrine disrupting chemicals, including BPA and dimethyl phthalate, further containing nonylphenol, methyl- and buthylparaben (initial concentration 25 μM , respectively for each compound) within two days of incubation. For none of the other fungal species employed, namely *C. aquatica*, *T. porosum*, *Acephala* sp., and *S. chlorohalonata*, removal of the mixture of endocrine disrupting agents was observed (Macellaro, 2014). Furthermore, in the same doctoral study *Phoma* sp. was reported to remove dimethyl phthalate (initial concentration 100 μM) within 7 days by solely biocatalytic attack. However, the conclusion of complete removal through biotransformation is questionable, as extraction of dimethyl phthalate from biomass might be incomplete and/or further degradation could have occurred. In a project preceding the present study, DBP removal within 24 h was observed by *Phoma* sp., though dominated by biosorption (Cowan, 2017). The results of the present study corroborate the reported fast biosorptive removal by *Phoma* sp. (Table 13). As for *Ascocoryne* sp., *P. arenariae* and *C. aquatica* no published literature was found with regard to phthalate degradation. In the aforementioned pre-study, complete removal of DBP was observed for these fungal strains without detectable exoenzyme activity (Cowan, 2017). Degradation rates in this study in cultures of *Ascocoryne* sp. and *P. arenariae* did not differ from those observed before, and the trend of biosorption dominated removal was repeated (Cowan, 2017). For *C. aquatica* the extent of DBP removal in this study was similar to results reported by Cowan (2017), although the biotransformation was found to be less important at the later stage of incubation.

Another major aim was to identify major enzyme classes involved in the biocatalytic removal of the target pollutants through the assessment of micropollutant removal under cytochrome P450 inhibiting conditions and concomitant monitoring of exoenzyme activities.

Involvement of cytochrome P450 was strongly indicated for the initial degradation of DBP and BPA by *S. rugosoannulata*. The presence of PB also affected DBP removal by *C. aquatica*, inhibiting degradation between 5 to 75% during the initial 48 h of incubation. In *S. chlorohalonata* cytochrome P450 contributed significantly to the DBP degradation after 48 h. Contribution of cytochrome P450 can not be ruled out for *P. arenariae*, as inhibition about 25% by PB after 24 h was observed. The initial specific degradation rate of *Phoma* sp. indicating contribution of cytochrome P450 contradicts the other indices in this study (Table 13). However, it is in accordance with results obtained previously by Cowan (2017) where total DBP removal remained unaffected, but a slight decrease in specific removal rates was observed. For all other fungal strains, major contribution of cytochrome P450 was not supported by the results.

As discernible in Appendix Figures 11 and 12, some removal of PB from the culture supernatant was observed over time for all fungi, and complete removal in case of *S. rugosoannulata*. A decrease in concentration can interfere with the intended cytochrome P450 inhibition. However, only for *S. rugosoannulata* a decrease in inhibition is suspected. The contribution of cytochrome P450 thus may have been underestimated and cytochrome P450 involved during the whole incubation. Furthermore, micropollutants and PB may have competed for enzymatic activities, as enzymes detoxifying PB can not simultaneously degrade the micropollutants. As a consequence of this assumption, the degradation of micropollutants would be diminished possibly not only by inhibition of the cytochrome P450 system. Further, the inhibitory effect is assumed to differ with regard to its efficiency among fungal strains. Additionally, inhibition of some esterase activities by PB can be achieved at high concentrations (see, for example, Young et al., 2005), so indiscriminate use of this synergist to infer P450 dependent metabolism is risky.

As previously mentioned, laccase activities were only detected in cultures of *S. rugosoannulata*. No Mn-peroxidase activities were observed in this study, nevertheless attack of both BPA and DBP would have been conceivable if present due to its higher oxidation potential. Detected exoenzymatic activities were negligible for *T. porosum* and *S. chlorohalonata*, though previous studies have proved that production of Mn-peroxidase by *T. porosum* and potentially lignin-modifying laccase in *Stachybotrys* sp. occurs (Janssen et al., 2004, Martorell et al., 2012). Singh et al. (2014) reported the lignin removal capacity of *S. chlorohalonata* (also *Phoma* sp. and *Acephala* sp.) to be only slightly lower than that of *S. rugosoannulata*. Laccase activity in *Phoma* sp. was witnessed by Cowan (2017), although due to the high redox potential catalysis of DBP by laccase (up to + 0.8 mV) is unlikely. However exoenzyme activities were not assessed in *Phoma* sp. in the present study.

To summarize, based on the observed results and studied literature esterases are assumed to be the major key enzymes involved in DBP and BPA degradation in the investigated fungi, in addition to cytochrome P450 in *S. rugosoannulata*, *C. aquatica* and *T. porosum* (Amir et al., 2005, Cartwright et al., 2000).

Evaluating the DBP removal efficiencies among employed fungal strains regarding taxonomy and ecophysiology, following tendencies were implied. Especially the white-rot fungus *S. rugosoannulata* showed higher efficiency in micropollutant degradation than the other fungal strains. Further, the degradation efficiencies of *S. rugosoannulata* and *Acephala* sp. being both terrestrial and of the aquatic strain *C. aquatica* imply ubiquitous degradation potential in the environment.

4.2. Biosorption of micropollutants

In the present study, biosorption occurred for both micropollutants to varying degree depending on the fungal strain. In some fungal cultures biosorption was completely accountable for observed removal. However, these results were observed in the presence of Tween 80, which may have diminished biosorption due to increased solubility of micropollutants. Previous studies have demonstrated hydrophobicity of organopollutants to control biosorption to fungal biomass and bacteria dominated activated sludge (Chen et al., 2010, Suárez et al., 2008). Comparing biosorption in *S. rugosoannulata* and *S. chlorohalonata*, for both fungi the biosorption of BPA was more pronounced than that of DBP despite the reversed hydrophobicity. However, the cell surface hydrophobicity differs among fungi, further depending on the growth conditions including particular habitats and presence of pollutants (Chau et al., 2009, Linder et al., 2005). It has previously been reported that biosorption by *Phoma* sp. and *C. aquatica* was more dominant for less hydrophobic pollutants (Hofmann and Schlosser, 2016, Cowan, 2017). For *S. rugosoannulata* a trend of improved BPA biotransformation over DBP was observed. This corroborates the results of previous studies where biosorptive enrichment of micropollutants has been implicated to enhance the biotransformation (Nguyen et al., 2014, Semple et al., 2007). However, in *S. chlorohalonata* and comparing DBP micropollutant removal among fungi in the present study, the opposite trend of decreasing biotransformation with increasing biosorption was observed.

4.3. DBP degradation pathway based on transformation products

To gain further insight into which enzymes are involved in DBP degradation by *T. porosum*, *S. rugosoannulata* and *S. chlorohalonata*, structure elucidation of DBP degradation metabolites via mass spectrometry was performed. No Tween 80 aided the aqueous solubility and thus DBP was likely less bioavailable than in the preceding experiment, as frequently the rate-limiting step in the degradation of

hydrophobic compounds is their solubility in water (Mulligan et al., 2001). At the same time, a stronger biosorption is to be expected due to partitioning from the aqueous phase. Further, separation of some DBP as NAPL was observed. Under these circumstances, the detected DBP concentration in samples from the aqueous supernatant possibly does not accurately reflect the total DBP amount contained in the respective entire degradation system. For DBP metabolites however, these effects are expected to decrease due to phase I metabolism which decreases hydrophobicity by incorporation of oxygen, and reduction in molecule size. Due to the matrix effect caused by PB and uncertainties related to the interpretation of cytochrome P450 inhibited reactions (as discussed in the preceding section), quantitative comparison to active cultures is flawed. Taking these points into consideration, the possible degradation pathways will be discussed with focus on presence or absence and the proposed structures of transformation products.

In Figure 13, the DBP transformation pathway based on most indicative metabolites detected in selected fungi is presented. For the yeast *T. porosum* no substantial amounts of oxidative products were detected and presumably hydrolytic metabolites were present in both active and cytochrome P450 inhibited cultures, though the second alkyl ester was seemingly not split (Figure 13). Therefore, it is unlikely that these products were actually formed by O-dealkylation and β -oxidation. The apparently less efficient removal of DBP by *T. porosum* in comparison to the previous DBP removal experiment is possibly a consequence of lower bioavailability. However, fungal biomass was not quantified in these experiments, so that a quantitative comparison has low meaningfulness. Contrasting to *T. porosum*, the white-rot *S. rugosoannulata* and the constructed wetland isolate *S. chlorohalonata* formed discernible amounts of oxidative and combined oxidative and hydrolytic degradation products beside the (possibly) hydrolytic metabolites. In PB inhibited cultures, oxidative and some combined oxidative and hydrolytic metabolites were absent, implying involvement of cytochrome P450 in these reactions. Since *S. rugosoannulata* was witnessed in the previous DBP removal experiment to degrade PB, increased removal of DBP over time in cytochrome P450 inhibited flasks is likely an effect of decreasing inhibition. In *S. rugosoannulata*, an appreciable decrease in monobutyl phthalate and oxidative product "DBP+2O" was observed after formation. While for monobutyl phthalate deesterification to finally phthalic acid is assumed, the continued degradation of "DBP+2O" remains unclear. A difference in peak area of presumably hydrolytic metabolites between active and PB inhibited cultures of *S. rugosoannulata* and *S. chlorohalonata* was observed. In this case, additionally to the discussed uncertainties caused by the presence of PB, it can not be excluded that the peak area in PB inhibited cultures was decreased by inhibited O-dealkylation and β -oxidation catalyzed by cytochrome P450. Removal by *S. chlorohalonata* was less effective than by

S. rugosoannulata and consequently lower amounts of metabolites were formed, and although not based on biomass normalized results it reflects observations from the previous DBP removal experiment. Contradicting the hypothesis of increased biosorption in absence of Tween 80, especially for *S. chlorohalonata* the opposite was observed.

The degradation pathways of DBP witnessed for *T. porosum*, *S. rugosoannulata* and *S. chlorohalonata* fit into the primary degradation described for bacteria and fungi in the literature and in the pre-study by Cowan (2017). Together with observed inhibitory effects of PB on DBP removal (Tables 20 and 22), the observed hydroxylation products suggest cytochrome P450 catalyzed oxidations of DBP in *S. rugosoannulata* and *S. chlorohalonata*, which may initiate the common β -oxidation processes. The observed ester cleavage reactions may indicate the action of esterases and the removal of one butyl chain to yield monobutyl phthalate appears as the key step in DBP biotransformation by the investigated fungi. Based on the investigated fungi, a difference in the degradative pathway was observed between yeast and filamentous fungi.

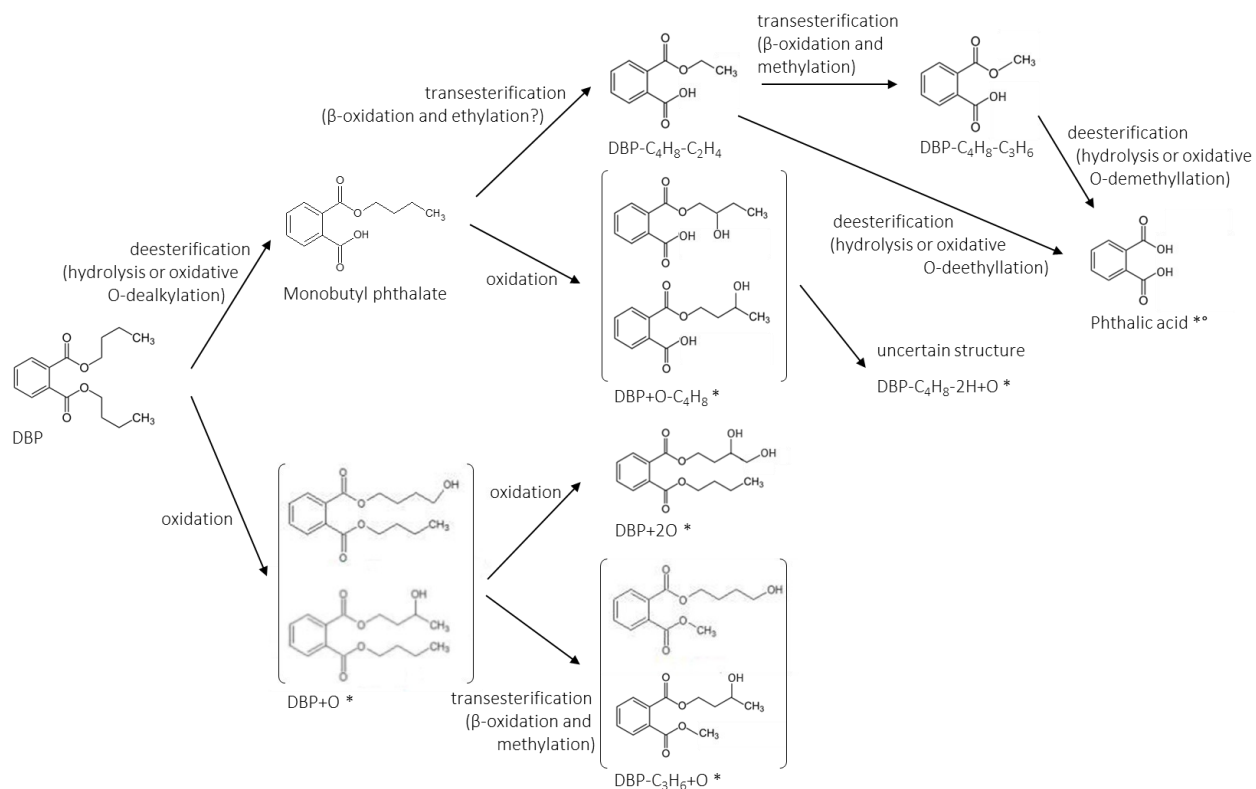


Figure 13 Proposed DBP transformation pathway in *T. porosum*, *S. rugosoannulata* and *S. chlorohalonata* based on most indicative metabolites detected by UPLC-QTOF-MS. * indicates metabolites not relevant for *T. porosum*. ** indicates transformation product not relevant for *S. chlorohalonata*.

5. Concluding remarks

In this study, varying dibutyl phthalate (DBP) and bisphenol A (BPA) removal efficiencies among fungal isolates were witnessed. Complete micropollutant removal was observed for all fungi with exception to *S. chlorohalonata* isolated from a constructed wetland. While biosorption was observed for all fungi to varying extent, biotransformation of DBP was most efficient for white-rot fungus *S. rugosoannulata* and the aquatic *C. aquatica*, followed by the peatland isolate *Acephala* sp., whereas all other strains had lower degradation efficiencies. Further, for *S. rugosoannulata* and *C. aquatica*, followed by *S. chlorohalonata* contribution of cytochrome P450 to DBP degradation was indicated, whereas for the soil inhabiting basidiomyceteous yeast *T. porosum* related evidence was missing. *S. rugosoannulata* also efficiently biotransformed BPA, seemingly involving cytochrome P450 and possibly laccase catalyzed reactions, whereas biosorption was a less important removal process. By contrast, biosorption was the only BPA removal process operative in *S. chlorohalonata*. Lignin-modifying exoenzymes could not be implicated in micropollutant removal by *S. chlorohalonata*, *T. porosum* and DBP degradation in *S. rugosoannulata*, which were investigated in this respect. The structure elucidation of DBP degradation metabolites for *S. rugosoannulata*, *T. porosum* and *S. chlorohalonata* enabled to suggest degradation pathways, which are in accordance with literature data. Esterases were likely involved in DBP degradation for all selected fungi. Moreover, oxidation catalyzed by cytochrome P450 seemingly played a prominent role in DBP removal by employed filamentous fungi, though not for the yeast *T. porosum*. A wide-spread micropollutant degradation potential in the environment was implied by investigated strains. Furthermore, an increased degradation efficiency in white-rot fungi *S. rugosoannulata* compared to other employed fungi was observed. Screening of a larger number of fungi would be required to firmly establish different trends suggested with regard to ecophysiological characteristics of degraders. For statistically meaningful evaluation, the number of replicates in degradation experiments should be increased. Moreover, future studies aimed at elucidating key enzymes (e.g. esterases and cytochrome P450) in more detail are merited. Finally, also degradation of micropollutants in mixture and removal by fungal consortia would increase the understanding of the micropollutant removal in the environment.

References

- Aksu, Z. & Karabayır, G. 2008. Comparison of biosorption properties of different kinds of fungi for the removal of Gryfalan Black RL metal-complex dye. *Bioresource Technology*, 99, 7730-7741.
- Amir, S., Hafidi, M., Merlina, G., Hamdi, H., Jouraiphy, A., El Gharous, M. & Revel, J.-C. 2005. Fate of phthalic acid esters during composting of both lagooning and activated sludges. *Process Biochemistry*, 40, 2183-2190.
- Baldy, V., Chauvet, E., Charcosset, J.-Y. & Gessner, M. O. 2002. Microbial dynamics associated with leaves decomposing in the mainstem and floodplain pond of a large river. *Aquatic Microbial Ecology*, 28, 25-36.
- Benjamin, S., Pradeep, S., Sarath Josh, M., Kumar, S. & Masai, E. 2015. A monograph on the remediation of hazardous phthalates. *Journal of Hazardous Materials*, 298, 58-72.
- Bergman, Å., Heindel, J. J., Jobling, S., Kidd, K. & Zoeller, T. R. 2013. State of the science of endocrine disrupting chemicals 2012. *In: WHO & UNEP (eds.)*.
- Cartwright, C. D., Owen, S. A., Thompson, I. P. & Burns, R. G. 2000. Biodegradation of diethyl phthalate in soil by a novel pathway. *FEMS Microbiology Letters*, 186, 27-34.
- Chai, W., Sakamaki, H., Kitanaka, S., Saito, M. & Horiuchi, C. A. 2003. Biodegradation of bisphenol A by cultured cells of *Caragana chamlagu*. *Bioscience, biotechnology, and biochemistry*, 67, 218-220.
- Chau, H. W., Si, B. C., Goh, Y. K. & Vujanovic, V. 2009. A novel method for identifying hydrophobicity on fungal surfaces. *Mycological Research*, 113, 1046-1052.
- Chauret, C., Mayfield, C. I. & Inniss, W. E. 1995. Biotransformation of di-n-butyl phthalate by a psychrotrophic *Pseudomonas fluorescens* (BGW) isolated from subsurface environment. *Canadian journal of microbiology*, 41, 54-63.
- Chen, B., Wang, Y. & Hu, D. 2010. Biosorption and biodegradation of polycyclic aromatic hydrocarbons in aqueous solutions by a consortium of white-rot fungi. *J Hazard Mater*, 179, 845-51.
- Cohen-Bazire, G., Sistrom, W. & Stanier, R. 1957. Kinetic studies of pigment synthesis by non-sulfur purple bacteria. *Journal of cellular physiology*, 49, 25-68.
- Coronado, J. E., Mneimneh, S., Epstein, S. L., Qiu, W. G. & Lipke, P. N. 2007. Conserved processes and lineage-specific proteins in fungal cell wall evolution. *Eukaryot Cell*, 6, 2269-77.
- Cowan, A. R. 2017. Biodegradation of Micropollutants DEP, DBP and BPA by Aquatic Fungi. Leipzig, Germany: Helmholtz Centre for Environmental Research UFZ.
- De Moura Carrara, S. M. C., Morita, D. M. & Boscov, M. E. G. 2011. Biodegradation of di(2-ethylhexyl)phthalate in a typical tropical soil. *Journal of Hazardous Materials*, 197, 40-48.
- Diamanti-Kandarakis, E., Bourguignon, J.-P., Giudice, L. C., Hauser, R., Prins, G. S., Soto, A. M., Zoeller, R. T. & Gore, A. C. 2009. Endocrine-disrupting chemicals: an Endocrine Society scientific statement. *Endocrine reviews*, 30, 293-342.
- Doerffel, K. 1966. *Statistik in der analytischen Chemie*, Deutscher Verlag für Grundstoffindustrie.
- Ec 2003. European Union Risk Assessment Report: 4, 4'-isopropylidenediphenol (Bisphenol-A). *EUR 20843 EN*. European Commission Joint Research Centre.

- Flint, S., Markle, T., Thompson, S. & Wallace, E. 2012. Bisphenol A exposure, effects, and policy: a wildlife perspective. *Journal of environmental management*, 104, 19-34.
- Gadd, G. M. 2009. Biosorption: critical review of scientific rationale, environmental importance and significance for pollution treatment. *Journal of Chemical Technology and Biotechnology*, 84, 13-28.
- Gao, D.-W. & Wen, Z.-D. 2016. Phthalate esters in the environment: A critical review of their occurrence, biodegradation, and removal during wastewater treatment processes. *Science of the Total Environment*, 541, 986-1001.
- Gow, N. A., Latge, J.-P. & Munro, C. A. 2017. The fungal cell wall: structure, biosynthesis, and function. *Microbiology spectrum*.
- Gu, J.-D., Li, J.-X. & Wang, Y.-Y. 2005. Biochemical pathway and degradation of phthalate ester isomers by bacteria. *Water Science and Technology*, 52, 241-248.
- Haneef, M., Ceseracciu, L., Canale, C., Bayer, I. S., Heredia-Guerrero, J. A. & Athanassiou, A. 2017. Advanced materials from fungal mycelium: fabrication and tuning of physical properties. *Scientific reports*, 7, 41292.
- Hansch, C., Leo, A., Hoekman, D. & Livingstone, D. 1995. *Exploring QSAR: hydrophobic, electronic, and steric constants*, American Chemical Society Washington, DC.
- Harms, H., Schlosser, D. & Wick, L. Y. 2011. Untapped potential: exploiting fungi in bioremediation of hazardous chemicals. *Nature Reviews Microbiology*, 9, 177-192.
- Hodgson, E. & Levi, P. E. 1999. Interactions of Piperonyl Butoxide with Cytochrome P450. *Piperonyl Butoxide*. London: Academic Press.
- Hofmann, U. & Schlosser, D. 2016. Biochemical and physicochemical processes contributing to the removal of endocrine-disrupting chemicals and pharmaceuticals by the aquatic ascomycete *Phoma* sp. UHH 5-1-03. *Applied microbiology and biotechnology*, 100, 2381-2399.
- Howard, P. 1989. Handbook of Environmental Fate and Exposure Data, Vol I. *Chelsea, MI: Lewis Publishers*.
- Huang, J., Nkrumah, P. N., Li, Y. & Appiah-Sefah, G. 2013. Chemical Behavior of Phthalates Under Abiotic Conditions in Landfills. In: WHITACRE, D. M. (ed.) *Reviews of Environmental Contamination and Toxicology Volume 224*. New York, NY: Springer New York.
- Ike, M., Chen, M. Y., Jin, C. S. & Fujita, M. 2002. Acute toxicity, mutagenicity, and estrogenicity of biodegradation products of bisphenol-A. *Environmental toxicology*, 17, 457-461.
- Jackson, M. A., Labeda, D. P. & Becker, L. A. 1996. Isolation for bacteria and fungi for the hydrolysis of phthalate and terephthalate esters. *Journal of Industrial Microbiology*, 16, 301-304.
- Jahangiri, E., Seiwert, B., Reemtsma, T. & Schlosser, D. 2017. Laccase- and electrochemically mediated conversion of triclosan: Metabolite formation and influence on antibacterial activity. *Chemosphere*, 168, 549-558.
- Janssen, G., Baldwin, T., Winetzky, D., Tierney, L., Wang, H. & Murray, C. 2004. Selective targeting of a laccase from *Stachybotrys chartarum* covalently linked to a carotenoid-binding peptide. *Chemical Biology & Drug Design*, 64, 10-24.
- Jin, L., Sun, X., Zhang, X., Guo, Y. & Shi, H. 2014. Co-metabolic biodegradation of DBP by *Paenibacillus* sp. S-3 and H-2. *Current microbiology*, 68, 708-716.
- Johannes, C. & Majcherczyk, A. 2000. Laccase activity tests and laccase inhibitors. *Journal of Biotechnology*, 78, 193-199.
- Junghanns, C., Krauss, G. & Schlosser, D. 2008. Potential of aquatic fungi derived from diverse freshwater environments to decolourise synthetic azo and anthraquinone dyes. *Bioresource Technology*, 99, 1225-1235.
- Junghanns, C., Moeder, M., Krauss, G., Martin, C. & Schlosser, D. 2005. Degradation of the xenoestrogen nonylphenol by aquatic fungi and their laccases. *Microbiology*, 151, 45-57.

- Kabiersch, G., Rajasärkkä, J., Ullrich, R., Tuomela, M., Hofrichter, M., Virta, M., Hatakka, A. & Steffen, K. 2011. Fate of bisphenol A during treatment with the litter-decomposing fungi *Stropharia rugosoannulata* and *Stropharia coronilla*. *Chemosphere*, 83, 226-232.
- Kapoor, A. & Viraraghavan, T. 1997. Heavy metal biosorption sites in *Aspergillus niger*. *Bioresource technology*, 61, 221-227.
- Kim, Y.-H., Min, J., Bae, K.-D., Gu, M. B. & Lee, J. 2005. Biodegradation of dipropyl phthalate and toxicity of its degradation products: a comparison of *Fusarium oxysporum* f. sp. pisi cutinase and *Candida cylindracea* esterase. *Archives of Microbiology*, 184, 25-31.
- Krauss, G., Barlocher, F., Schreck, P., Wennrich, R., Glasser, W. & Krauss, G.-J. 2001. Aquatic hyphomycetes occur in hyperpolluted waters in Central Germany. *Nova Hedwigia*, 72, 419-428.
- Krueger, M. C., Harms, H. & Schlosser, D. 2015. Prospects for microbiological solutions to environmental pollution with plastics. *Applied microbiology and biotechnology*, 99, 8857-8874.
- Lau, T., Chu, W. & Graham, N. 2005. The degradation of endocrine disruptor di-n-butyl phthalate by UV irradiation: a photolysis and product study. *Chemosphere*, 60, 1045-1053.
- Leinberger, J. 2017. Research Project: Potential for biodegradation of micropollutants BPA, DEP and DBP by fungal isolates. Leipzig, Germany: Helmholtz Centre for Environmental Research UFZ.
- Lertsirisophon, R., Soda, S., Sei, K. & Ike, M. 2009. Abiotic degradation of four phthalic acid esters in aqueous phase under natural sunlight irradiation. *Journal of environmental sciences*, 21, 285-290.
- Liang, D.-W., Zhang, T., Fang, H. H. P. & He, J. 2008. Phthalates biodegradation in the environment. *Applied Microbiology and Biotechnology*, 80, 183.
- Liao, C.-S., Chen, L.-C., Chen, B.-S. & Lin, S.-H. 2010. Bioremediation of endocrine disruptor di-n-butyl phthalate ester by *Deinococcus radiodurans* and *Pseudomonas stutzeri*. *Chemosphere*, 78, 342-346.
- Liers, C., Ullrich, R., Hofrichter, M., Minibayeva, F. V. & Beckett, R. P. 2011. A heme peroxidase of the ascomyceteous lichen *Leptogium saturninum* oxidizes high-redox potential substrates. *Fungal Genetics and Biology*, 48, 1139-1145.
- Linder, M. B., Szilvay, G. R., Nakari-Setälä, T. & Penttilä, M. E. 2005. Hydrophobins: the protein-amphiphiles of filamentous fungi. *FEMS Microbiology Reviews*, 29, 877-896.
- Lobos, J. H., Leib, T. & Su, T.-M. 1992. Biodegradation of bisphenol A and other bisphenols by a gram-negative aerobic bacterium. *Applied and environmental microbiology*, 58, 1823-1831.
- Luo, H., Li, X., Li, G., Pan, Y. & Zhang, K. 2006. Acanthocytes of *Stropharia rugosoannulata* Function as a Nematode-Attacking Device. *Applied and Environmental Microbiology*, 72, 2982-2987.
- Luo, Y., Guo, W., Ngo, H. H., Nghiem, L. D., Hai, F. I., Zhang, J., Liang, S. & Wang, X. C. 2014. A review on the occurrence of micropollutants in the aquatic environment and their fate and removal during wastewater treatment. *Science of the Total Environment*, 473, 619-641.
- Macellaro, G. 2014. Development of biosystems for the detection and degradation of endocrine disrupting chemicals (EDCs).
- Martorell, M. M., Pajot, H. F. & De Figueroa, L. I. C. 2012. Dye-decolourizing yeasts isolated from Las Yungas rainforest. Dye assimilation and removal used as selection criteria. *International Biodeterioration & Biodegradation*, 66, 25-32.
- Matsumoto, M., Hirata-Koizumi, M. & Ema, M. 2008. Potential adverse effects of phthalic acid esters on human health: a review of recent studies on reproduction. *Regulatory Toxicology and Pharmacology*, 50, 37-49.
- McIlvaine, T. 1921. A buffer solution for colorimetric comparison. *Journal of Biological Chemistry*, 49, 183-186.
- Middelhoven, W. J., Scorzetti, G. & Fell, J. W. 2001. *Trichosporon porosum* comb. nov., an anamorphic basidiomycetous yeast inhabiting soil, related to the *loubieri/laiibachii* group of species that assimilate hemicelluloses and phenolic compounds. *FEMS Yeast Research*, 1, 15-22.

- Mori, T. & Kondo, R. 2002. Oxidation of chlorinated dibenzo-p-dioxin and dibenzofuran by white-rot fungus, *Phlebia lindtneri*. *FEMS Microbiology Letters*, 216, 223-227.
- Morohoshi, K., Shiraishi, F., Oshima, Y., Koda, T., Nakajima, N., Edmonds, J. S. & Morita, M. 2003. Synthesis and estrogenic activity of bisphenol A mono- and di- β -D-glucopyranosides, plant metabolites of bisphenol A. *Environmental toxicology and chemistry*, 22, 2275-2279.
- Mulligan, C. N., Yong, R. & Gibbs, B. 2001. Surfactant-enhanced remediation of contaminated soil: a review. *Engineering geology*, 60, 371-380.
- Navacharoen, A. & Vangnai, A. S. 2011. Biodegradation of diethyl phthalate by an organic-solvent-tolerant *Bacillus subtilis* strain 3C3 and effect of phthalate ester coexistence. *International Biodeterioration & Biodegradation*, 65, 818-826.
- Nguyen, L. N., Hai, F. I., Yang, S., Kang, J., Leusch, F. D., Roddick, F., Price, W. E. & Nghiem, L. D. 2014. Removal of pharmaceuticals, steroid hormones, phytoestrogens, UV-filters, industrial chemicals and pesticides by *Trametes versicolor*: role of biosorption and biodegradation. *International Biodeterioration & Biodegradation*, 88, 169-175.
- Nikolcheva, L. G., Cockshutt, A. M. & Bärlocher, F. 2003. Determining diversity of freshwater fungi on decaying leaves: comparison of traditional and molecular approaches. *Applied and environmental microbiology*, 69, 2548-2554.
- Peng, X. & Li, X. 2012. Compound-specific isotope analysis for aerobic biodegradation of phthalate acid esters. *Talanta*, 97, 445-449.
- Sabev, H. A., Handley, P. S. & Robson, G. D. 2006. Fungal colonization of soil-buried plasticized polyvinyl chloride (pPVC) and the impact of incorporated biocides. *Microbiology*, 152, 1731-1739.
- Sakurai, A., Toyoda, S. & Sakakibara, M. 2001. Removal of bisphenol A by polymerization and precipitation method using *Coprinus cinereus* peroxidase. *Biotechnology letters*, 23, 995-998.
- Sasaki, M., Maki, J.-I., Oshiman, K.-I., Matsumura, Y. & Tsuchido, T. 2005. Biodegradation of bisphenol A by cells and cell lysate from *Sphingomonas* sp. strain AO1. *Biodegradation*, 16, 449-459.
- Schlosser, D. & Hofer, C. 2002. Laccase-catalyzed oxidation of Mn(2+) in the presence of natural Mn(3+) chelators as a novel source of extracellular H₂O₂ production and its impact on manganese peroxidase. *Appl Environ Microbiol*, 68, 3514-21.
- Scholz, N. 2003. Ecotoxicity and biodegradation of phthalate monoesters. *Chemosphere*, 53, 921-926.
- Schwarzenbach, R. P., Escher, B. I., Fenner, K., Hofstetter, T. B., Johnson, C. A., Von Gunten, U. & Wehrli, B. 2006. The challenge of micropollutants in aquatic systems. *Science*, 313, 1072-1077.
- Semple, K. T., Doick, K. J., Wick, L. Y. & Harms, H. 2007. Microbial interactions with organic contaminants in soil: Definitions, processes and measurement. *Environmental Pollution*, 150, 166-176.
- Shareef, A., Angove, M. J., Wells, J. D. & Johnson, B. B. 2006. Aqueous solubilities of estrone, 17 β -estradiol, 17 α -ethynylestradiol, and bisphenol A. *Journal of Chemical & Engineering Data*, 51, 879-881.
- Singh, S., Harms, H. & Schlosser, D. 2014. Screening of ecologically diverse fungi for their potential to pretreat lignocellulosic bioenergy feedstock. *Applied microbiology and biotechnology*, 98, 3355-3370.
- Spivack, J., Leib, T. & Lobos, J. 1994. Novel pathway for bacterial metabolism of bisphenol A. Rearrangements and stilbene cleavage in bisphenol A metabolism. *Journal of Biological Chemistry*, 269, 7323-7329.
- Stanier, R. Y., Palleroni, N. J. & Doudoroff, M. 1966. The aerobic pseudomonads a taxonomic study. *Microbiology*, 43, 159-271.
- Staples, C. A., Dome, P. B., Klecka, G. M., Oblock, S. T. & Harris, L. R. 1998. A review of the environmental fate, effects, and exposures of bisphenol A. *Chemosphere*, 36, 2149-2173.
- Staples, C. A., Peterson, D. R., Parkerton, T. F. & Adams, W. J. 1997. The environmental fate of phthalate esters: A literature review. *Chemosphere*, 35, 667-749.

- Suárez, S., Carballa, M., Omil, F. & Lema, J. M. 2008. How are pharmaceutical and personal care products (PPCPs) removed from urban wastewaters? *Reviews in Environmental Science and Bio/Technology*, 7, 125-138.
- Subramanian, V. & Yadav, J. S. 2009. Role of P450 monooxygenases in the degradation of the endocrine-disrupting chemical nonylphenol by the white rot fungus *Phanerochaete chrysosporium*. *Applied and environmental microbiology*, 75, 5570-5580.
- Tomlin, C. D. 2009. *The pesticide manual: a world compendium*, British Crop Production Council.
- Uchida, H., Fukuda, T., Miyamoto, H., Kawabata, T., Suzuki, M. & Uwajima, T. 2001. Polymerization of bisphenol A by purified laccase from *Trametes villosa*. *Biochemical and Biophysical Research Communications*, 287, 355-358.
- Wang, J., Yamada, Y., Notake, A., Todoroki, Y., Tokumoto, T., Dong, J., Thomas, P., Hirai, H. & Kawagishi, H. 2014. Metabolism of bisphenol A by hyper lignin-degrading fungus *Phanerochaete sordida* YK-624 under non-ligninolytic condition. *Chemosphere*, 109, 128-133.
- Wang, J., Yamamoto, R., Yamamoto, Y., Tokumoto, T., Dong, J., Thomas, P., Hirai, H. & Kawagishi, H. 2013a. Hydroxylation of bisphenol A by hyper lignin-degrading fungus *Phanerochaete sordida* YK-624 under non-ligninolytic condition. *Chemosphere*, 93, 1419-1423.
- Wang, J., Yamamoto, Y., Hirai, H. & Kawagishi, H. 2013b. Dimerization of Bisphenol A by Hyper Lignin-Degrading Fungus *Phanerochaete sordida* YK-624 Under Ligninolytic Condition. *Current Microbiology*, 66, 544-547.
- Yang, S., Hai, F. I., Nghiem, L. D., Nguyen, L. N., Roddick, F. & Price, W. E. 2013a. Removal of bisphenol A and diclofenac by a novel fungal membrane bioreactor operated under non-sterile conditions. *International Biodeterioration & Biodegradation*, 85, 483-490.
- Yang, X., Zhang, C., He, Z., Hu, X., Guo, J., Zhong, Q., Wang, J., Xiong, L. & Liu, D. 2013b. Isolation and characterization of two n-butyl benzyl phthalate degrading bacteria. *International Biodeterioration & Biodegradation*, 76, 8-11.
- Yordanova, G., Godjevargova, T., Nenkova, R. & Ivanova, D. 2013. Biodegradation of phenol and phenolic derivatives by a mixture of immobilized cells of *aspergillus awamori* and *trichosporon cutaneum*. *Biotechnology & Biotechnological Equipment*, 27, 3681-3688.

Acknowledgements

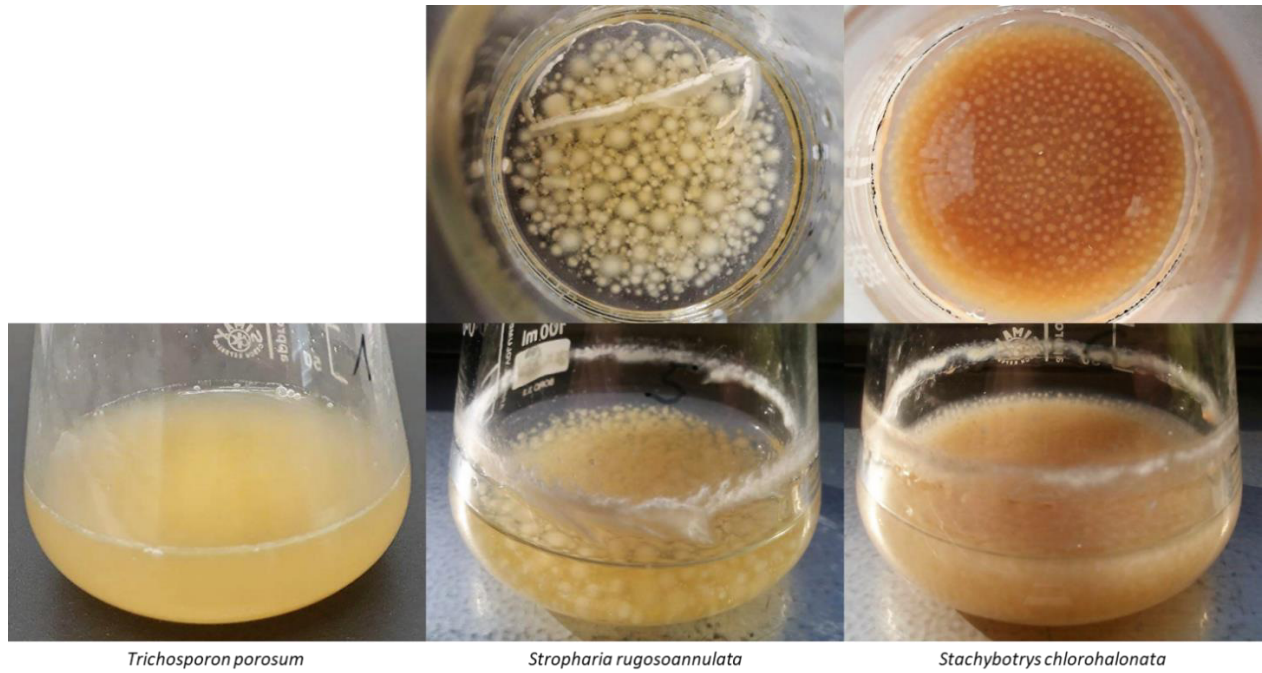
I am particularly grateful for the opportunity given by Dr. Dietmar Schlosser to write my thesis in his lab. I would like to express my appreciation to Dietmar for his patient guidance, enthusiastic encouragement, and useful feedback. I did benefit a lot from our discussions!

Advice by Dr. Harald Cederlund has been a great help for the progress of writing, thank you for being such a cheerful long-distance supervisor! Further, I am grateful to Dr. Bettina Seivert for running the UPLC-QTOF-MS for my metabolite samples and dealing with the data.

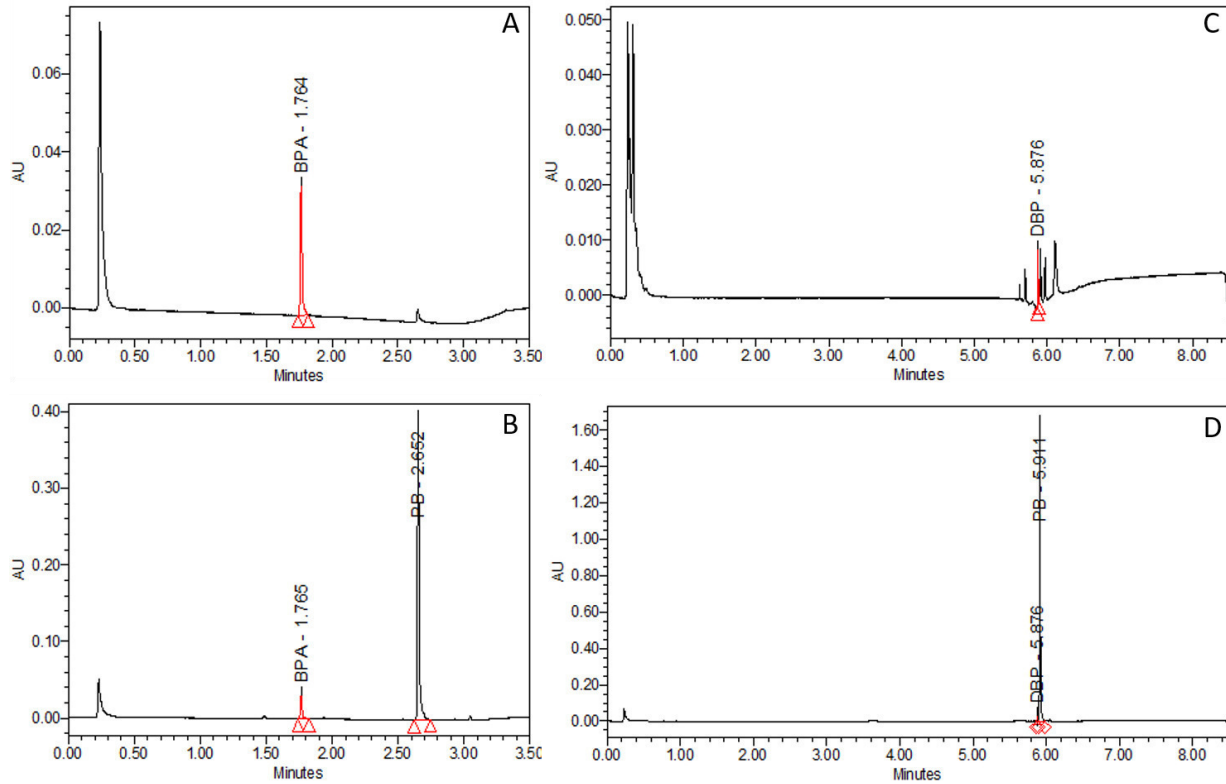
My special thanks are extended to all group members and Kamyar Mogodiniyai Kasmaei for their technical support on this project and the good times in the lab.

Lena

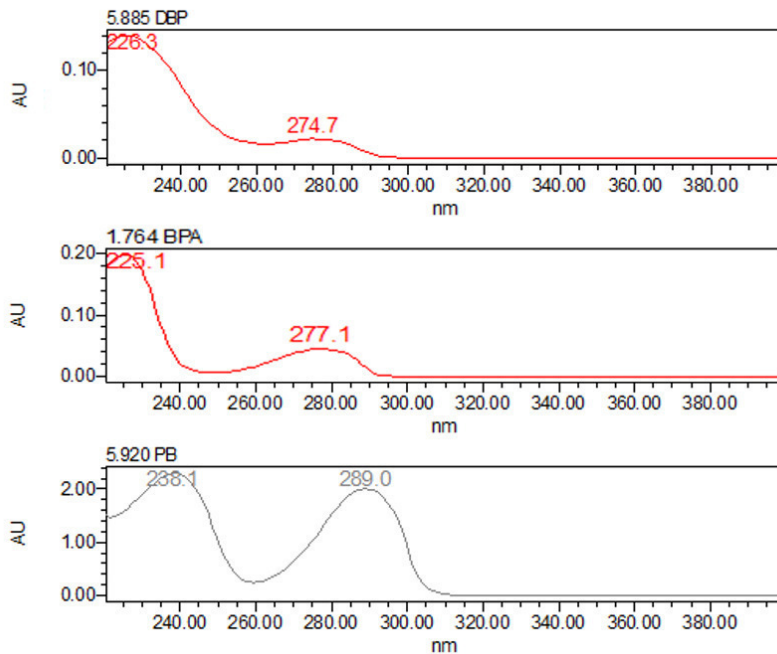
Appendix



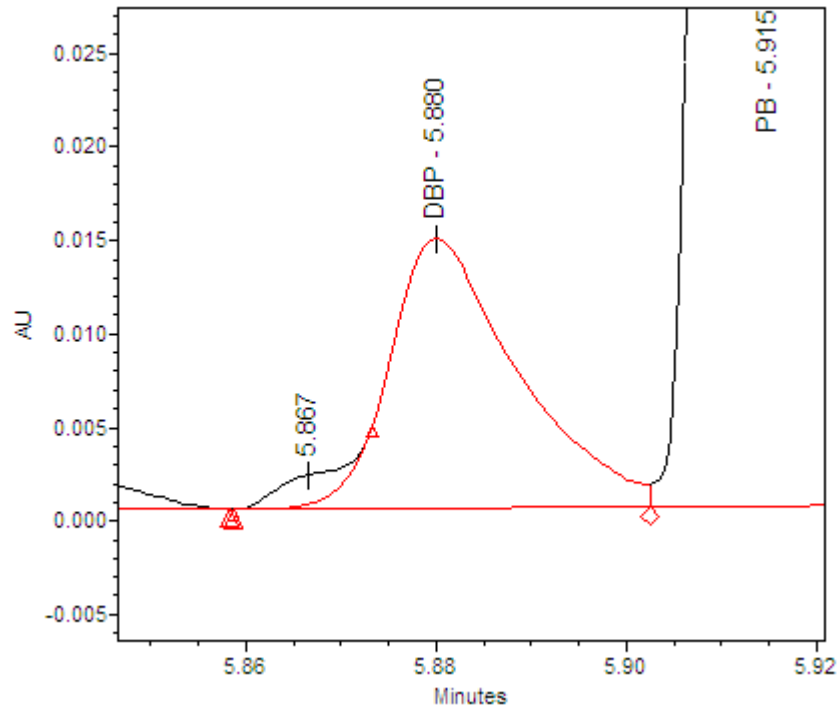
Appendix Figure 1 Pictures of 100 ml Erlenmeyer flasks containing cultures of *T. porosum*, *S. rugosoannulata* and *S. chlorohalonata* in pre-cultivation (day 6) in 30 ml 2% malt extract media.



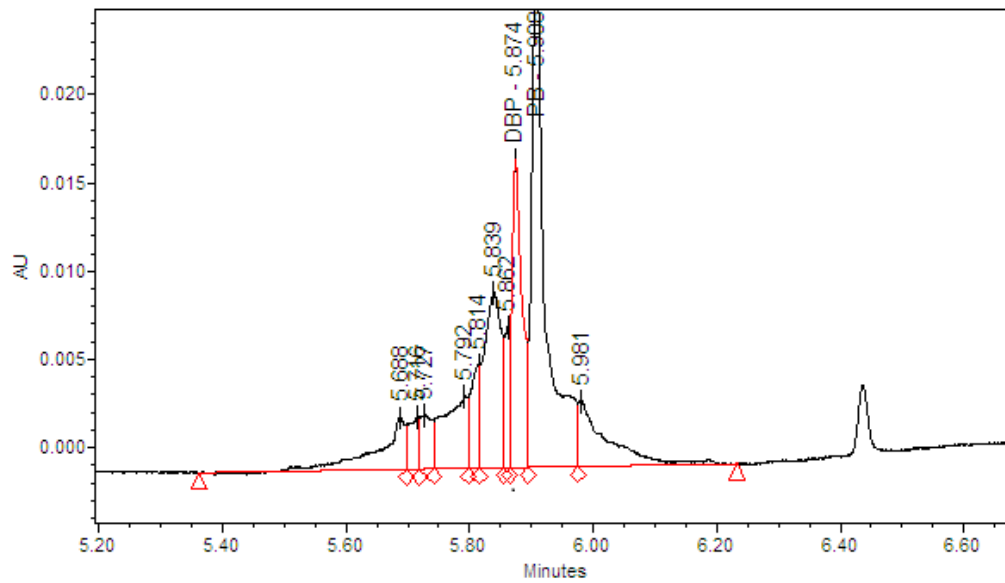
Appendix Figure 2 Representative UPLC chromatograms by an Aquity™ eλ photodiode array detector at wavelength 278 nm. A BPA in an active culture of *T. porosum*. B BPA and PB in a PB 1 mM inhibited culture of *S. rugosoannulata*. C DBP in a onetime NaN_3 inactivated culture of *Acephala* sp. D DBP and PB in a PB 5 mM inhibited culture of *C. aquatica*. All chromatograms are from samples taken 1.5 h after incubation.



Appendix Figure 3 Characteristic absorbance spectra of DBP, BPA and PB from 230 to 390 nm wavelength by an Aquity™ eλ photodiode array detector.



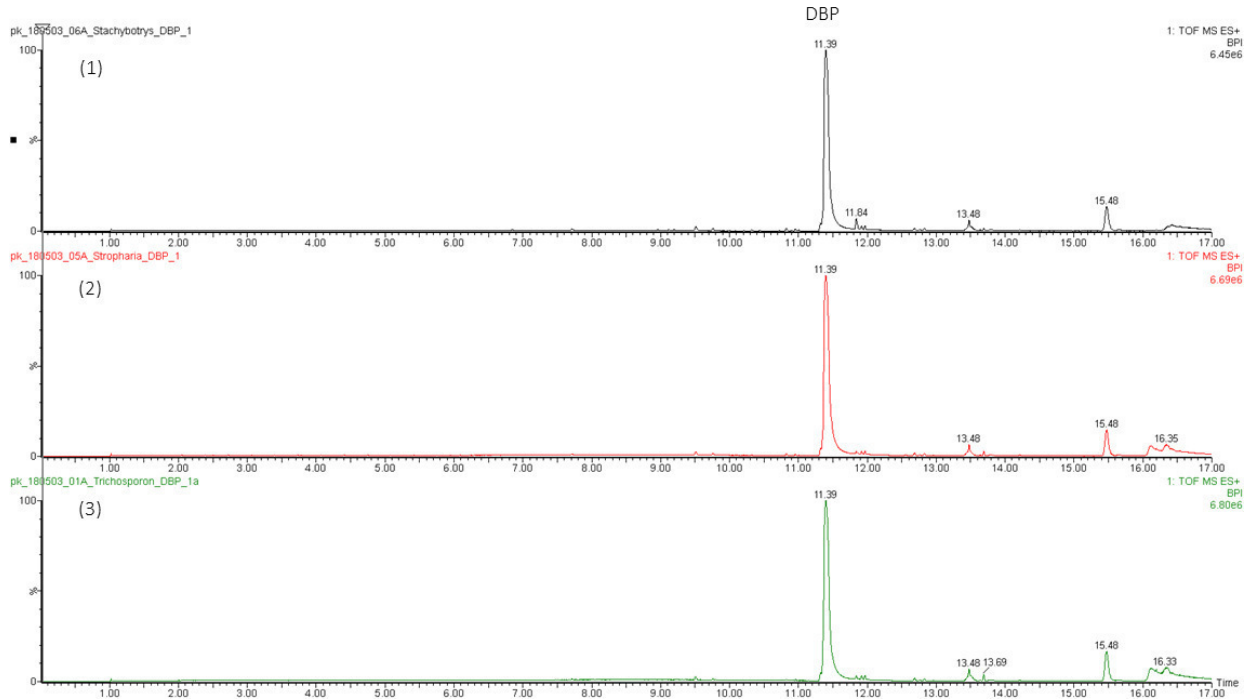
Appendix Figure 4 UPLC target peak integration improved by automatic peak shoulder detection and Gaussian skim.



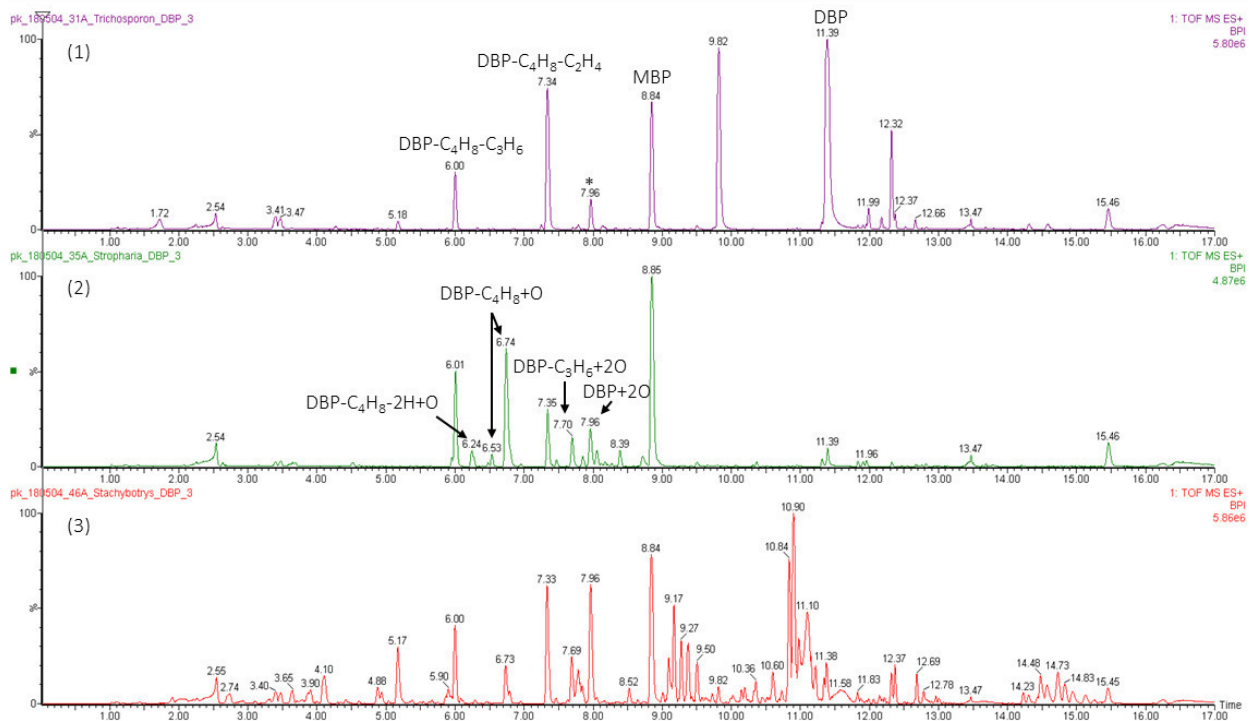
Appendix Figure 5 UPLC peak integration by height in case of DBP quantification of *S. chlorohalonata*.

S. rugosoannulata		S. chlorohalonata		Time	Assay
	Blank	Blank	Blank	0	Laccase activity
	Active	Active	Active	1.5	
	PB 1mM inhibited	PB 1mM inhibited	PB 1mM inhibited	3.5	
	NaN3 inactivated	NaN3 inactivated	NaN3 inactivated	24	
				48	
				120	Laccase activity
				216	
				336	
	Blank	Blank	Blank	0	
	Active	Active	Active	1.5	
	PB 1mM inhibited	PB 1mM inhibited	PB 1mM inhibited	3.5	A. Laccase activity
	NaN3 inactivated	NaN3 inactivated	NaN3 inactivated	24	
				48	
				120	
				216	
				336	C. Laccase activity
	Blank	Blank	Blank	0	
	Active	Active	Active	1.5	
	PB 1mM inhibited	PB 1mM inhibited	PB 1mM inhibited	3.5	
	NaN3 inactivated	NaN3 inactivated	NaN3 inactivated	24	
				48	B. Laccase and Mn-independent peroxidase activity
				120	
				216	
				336	
	Blank	Blank	Blank	0	
	Active	Active	Active	1.5	D. Laccase and all peroxidase activity
	PB 1mM inhibited	PB 1mM inhibited	PB 1mM inhibited	3.5	
	NaN3 inactivated	NaN3 inactivated	NaN3 inactivated	24	
				48	
				120	
				216	336
				336	

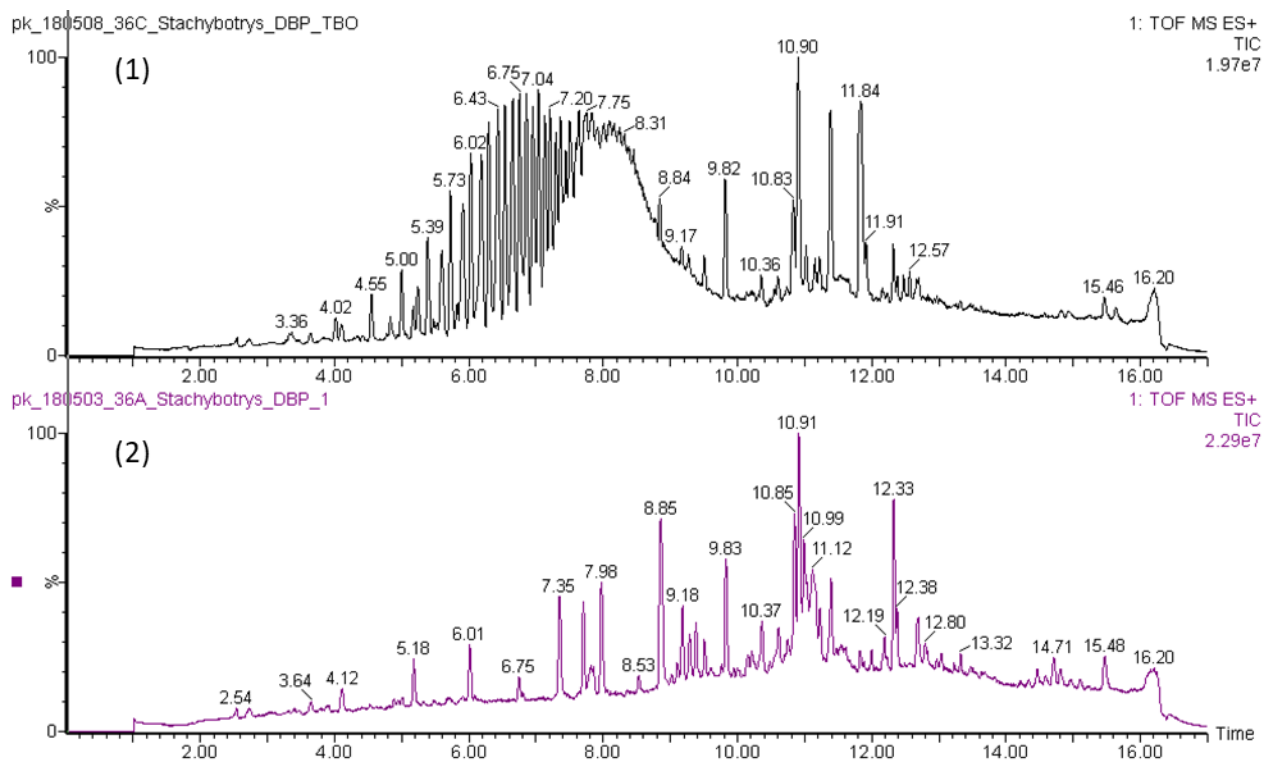
Appendix Figure 6 Picture of 96-well plates in exoenzyme activity assay of *S. rugosoannulata* (left column) and *S. chlorohalonata* (right column) for DBP removal experiment. The Table gives information about location of samples within the plates. The laccase activity assay is in the first row, and assays A, B, C and D are part of the Mn-dependent and Mn-independent peroxidase activity determination (see also Table 4). The green-blue colorization arises from oxidized ABTS to radical ABTS^{•+}.



Appendix Figure 7 Representative base peak chromatograms of UPLC-QTOF-MS for DBP metabolites. Respective samples were taken at 0 h i.e. before biomass addition of (1) *S. chlorohalonata*, (2) *S. rugosoannulata* and (3) *T. porosum*. DBP peak at retention time of 11.39 min.



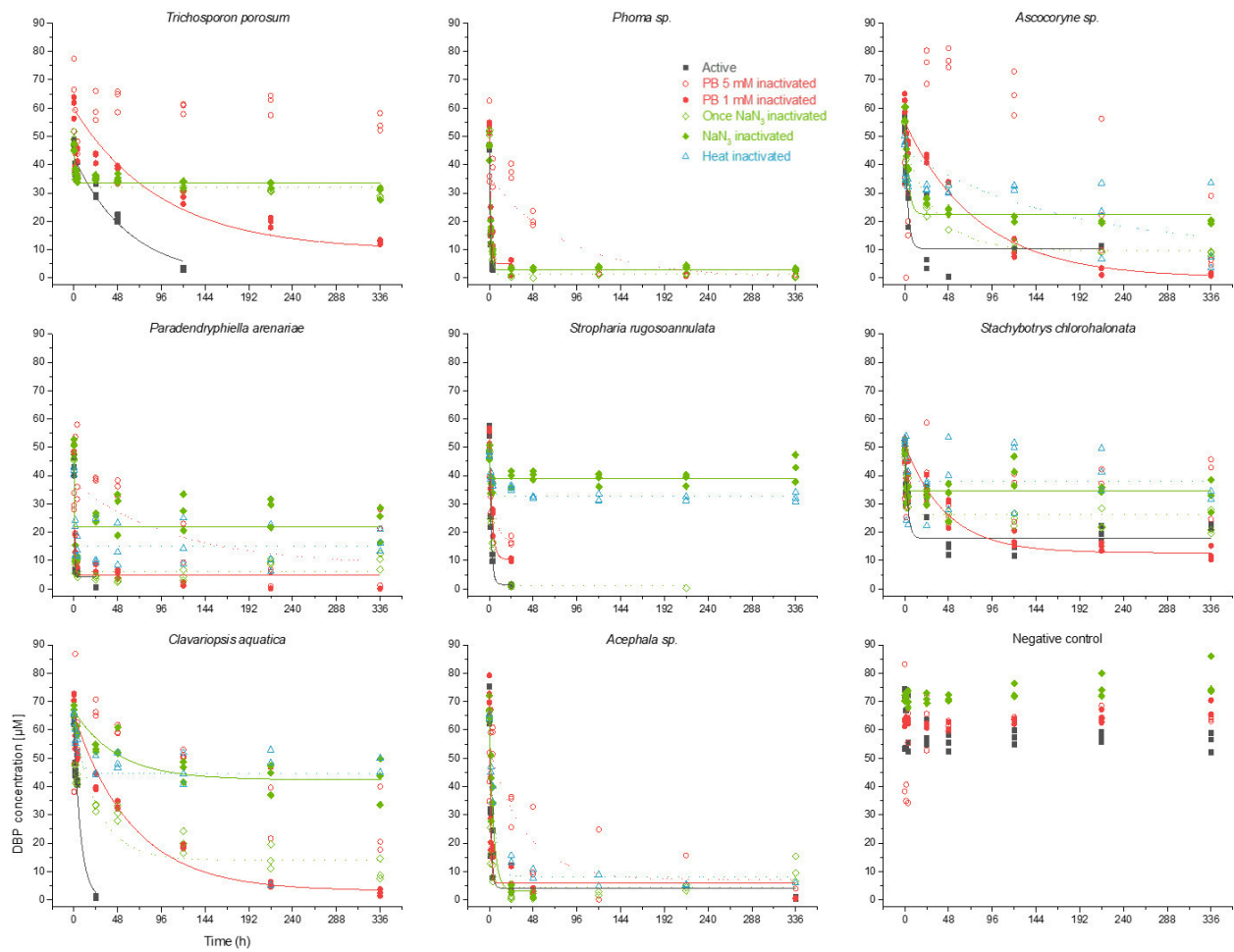
Appendix Figure 8 Representative base peak chromatograms of UPLC-QTOF-MS for DBP metabolites in active fungal cultures. Respective samples were taken 96 h after biomass addition of (1) *T. porosum*, (2) *S. rugosoannulata* and after 216 h in case of (3) *S. chlorohalonata*. Retention times and description as inferred from measured compound mass of DBP and (major) DBP metabolite peaks are visible. * Peak at 7.96 min in sample of *T. porosum* supernatant is not related to "DBP+2O" and was also present in NaN₃ inactivated fungal culture.



Appendix Figure 9 Total ion chromatograms of UPLC-QTOF-MS for DBP metabolites in *S. chlorohalonata* culture supernatant taken 96 h after biomass addition. (1) In cytochrome P450 inhibited cultures, target peaks (i.e. retention times in between approximately 6 to 9 minutes) were affected by matrix interference caused by PB. This perturbation was observed in all PB amended samples for all fungal strains. For comparison, (2) the identical active fungal culture.

Appendix Table 1 Fungal dry biomass values (g) after 14 days of cultivation in presence of micropollutants and, where applicable, PB inhibited or inactivation by NaN_3 or moist heat. Biomass was determined in triplicates for each strain and experiment. Values of alternative inhibition methods are presented in italic letters. ° indicates biomass increase compared to initial fungal dry biomass. * labels where the significantly (student's paired t-test, two-tailed, $\alpha = 0.05$) difference between initial and final biomass values

		Final fungal dry biomass weight (g)							
		<i>T. porosum</i>	<i>S. rugosoannul.</i>	<i>S. chlorothalon.</i>	<i>Phoma</i> sp.	<i>Ascocoryne</i> sp.	<i>P. arenariae</i>	<i>C. aquatica</i>	<i>Acephala</i> sp.
Active	DBP	0.200 ± 0.033	*0.058 ± 0.003	*0.125 ± 0.011	°0.400 ± 0.031	0.047 ± 0.005	0.227 ± 0.012	*0.055 ± 0.002	0.259 ± 0.014
	BPA	0.052 ± 0.007	°0.079 ± 0.014	0.120 ± 0.020	-	-	-	-	-
PB 5 mM inhibited	DBP	0.201 ± 0.034	*0.079 ± 0.000	*0.143 ± 0.013	*0.294 ± 0.011	*0.056 ± 0.005	*0.221 ± 0.011	*0.049 ± 0.001	°0.292 ± 0.022
	DBP	0.179 ± 0.049	*0.046 ± 0.003	*0.107 ± 0.011	°0.355 ± 0.038	0.053 ± 0.003	0.215 ± 0.020	*0.043 ± 0.003	°0.267 ± 0.017
PB 1 mM inhibited	BPA	0.057 ± 0.003	°0.075 ± 0.011	0.099 ± 0.005	-	-	-	-	-
	DBP	*0.122 ± 0.008	*0.035 ± 0.001	*0.113 ± 0.022	0.262 ± 0.020	*0.025 ± 0.001	*0.100 ± 0.006	*0.025 ± 0.005	*0.235 ± 0.010
$1 \times \text{NaN}_3$ inactivated	DBP	0.117 ± 0.025	0.048 ± 0.003	*0.111 ± 0.029	0.227 ± 0.008	*0.041 ± 0.003	*0.147 ± 0.013	0.028 ± 0.002	0.203 ± 0.008
	BPA	*0.047 ± 0.003	0.049 ± 0.008	*0.089 ± 0.004	-	-	-	-	-
Heat inactivated	DBP	-	0.049 ± 0.003	0.108 ± 0.012	-	*0.031 ± 0.005	*0.156 ± 0.023	*0.036 ± 0.007	°0.242 ± 0.002



Appendix Figure 10 Time course of DBP concentrations for active (solid black squares), PB 1mM inhibited (solid red circles), PB 5 mM inhibited (open red circles), double NaN_3 inactivated cultures (solid green diamonds) and once NaN_3 inactivated cultures (open green diamonds). The corresponding solid and dashed lines arise from data fitting of measured micropollutant concentration by exponential regression. Symbols represent means \pm standard deviations from triplicate cultures. Where PB 5 mM regression curves are missing, the exponential fit did not converge (*T. porosum*, *Ascocoryne sp.*, *S. chlorohalonata* and *C. aquatica*).

Appendix Table 2 Initial and specific (initial) removal rates of DBP observed with 5 mM PB inhibited, once NaN₃ inactivated and heat inactivates cultures of T.porosum. A difference of rates of 5 mM PB inhibited and double NaN₃ inactivated cultures is accounted as PB 5 mM (inhibited) biotransformation.

<i>T. porosum</i>						
Removal rate ¹	PB 5 mM inhibited		once NaN ₃ inactivated		Heat inactivated	Biotransformation PB 5 mM
Initial rate (μM h ⁻¹)	0.00 ±	0.00	§10.92 ±	2.54	-	
Specific initial rate (μM h ⁻¹ g ⁻¹)	0.00 ±	0.00	§43.75 ±	10.36	-	0
Specific 3.5 h rate (μM h ⁻¹ g ⁻¹)	18.83 ±	0.11	15.55 ±	0.18	-	4.43
Specific 24 h rate (μM h ⁻¹ g ⁻¹)	0.85 ±	40.90	2.37 ±	1.36	-	0
Specific 48 h rate (μM h ⁻¹ g ⁻¹)	0.18 ±	523.58	1.25 ±	2.42	-	0
Specific overall rate (μM h ⁻¹ g ⁻¹)	0.13 ±	166.33	0.25 ±	7.67	-	0

¹ Initial (volume-based) and specific (fungal dry biomass-based) initial removal rates obtained by exponential regression fit, and manually calculated specific removal rates for different time points, and the whole cultivation time 'overall'. § indicates non-linear regression fitting with a R2 < 0.9.

Appendix Table 3 Initial and specific (initial) removal rates of DBP observed with 5 mM PB inhibited, once NaN₃ inactivated and heat inactivates cultures of S. rugosoannulata. A difference of rates of 5 mM PB inhibited and double NaN₃ inactivated cultures is accounted as PB 5 mM (inhibited) biotransformation.

<i>S. rugosoannulata</i>						
Removal rate ¹	PB 5 mM inhibited		once NaN ₃ inactivated		Heat inactivated	Biotransformation PB 5 mM
Initial rate (μM h ⁻¹)	§4.51 ±	2.40	17.93 ±	1.45	6.21 ±	1.07
Specific initial rate (μM h ⁻¹ g ⁻¹)	§43.33 ±	23.18	172.24 ±	17.94	91.75 ±	31.43
Specific 3.5 h rate (μM h ⁻¹ g ⁻¹)	82.41 ±	0.01	89.53 ±	0.00	45.63 ±	0.00
Specific 24 h rate (μM h ⁻¹ g ⁻¹)	11.39 ±	0.20	18.83 ±	0.00	7.33 ±	0.02
Specific 48 h rate (μM h ⁻¹ g ⁻¹)	9.08 ±	0.20	9.64 ±	0.02	4.67 ±	0.03
Specific overall rate (μM h ⁻¹ g ⁻¹)	1.30 ±	1.37	1.38 ±	0.12	0.67 ±	0.30

¹ Initial (volume-based) and specific (fungal dry biomass-based) initial removal rates obtained by exponential regression fit, and manually calculated specific removal rates for different time points, and the whole cultivation time 'overall'. § indicates non-linear regression fitting with a R2 < 0.9 and therefore not considered as accurate (n.a.) and not used for calculation of biotransformation.

Appendix Table 4 Initial and specific (initial) removal rates of DBP observed with 5 mM PB inhibited, once NaN₃ inactivated and heat inactivates cultures of S. chlorohalonata. A difference of rates of 5 mM PB inhibited and double NaN₃ inactivated cultures is accounted as PB 5 mM (inhibited) biotransformation.

<i>S. chlorohalonata</i>						
Removal rate ¹	PB 5 mM inhibited		once NaN ₃ inactivated		Heat inactivated	Biotransformation PB 5 mM
Initial rate (μM h ⁻¹)	-		§11.94 ± 4.07		§21.16 ± 41.94	
Specific initial rate (μM h ⁻¹ g ⁻¹)	-		§55.13 ± 19.26		§106.39 ± 210.95	-
Specific 3.5 h rate (μM h ⁻¹ g ⁻¹)	13.30 ±	0.31	21.58 ±	0.09	22.17 ± 0.80	0
Specific 24 h rate (μM h ⁻¹ g ⁻¹)	-0.51 ±	-52.66	3.27 ±	0.09	4.14 ± 2.31	0
Specific 48 h rate (μM h ⁻¹ g ⁻¹)	1.58 ±	3.21	2.31 ±	0.26	1.21 ± 20.20	0
Specific overall rate (μM h ⁻¹ g ⁻¹)	0.06 ±	127.83	0.37 ±	3.24	0.45 ± 32.55	0

¹ Initial (volume-based) and specific (fungal dry biomass-based) initial removal rates obtained by exponential regression fit, and manually calculated specific removal rates for different time points, and the whole cultivation time 'overall'. § indicates non-linear regression fitting with a R² < 0.9.

Appendix Table 5 Initial and specific (initial) removal rates of DBP observed with 5 mM PB inhibited, once NaN₃ inactivated and heat inactivates cultures of Phoma sp. A difference of rates of 5 mM PB inhibited and double NaN₃ inactivated cultures is accounted as PB 5 mM (inhibited) biotransformation.

<i>Phoma sp.</i>						
Removal rate ¹	PB 5 mM inhibited		once NaN ₃ inactivated		Heat inactivated	Biotransformation PB 5 mM
Initial rate (μM h ⁻¹)	§0.43 ±	0.16	44.60 ±	3.04	-	
Specific initial rate (μM h ⁻¹ g ⁻¹)	§1.28 ±	0.48	132.22 ±	17.34	-	n.a.
Specific 3.5 h rate (μM h ⁻¹ g ⁻¹)	35.00 ±	0.02	37.58 ±	0.00	-	4.60
Specific 24 h rate (μM h ⁻¹ g ⁻¹)	0.81 ±	23.14	6.30 ±	0.02	-	0
Specific 48 h rate (μM h ⁻¹ g ⁻¹)	1.45 ±	3.53	3.18 ±	0.05	-	0
Specific overall rate (μM h ⁻¹ g ⁻¹)	0.38 ±	8.69	0.45 ±	0.26	-	0.01

¹ Initial (volume-based) and specific (fungal dry biomass-based) initial removal rates obtained by exponential regression fit, and manually calculated specific removal rates for different time points, and the whole cultivation time 'overall'. § indicates non-linear regression fitting with a R² < 0.9 and therefore not considered as accurate (n.a.) and not used for calculation of biotransformation.

Appendix Table 6 Initial and specific (initial) removal rates of DBP observed with 5 mM PB inhibited, once NaN₃ inactivated and heat inactivates cultures of Ascocoryne sp. A difference of rates of 5 mM PB inhibited and double NaN₃ inactivated cultures is accounted as PB 5 mM (inhibited) biotransformation.

<i>Ascocoryne sp.</i>							
Removal rate ¹	PB 5 mM inhibited		once NaN ₃ inactivated		Heat inactivated*		Biotransformation PB 5 mM
Initial rate (μM h ⁻¹)	-		§1.09 ±	0.20	§0.21 ±	0.05	
Specific initial rate (μM h ⁻¹ g ⁻¹)	-		§15.69 ±	3.36	§3.09 ±	0.83	-
Specific 3.5 h rate (μM h ⁻¹ g ⁻¹)	64.39 ±	0.01	172.47 ±	0.03	61.83 ±	0.00	0
Specific 24 h rate (μM h ⁻¹ g ⁻¹)	-23.26 ±	-0.03	18.64 ±	0.03	10.05 ±	0.03	0
Specific 48 h rate (μM h ⁻¹ g ⁻¹)	-12.35 ±	-0.01	9.36 ±	0.24	5.25 ±	0.02	0
Specific overall rate (μM h ⁻¹ g ⁻¹)	0.99 ±	3.83	2.00 ±	0.06	1.44 ±	2.76	0

¹ Initial (volume-based) and specific (fungal dry biomass-based) initial removal rates obtained by exponential regression fit, and manually calculated specific removal rates for different time points, and the whole cultivation time 'overall'. § indicates non-linear regression fitting with a R² < 0.9.

Appendix Table 7 Initial and specific (initial) removal rates of DBP observed with 5 mM PB inhibited, once NaN₃ inactivated and heat inactivates cultures of P. arenariae. A difference of rates of 5 mM PB inhibited and double NaN₃ inactivated cultures is accounted as PB 5 mM (inhibited) biotransformation.

<i>P. arenariae</i>							
Removal rate ¹	PB 5 mM inhibited		once NaN ₃ inactivated		Heat inactivated		Biotransformation PB 5 mM
Initial rate (μM h ⁻¹)	§0.26 ±	0.25	83.50 ±	26.71	§32.91 ±	16.08	
Specific initial rate (μM h ⁻¹ g ⁻¹)	§1.00 ±	0.95	318.85 ±	104.97	§125.68 ±	62.19	n.a.
Specific 3.5 h rate (μM h ⁻¹ g ⁻¹)	43.44 ±	0.01	45.40 ±	0.01	29.66 ±	0.04	0
Specific 24 h rate (μM h ⁻¹ g ⁻¹)	-1.32 ±	-2.95	6.73 ±	0.02	4.28 ±	0.86	0
Specific 48 h rate (μM h ⁻¹ g ⁻¹)	-0.43 ±	-6.92	3.45 ±	0.04	2.14 ±	1.43	0
Specific overall rate (μM h ⁻¹ g ⁻¹)	0.15 ±	71.11	0.41 ±	1.63	0.28 ±	4.86	0

¹ Initial (volume-based) and specific (fungal dry biomass-based) initial removal rates obtained by exponential regression fit, and manually calculated specific removal rates for different time points, and the whole cultivation time 'overall'. § indicates non-linear regression fitting with a R² < 0.9 and therefore not considered as accurate (n.a.) and not used for calculation of biotransformation.

Appendix Table 8 Initial and specific (initial) removal rates of DBP observed with 5 mM PB inhibited, once NaN₃ inactivated and heat inactivates cultures of Acephala sp. A difference of rates of 5 mM PB inhibited and double NaN₃ inactivated cultures is accounted as PB 5 mM (inhibited) biotransformation.

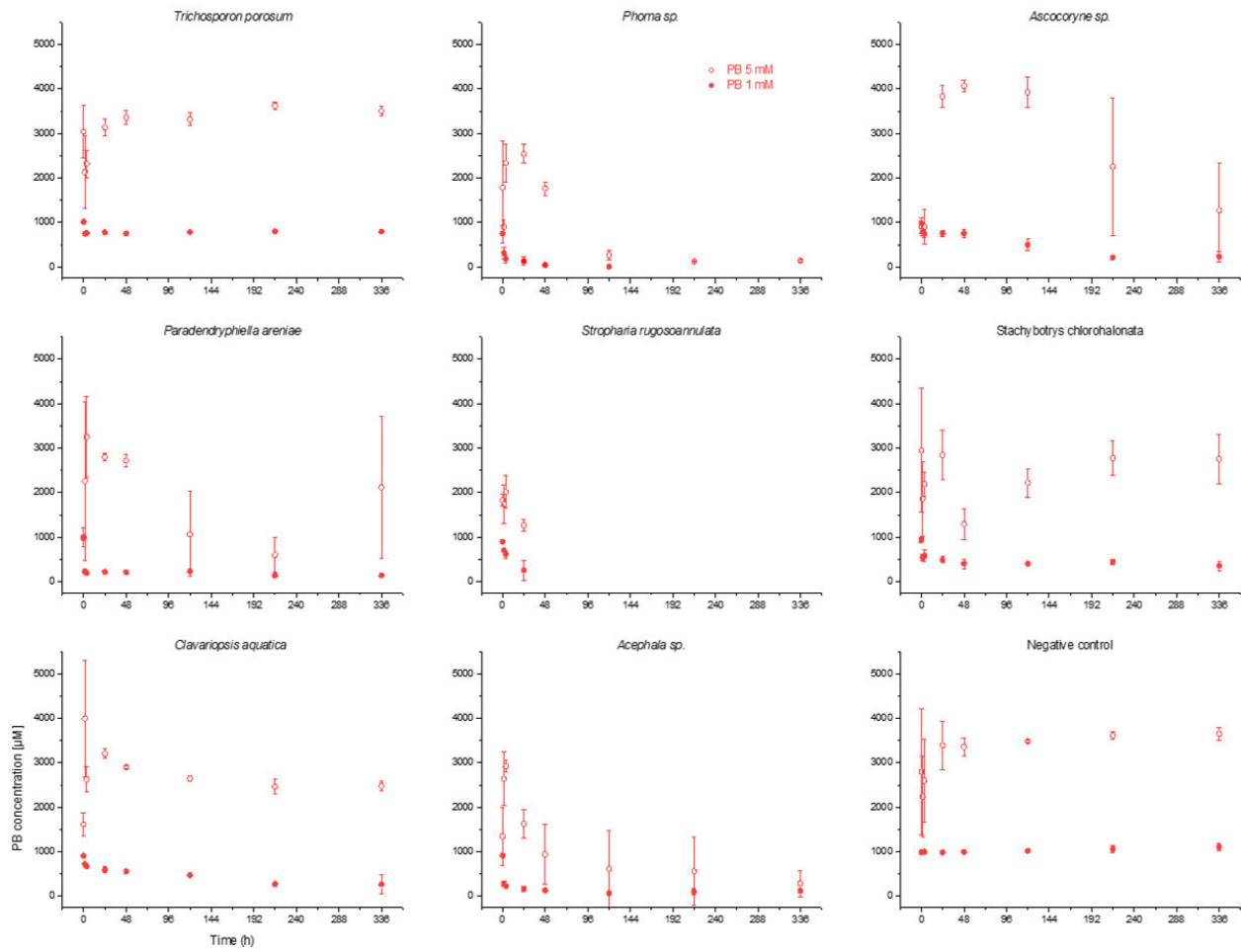
<i>Acephala sp.</i>							
Removal rate ¹	PB 5 mM inhibited		once NaN ₃ inactivated		Heat inactivated		Biotransformation PB 5 mM
Initial rate (μM h ⁻¹)	[§] 1.19 ±	0.49	56.61 ±	7.61	10.69 ±	1.64	
Specific initial rate (μM h ⁻¹ g ⁻¹)	[§] 4.50 ±	1.84	214.13 ±	29.35	44.48 ±	6.92	n.a.
Specific 3.5 h rate (μM h ⁻¹ g ⁻¹)	61.30 ±	0.03	59.99 ±	0.01	32.72 ±	0.20	20.56
Specific 24 h rate (μM h ⁻¹ g ⁻¹)	1.61 ±	10.94	10.05 ±	0.09	8.73 ±	0.05	0
Specific 48 h rate (μM h ⁻¹ g ⁻¹)	2.02 ±	4.76	4.93 ±	0.13	4.82 ±	0.16	0
Specific overall rate (μM h ⁻¹ g ⁻¹)	0.47 ±	20.58	0.61 ±	3.05	0.73 ±	0.89	0

¹ Initial (volume-based) and specific (fungal dry biomass-based) initial removal rates obtained by exponential regression fit, and manually calculated specific removal rates for different time points, and the whole cultivation time 'overall'. § indicates non-linear regression fitting with a R² < 0.9 and therefore not considered as accurate (n.a.) and not used for calculation of biotransformation.

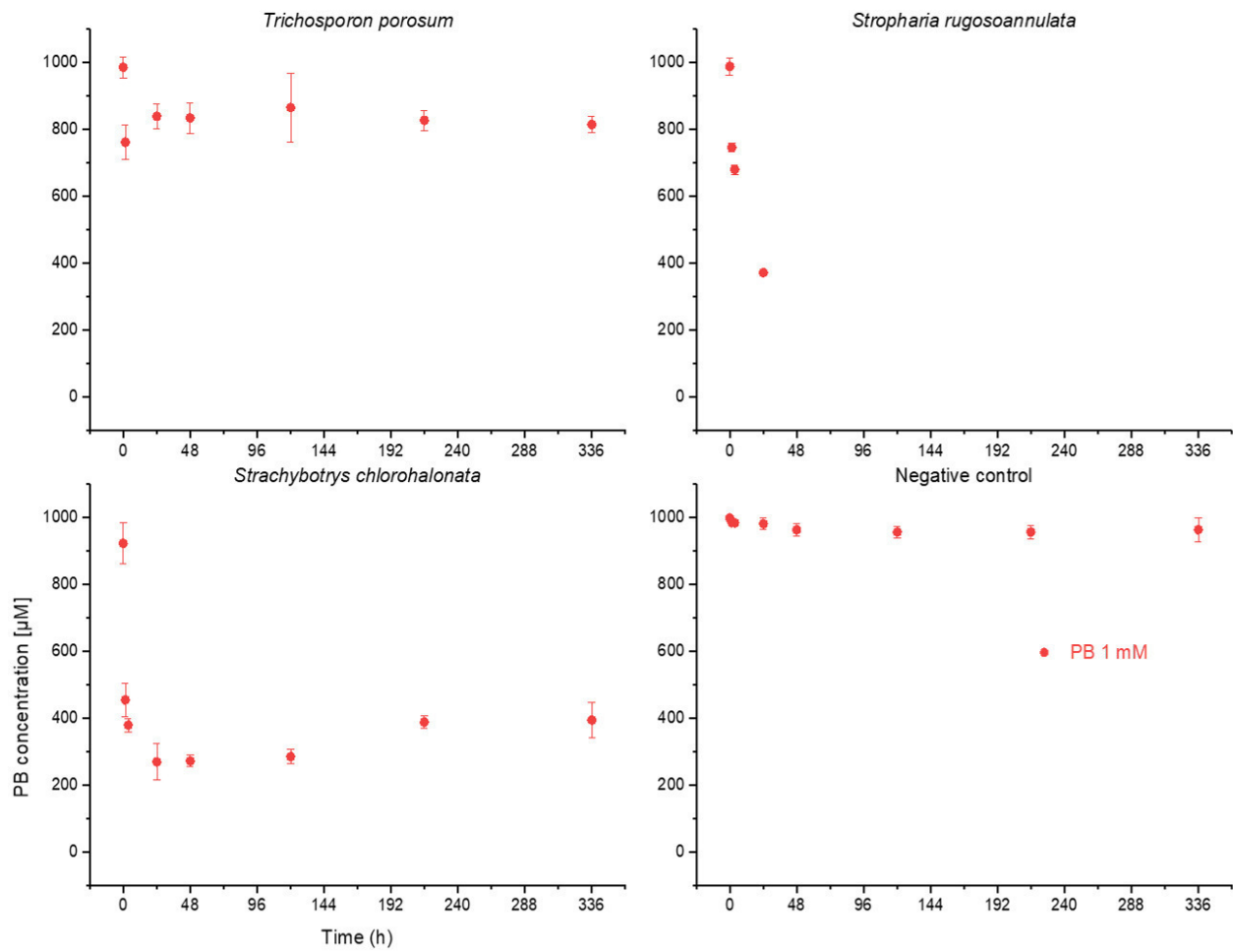
Appendix Table 9 Initial and specific (initial) removal rates of DBP observed with 5 mM PB inhibited, once NaN₃ inactivated and heat inactivates cultures of C. aquatica. A difference of rates of 5 mM PB inhibited and double NaN₃ inactivated cultures is accounted as PB 5 mM (inhibited) biotransformation.

<i>C. aquatica</i>							
Removal rate ¹	PB 5 mM inhibited		once NaN ₃ inactivated*		Heat inactivated		Biotransformation PB 5 mM
Initial rate (μM h ⁻¹)	-		[§] 1.81 ±	0.38	[§] 3.25 ±	3.42	
Specific initial rate (μM h ⁻¹ g ⁻¹)	-		[§] 22.21 ±	4.82	[§] 69.49 ±	74.44	-
Specific 3.5 h rate (μM h ⁻¹ g ⁻¹)	73.54 ±	0.01	81.24 ±	0.01	53.93 ±	0.02	33.71
Specific 24 h rate (μM h ⁻¹ g ⁻¹)	-13.29 ±	-0.16	16.91 ±	0.03	16.14 ±	0.05	0
Specific 48 h rate (μM h ⁻¹ g ⁻¹)	-4.74 ±	-0.92	8.98 ±	0.09	7.08 ±	0.08	0
Specific overall rate (μM h ⁻¹ g ⁻¹)	0.56 ±	15.53	2.03 ±	0.45	2.10 ±	2.11	0

¹ Initial (volume-based) and specific (fungal dry biomass-based) initial removal rates obtained by exponential regression fit, and manually calculated specific removal rates for different time points, and the whole cultivation time 'overall'. § indicates non-linear regression fitting with a R² < 0.9.



Appendix Figure 11 Time course of PB nominal 1 mM (solid red circles) and 5 mM (open red circles) concentrations in the DBP degradation experiment.



Appendix Figure 12 Time course of PB concentrations in the BPA degradation experiment.

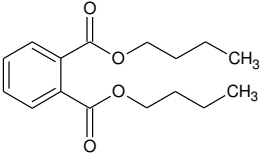
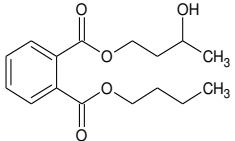
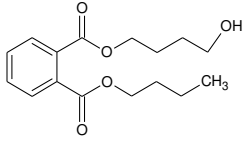
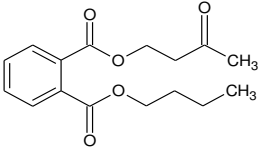
Appendix Table 10 Exoenzyme activities in active, PB inhibited and NaN₃ inactivated cultures of *T. porosum*, *S. rugosoannulata* and *S. chlorohalonata* during the **DBP** removal experiment.

Time [h]	Laccase activity [U l ⁻¹]			All peroxidase activity [U l ⁻¹]			Mn-independant peroxidase activity [U l ⁻¹]			Mn-dependant peroxidase activity [U l ⁻¹]		
	Active	PB inhibited	NaN ₃ inactivated	Active	PB inhibited	NaN ₃ inactivated	Active	PB inhibited	NaN ₃ inactivated	Active	PB inhibited	NaN ₃ inactivated
<i>T. porosum</i>												
0	0.10 ± 0.04	0.03 ± 0.29	0.05 ± 0.11	n.d.	n.d.	0.26 ± 1.45	n.d.	n.d.	n.d.	n.d.	n.d.	0.26 ± 1.45
1.5	n.d.	n.d.	0.10 ± 0.10	n.d.	n.d.	n.d.	n.d.	n.d.	0.99 ± 2.14	n.d.	n.d.	n.d.
3.5	n.d.	n.d.	n.d.	0.31 ± 0.77	n.d.	n.d.	n.d.	n.d.	n.d.	0.31 ± 0.77	n.d.	n.d.
24	0.12 ± 0.20	0.19 ± 0.52	0.03 ± 0.13	n.d.	n.d.	n.d.	n.d.	n.d.	n.d.	n.d.	n.d.	n.d.
48	0.38 ± 0.06	0.11 ± 0.07	0.05 ± 0.05	0.07 ± 0.33	n.d.	n.d.	n.d.	n.d.	n.d.	0.07 ± 0.33	n.d.	n.d.
120	0.16 ± 0.10	0.33 ± 0.14	0.13 ± 0.08	0.05 ± 0.25	0.01 ± 0.17	n.d.	0.06 ± 0.33	0.09 ± 0.32	n.d.	n.d.	n.d.	n.d.
216	0.46 ± 0.16	0.34 ± 0.16	0.06 ± 0.21	n.d.	n.d.	n.d.	n.d.	0.06 ± 0.17	n.d.	n.d.	n.d.	n.d.
336	0.47 ± 0.24	0.33 ± 0.04	0.16 ± 0.20	0.21 ± 0.43	n.d.	0.06 ± 0.33	0.09 ± 0.19	0.02 ± 1.15	0.03 ± 0.15	0.11 ± 0.62	n.d.	0.03 ± 0.48
<i>S. rugosoannulata</i>												
0	0.08 ± 0.10	-	0.08 ± 0.30	0.06 ± 0.12	-	n.d.	n.d.	-	n.d.	0.06 ± 0.12	-	n.d.
1.5	0.82 ± 0.41	0.21 ± 0.06	n.d.	n.d.	n.d.	n.d.	n.d.	n.d.	n.d.	n.d.	n.d.	n.d.
3.5	0.87 ± 0.33	0.36 ± 0.10	n.d.	0.07 ± 0.18	n.d.	n.d.	n.d.	n.d.	n.d.	0.07 ± 0.18	n.d.	n.d.
24	1.24 ± 0.29	1.03 ± 0.22	0.05 ± 0.04	0.05 ± 0.31	n.d.	n.d.	0.10 ± 0.14	0.16 ± 0.31	0.01 ± 0.12	n.d.	n.d.	n.d.
48	13.02 ± 2.95	4.88 ± 3.05	n.d.	n.d.	n.d.	0.58 ± 1.29	n.d.	n.d.	0.31 ± 9.49	n.d.	n.d.	0.27 ± 10.78
120	22.42 ± 4.85	14.85 ± 9.74	0.10 ± 0.07	n.d.	n.d.	n.d.	n.d.	n.d.	n.d.	n.d.	n.d.	n.d.
216	42.35 ± 15.06	19.73 ± 10.10	0.16 ± 0.20	n.d.	0.24 ± 1.89	n.d.	n.d.	n.d.	n.d.	n.d.	0.24 ± 1.89	n.d.
336	102.85 ± 18.51	22.92 ± 9.52	0.16 ± 0.11	n.d.	n.d.	n.d.	n.d.	n.d.	n.d.	n.d.	n.d.	n.d.
<i>S. chlorohalonata</i>												
0	0.08 ± 0.20	n.d.	n.d.	n.d.	-	0.22 ± 0.83	n.d.	-	n.d.	n.d.	-	0.22 ± 0.83
1.5	n.d.	n.d.	n.d.	n.d.	n.d.	n.d.	n.d.	n.d.	n.d.	n.d.	n.d.	n.d.
3.5	n.d.	n.d.	n.d.	n.d.	0.13 ± 1.05	n.d.	n.d.	n.d.	n.d.	n.d.	0.13 ± 1.05	n.d.
24	n.d.	n.d.	n.d.	n.d.	n.d.	n.d.	n.d.	n.d.	n.d.	n.d.	n.d.	n.d.
48	n.d.	n.d.	-	n.d.	n.d.	n.d.	n.d.	n.d.	n.d.	n.d.	n.d.	n.d.
120	n.d.	1.59 ± 2.33	n.d.	n.d.	n.d.	n.d.	n.d.	n.d.	n.d.	n.d.	n.d.	n.d.
216	n.d.	1.90 ± 0.31	n.d.	n.d.	0.13 ± 1.43	n.d.	n.d.	0.26 ± 1.28	n.d.	n.d.	n.d.	n.d.
336	n.d.	0.36 ± 0.14	n.d.	n.d.	0.05 ± 0.44	n.d.	n.d.	n.d.	n.d.	n.d.	0.05 ± 0.44	n.d.

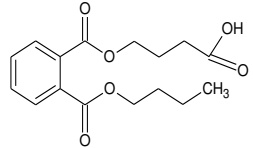
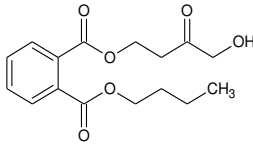
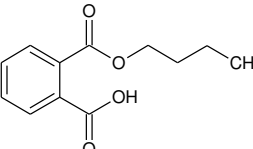
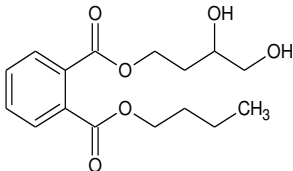
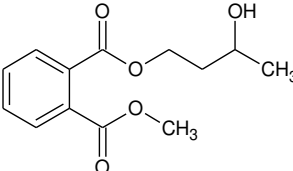
Appendix Table 11 Exoenzyme activities in active, PB inhibited and NaN₃ inactivated cultures of *T. porosum*, *S. rugosannulata* and *S. chlorohalonata* during the BPA removal experiment.

Time [h]	Laccase activity [U l ⁻¹]			All peroxidase activity [U l ⁻¹]			Mn-independent peroxidase activity [U l ⁻¹]			Mn-dependant peroxidase activity [U l ⁻¹]		
	Active	PB inhibited	NaN ₃ inactivated	Active	PB inhibited	NaN ₃ inactivated	Active	PB inhibited	NaN ₃ inactivated	Active	PB inhibited	NaN ₃ inactivated
<i>T. porosum</i>												
0	n.d.	n.d.	n.d.	-	-	-	n.d.	n.d.	n.d.	-	-	-
1.5	n.d.	n.d.	n.d.	-	-	-	0.13 ± 1.23	n.d.	n.d.	-	-	-
3.5	0.01 ± 0.05	n.d.	n.d.	-	-	-	n.d.	n.d.	n.d.	-	-	-
24	0.02 ± 0.16	0.09 ± 0.09	n.d.	-	-	-	n.d.	n.d.	n.d.	-	-	-
48	0.12 ± 0.11	0.06 ± 0.13	n.d.	-	-	-	0.05 ± 2.22	n.d.	3.73 ± 7.70	-	-	-
120	0.14 ± 0.17	n.d.	0.04 ± 0.16	-	-	-	n.d.	n.d.	n.d.	-	-	-
216	0.07 ± 0.07	0.03 ± 0.07	0.00 ± 0.10	-	-	-	n.d.	n.d.	n.d.	-	-	-
336	0.27 ± 0.09	0.21 ± 0.07	0.12 ± 0.21	-	-	-	n.d.	n.d.	n.d.	-	-	-
<i>S. rugosannulata</i>												
0	n.d.	-	n.d.	n.d.	-	n.d.	n.d.	-	n.d.	n.d.	-	n.d.
1.5	0.12 ± 0.08	0.02 ± 0.30	n.d.	0.47 ± 0.80	n.d.	n.d.	n.d.	0.03 ± 0.34	n.d.	0.47 ± 0.80	n.d.	n.d.
3.5	0.11 ± 0.15	0.21 ± 0.22	n.d.	1.03 ± 0.44	n.d.	n.d.	0.03 ± 0.16	n.d.	n.d.	1.00 ± 0.59	n.d.	n.d.
24	0.71 ± 0.34	0.03 ± 0.26	0.01 ± 0.09	0.83 ± 0.31	n.d.	n.d.	n.d.	n.d.	n.d.	0.83 ± 0.31	n.d.	n.d.
48	3.13 ± 2.63	1.37 ± 1.31	0.11 ± 0.12	n.d.	n.d.	n.d.	n.d.	0.25 ± 0.27	n.d.	n.d.	n.d.	n.d.
120	26.74 ± 20.00	19.99 ± 8.23	0.12 ± 0.12	n.d.	n.d.	n.d.	n.d.	n.d.	n.d.	n.d.	n.d.	n.d.
216	35.23 ± 30.86	30.64 ± 3.14	0.08 ± 0.07	n.d.	n.d.	n.d.	n.d.	n.d.	n.d.	n.d.	n.d.	n.d.
336	51.16 ± 36.41	66.94 ± 86.85	0.13 ± 0.04	n.d.	n.d.	n.d.	n.d.	n.d.	n.d.	n.d.	n.d.	n.d.
<i>S. chlorohalonata</i>												
0	0.01 ± 0.10	0.01 ± 0.07	n.d.	n.d.	n.d.	n.d.	n.d.	n.d.	n.d.	n.d.	n.d.	n.d.
1.5	n.d.	0.51 ± 1.19	0.78 ± 0.85	n.d.	n.d.	n.d.	n.d.	n.d.	n.d.	n.d.	n.d.	n.d.
3.5	n.d.	0.13 ± 0.73	0.61 ± 1.57	n.d.	n.d.	n.d.	n.d.	n.d.	n.d.	n.d.	n.d.	n.d.
24	n.d.	n.d.	n.d.	n.d.	n.d.	n.d.	n.d.	n.d.	n.d.	n.d.	n.d.	n.d.
48	0.67 ± 0.40	0.70 ± 0.14	n.d.	n.d.	n.d.	n.d.	n.d.	n.d.	n.d.	n.d.	n.d.	n.d.
120	1.35 ± 1.41	10.49 ± 0.68	0.19 ± 1.62	0.09 ± 2.18	n.d.	n.d.	n.d.	n.d.	0.60 ± 28.87	0.09 ± 2.18	n.d.	n.d.
216	0.47 ± 0.72	5.24 ± 1.07	n.d.	0.13 ± 1.24	n.d.	n.d.	n.d.	n.d.	n.d.	0.13 ± 1.24	n.d.	n.d.
336	0.06 ± 0.10	1.72 ± 0.34	n.d.	n.d.	n.d.	n.d.	n.d.	n.d.	n.d.	n.d.	n.d.	n.d.

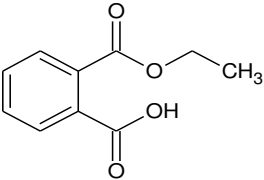
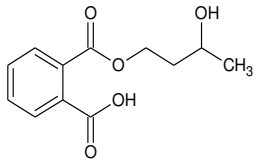
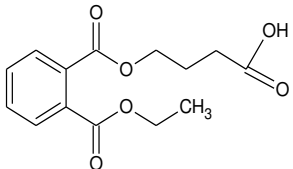
Appendix Table 12 Structures proposed for the fungal products of DBP measured with UPLC-QTOF-MS. ESI: Electron spray ionization.

Compound	Structure(s) Proposed	[M-H] ⁻ experimental exact mass (U)	Elemental Composition	Average retention time(s) (min)	ESI	Fragments
Dibutyl Phthalate (DBP)		301.143	C ₁₆ H ₂₃ O ₄ Na	11.39	Positive	Low abundance
TP 317 (DBP +O)	  Two possible structure shown	317.139	C ₁₆ H ₂₂ O ₅ Na	9.15	Positive	Low abundance
TP 259 (DBP -C ₄ H ₈ -2H +O)	Structure uncertain	259.059	C ₁₂ H ₁₂ O ₅ Na	6.26	Positive	163.04 (C ₉ H ₇ O ₃)
TP 315 (DBP +O -2H)		315.121	C ₁₆ H ₂₀ O ₅ Na	8.79	Positive	Low abundance

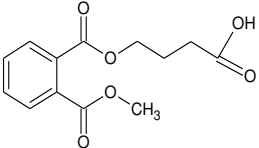
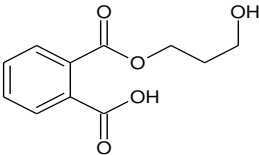
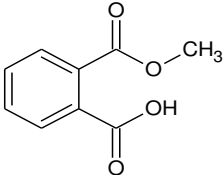
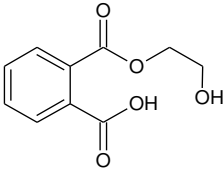
continued on next page

Compound	Structure(s) Proposed	[M-H] ⁻ experimental exact mass (U)	Elemental Composition	Average retention time(s) (min)	ESI	Fragments
TP 331 (DBP +2O -2H)	  <p>Two possible structure shown</p>	331.116	C ₁₆ H ₂₀ O ₆ Na	7.58	Positive	267.061 (C ₁₂ H ₁₃ O ₄ Na ₂) 261.074 (C ₁₂ H ₁₄ O ₅ Na)
Monobutyl Phthalate		245.08	C ₁₂ H ₁₄ O ₄ Na	8.85	Positive	Low abundance
TP 333 (DBP +2O)		333.141	C ₁₆ H ₂₂ O ₆ Na	8.14, 7.96, 8.07, 8.18	Positive	Low abundance
TP 275 (DBP -C ₃ H ₆ +O)		275.089	C ₁₃ H ₁₆ O ₅ Na	7.69, 7.85, 7.95	Positive	Low abundance

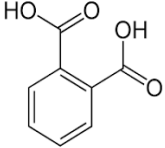
continued on next page

Compound	Structure(s) Proposed	[M-H] ⁻ experimental exact mass (U)	Elemental Composition	Average retention time(s) (min)	ESI	Fragments
TP 217 (DBP -C ₄ H ₈ -C ₂ H ₄)		217.048	C ₁₀ H ₁₀ O ₄ Na	7.03, 7.33	Positive	Low abundance
TP 261 (DBP +O -C ₄ H ₈)		261.075	C ₁₂ H ₁₄ O ₅ Na	6.73, 6.55	Positive	Low abundance
TP 305 (DBP -C ₂ H ₄ +2O)	 Two possible structure shown	305.101	C ₁₄ H ₁₈ O ₆ Na	6.78, 6.90	Positive	163.04 (C ₉ H ₇ O ₃)

continued on next page

Compound	Structure(s) Proposed	[M-H] ⁻ experimental exact mass (U)	Elemental Composition	Average retention time(s) (min)	ESI	Fragments
TP 291 (DBP +2O -C ₃ H ₆)		291.085	C ₁₃ H ₁₆ O ₆ Na	6.19, 6.55, 6.65	Positive	Low abundance
TP 247 (DBP -C ₄ H ₈ -CH ₂ +O)		247.059	C ₁₁ H ₁₂ O ₅ Na	6.13	Positive	Low abundance
TP 203 (DBP -C ₄ H ₈ -C ₃ H ₆)		203.032	C ₉ H ₈ O ₄ Na	6.00	Positive	163.04 (C ₉ H ₇ O ₃)
TP 233 (DBP -C ₄ H ₈ -C ₂ H ₄ +O)		233.043	C ₁₀ H ₁₀ O ₅ Na	5.24	Positive	163.04 (C ₉ H ₇ O ₃)

continued on next page

Compound	Structure(s) Proposed	[M-H] ⁻ experimental exact mass (U)	Elemental Composition	Average retention time(s) (min)	ESI	Fragments
Phthalic Acid		163.04	C ₈ H ₆ O ₄	4.55	Positive	Low abundance